A study of the preparation and pyrolysis of -diketonate and carboxylate precursors to semiconducting zinc oxide films

Philip Douglas Coates

A Study of the Preparation and Pyrolysis of β-Diketonate and Carboxylate Precursors to Semiconducting Zinc Oxide Films.

by

Philip Douglas Coates

A thesis submitted towards the degree of Ph.D. to the University of Durham.

June1994.

Acknowledgements

The following people are gratefully acknowledged for their help in making this thesis possible.

Dr. Arthur Banister, my supervisor, for his unending enthusiasm and belief in his projects and his students.

Dr. Stan Hauptman for technical wizardry, sound advice and discussions on European Politics.

Dr. Jeremy Rawson for computer software, much practical assistance and a lot of typing.

Dr. Ian Lavender for practical advice, typing and accommodation.

Dr. Euan Ross for administrative expertise, encouragement and company on the fells.

Prof. John Woods, Drs. Andy Brinkman and Ken Durose, James Fiddes and Norman, Harry and Brian - the team from Applied Physics (Durham) for knowledge in fields largely unknown to me.

Drs. Richard Marbrow, Jonathan Lloyd, Eric Neild and Ed West of ICI for providing enthusiastic and supportive industrial backing.

ICI Paints (Slough) for money.

Prof. Bill Clegg (University of Newcastle-upon-Tyne) for solid state crystallography.

Mr I.D. Luscombe (ICI, Wilton) for d.s.c. work.

All technical staff in the Department of Chemistry (I made use of nearly everyone in three years) who were consistently both helpful and interested.

Moira for further typing and sarcasm.

Fellow chemists, Ant, Simon, Christine, Simon, Iain, Neil, Colin plus the inhabitants of CG101/19 ("Matt Jolly Experience") for beer and company.

Fellow 5-a-siders, Mark x 2, Paul, John, Steve, Martin, Jon and Peter for intense relaxation.

All friends and family for their encouragement.

Memorandum

The work described in this thesis was carried out by me in the Chemistry Department of the University of Durham between October 1988 and September 1991. I declare that the work has not been submitted previously for a degree at this, or any other, University. This thesis is a report of my own original work, except where acknowledged by reference. The copyright of this thesis rests with the author. No quotation should be published without his written consent and information derived from it should be acknowledged. This work is covered by an I.C.I. secrecy agreement. It is intended to use material from this thesis in future publications, given the consent of I.C.I. plc.

Abstract

This work primarily concerns the chemistry involved in the preparation of zinc oxide semiconducting films.

Chapter One is an outline of the background to this project. It also indicates the reasons for studying the areas described in the subsequent chapters.

General details of experimental techniques are described in Chapter Two.

The third chapter covers the synthetic work carried out during this project. This includes the preparation and characterisation of $Zn(acac)_2.H_2O$, related zinc compounds and acetylacetonate complexes of group III metals (Al, Ga, In). It also includes details of the reaction between alcoholic solutions of $Zn(acac)_2.H_2O$ and water.

Chapter Four describes the study, by differential scanning calorimetry, of $Zn(acac)_2.H_2O$ and $Zn(acac)_2$. This includes d.s.c. traces carried out for a variety of conditions (including heating rate and particle size). Particular attention is paid to enthalpies and peak-maxima temperatures.

The experiments described in Chapter Five were designed to gain further insight into the complex thermal behaviour of $Zn(acac)_2.H_2O$. Infra-red spectroscopy, proton n.m.r. , elemental analysis and X-ray powder photography were used to identify the compounds involved.

The sixth chapter outlines the synthesis of zinc oxide films from aqueous solutions of zinc formate dihydrate using spray equipment designed and assembled at the University of Durham. X-ray photography, and thickness and transparency measurements were carried out on the films produced.

Abbreviations

acac	$CH_3COCHCOCH_3^-$
d.s.c.	differential scanning calorimetry
Hacac	acetylacetone (2,4-pentanedione)
OAc	acetate
t.g.a.	thermal gravimetric analysis
DTA	differential thermal analysis
etaa	ethylacetoacetate
Me	Methyl
IPA	iso-propyl alcohol
MeOH	methanol
DPM	dipivaloylmethanido

Table of Contents

Chapter 1

Introduction

The connecting theme for all the work described in this thesis is the production of zinc oxide films. Zinc oxide is an n-type semiconductor[1] in which excess zinc acts as an electron donor[2]. If, instead of zinc, there are small quantities of a group III metal (dopant) in the ZnO lattice there is a further increase in the conductivity of the material. Crystalline ZnO is transparent[3] and good quality films (in terms of crystallinity and dopant level) have the unusual ability of allowing light to pass through whilst conducting electricity. In addition to these two characteristics, zinc oxide films are also relatively cheap to produce.

Together, these three properties were necessary for the intended end application, which was principally the manufacture of zinc oxide-based photovoltaic devices. The crux of the problem was to produce a good enough quality film, in terms of conductivity and transparency, at a temperature low enough for plastic [e.g. poly(ethyleneterephthalate)] films to be used as the substrate.

The preceding work to that described in this thesis was carried out by Dr. S. Oktik (School of Engineering and Applied Sciences, University of Durham)[4] . His attempts to produce a good quality semiconducting zinc oxide at low deposition temperatures concentrated on the spray pyrolysis of solutions of zinc acetate in H_2O/IPA mixtures, using $InCl_3$ as a dopant. This work produced reasonable quality films at substrate temperatures as low as 350°C, but this was still too high for successful deposition onto a plastic substrate. Following the suggestion of Dr. P O'Brien (Queen Mary College, University of London), Dr Oktik used zinc acetylacetonate (in IPA) as an

alternative to zinc acetate. Early results were encouraging (although some doubt existed as to the exact composition of the spray solution), and these experiments were continued by Mr. A.J.C. Fiddes (SEAS, University of Durham), whose project ran concurrently with this author's.

Given the situation at the onset of the project, it was decided that there would be three main areas of interest: (1) synthesis and characterisation of possible precursors, (2) analysis of the thermal behaviour of the major precursor(s) used by Mr A.J.C. Fiddes (subsequently identified as $Zn(acac)_2.H_2O$) and (3) spray deposition of zinc oxide films using solvent-free solutions.

The main precursors considered were the three different forms of zinc acetylacetonate, i.e. $Zn(acac)_2.H_2O$, $[Zn(acac)_2]_3$ and $Zn(acac)_2$, as well as adducts of the general formula $Zn(acac)_2.X$. Other β-diketonates and carboxylates of zinc were also to be characterised with special attention paid to their suitability as precursors to spray-pyrolysed zinc oxide films.

It was hoped that the thermal studies of the major precursor, $Zn(acac)_2.H_2O$, would indicate the mechanism and onset temperature of decomposition to zinc oxide. It was hoped that an understanding of the mechanism would lead to a more successful precursor. Pin-pointing the onset temperature of decomposition would also allow improvement of the spray equipment, i.e. for efficient film manufacture at the lowest possible temperature.

Given heightened environmental concerns in recent years and the desire to increase the safety of the spraying process, it was considered desirable to investigate the possibility of producing semi-conducting zinc oxide films at low temperatures using solutions free from organic solvent. Thus it was hoped that an initial study would enable the identification of optimum conditions.

References

1. W. Jander and W. Stamm, *Z. Anorg. Allg. Chem.* 1931, **199**, 165
2. Current topics in Materials Science, volume 7, sub-chapter 3.0, 149, edited by E. Kaldis.
3. M.N. Islam, M.O. Hakim and H. Rahman, *J. Mater. Sci.*, 1987, **22**, 1379.
4. S. Oktik, post-doctoral report, 1988.

Chapter Two

Experimental Techniques

2.1 General Experimental Techniques

Glassware

All glassware was cleaned using a hot aqueous solution of alkaline detergent followed by rinsing with acetone. Glassware used in experiments where water was to be excluded was oven-dried at approximately 130°C for a minimum of 30 minutes.

Bench Manipulations

Manipulations of moisture-sensitive compounds, hygroscopic materials and solvent distillations were carried out *in vacuo* or under an atmosphere of 'white spot' cylinder nitrogen which was dried by passing through a P_4O_{10} tower.

The Dry Box

Where necessary, a dry box was used for the manipulation of moisture sensitive materials. A pressure regulated Vacuum Atmospheres glove box (type HE43-2) fitted with an HE-493 Dri-Train was used for this purpose.

Infra-Red Spectra

These were recorded as Nujol mulls between CsI plates on a Perkin-Elmer 477 or 577 grating spectrophotometer.

Mass Spectra

These were recorded using a VG Analytical 7070E spectrometer using either electron impact or chemical ionisation techniques.

Elemental Analyses

C,H and N analyses were carried out on a Carlo-Erba 1106 Elemental Analyser by Mrs. M. Cocks (Chemistry Department, University of Durham).

Aluminium, gallium, indium and zinc were determined by decomposition of a solid sample in acid and concentration measured by atomic absorption

spectrophotometry using a Perkin Elmer 5000 atomic absorption spectrophotometer by Mrs. J. Dostal and Mr. R. Coult (both Chemistry Department , University of Durham).

Nuclear Magnetic Resonance

^{1}H and ^{13}C solution n.m.r. spectra were recorded using a Brüker AMX 500 MHz, Varian Gemini 400 or 200MHz n.m.r. spectrometers. Solid state ^{13}C n.m.r. spectra were recorded on a Varian VCR 300MHz n.m.r. spectrometer.

Temperature Regulation

Elevated temperatures were achieved and maintained by the use of an oil or water bath. Temperatures between 0°C and 20°C were obtained using an ice/water bath. For temperatures below this, a solid CO_2/acetone bath was used.

X-Ray Powder Photographs

X-Ray powder photographs were obtained from either silicone oil mulls, using a Guinier de Wolff camera No. II (Enraf-Nonius, Delft), or the pure powder using a 14mm Debye-Scherrer camera. Both used Cu-Kα filtered radiation (λ = 1.5418Å, generated at 42kV and 16mA) and Agfa-Gevaert Osray X-ray film.

Crystal Growth

Single crystals were grown by placing the sample in the bottom of a vertical pyrex tube (15mm o.d.). The tube had two constrictions (diameter 3mm) approximately 50mm and 100mm from the bottom of the tube. Fine glass wool was placed over the sample. A vacuum of approximately $10^{-7}\tau$ was produced using a high-vacuum line designed by Dr. Z.V. Hauptman (University of Durham) incorporating an Edwards No.5 two-stage rotary oil pump and an Edwards vapour pump (model EO2) using Santovac fluid (Edwards). An oscillating temperature control was provided by a cylindrical coiled wire furnace (built by Dr. Z.V. Hauptman) connected to a Eurotherm 818 temperature controller.

Crystal Structure Determination

Preliminary studies were carried out by mounting crystals in glass or quartz Lindemann tubes and taking oscillation photographs using a Nonius integrating Weissenburg goniometer with a Philips X-ray generator (type PW1009 130) fitted with an X-ray tube (Cu anode, Ni filter) operating at 42kV and 16mA.

A full X-ray structure determination was carried out by Dr. W. Clegg (Univeristy of Newcastle upon Tyne) on a Siemens AED2 diffractometer with a graphite monochromator using Mo-Kα radiation (λ = 0.71073Å). An ω-θ scan mode was used for data collection with appropriately chosen scan width and time. Programs (SHELXTL and local software) were run on a Data General Model 30 computer.

2.2 More Specialised Techniques

"The Dog".

This is a two-limbed reaction vessel where each limb is surmounted by a J.Young tap and the two limbs are separated by a medium porosity (grade 3) glass sinter.
See Diagram 2.2.1

The Closed Extractor.

This is based on the soxhlet extraction system where the solvent is heated in the lower bulb and condensed by means of a water-jacket above the medium porosity (grade 3) glass sinter.
See Diagram 2.2.2

Diagram 2.2.1

"The Dog"

1. Reaction Bulb.
2. Glass sinter (usually porosity grade 3).
3. J. Young teflon tap.
4. $^1/_4$" ground glass connector.

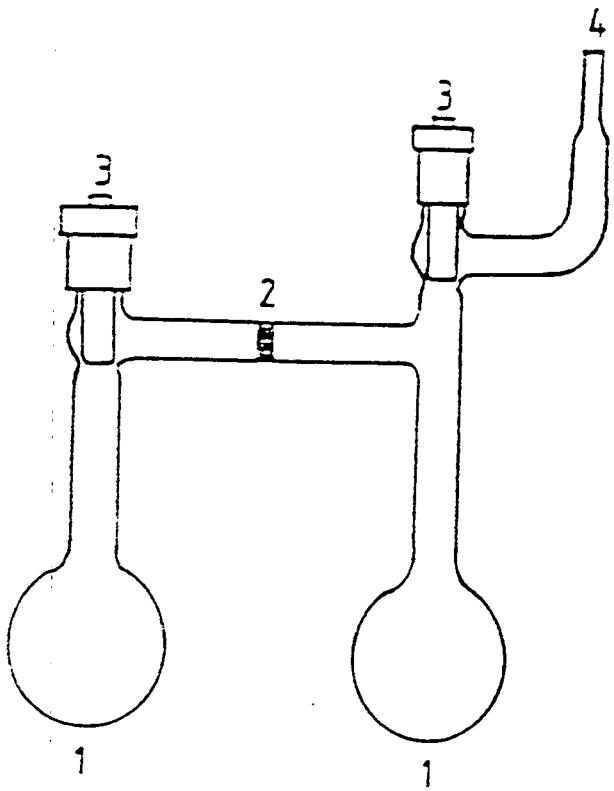

Diagram 2.2.2

The Closed Extractor.

1. J. Young teflon tap.
2. $^1/_4$" ground glass connector.
3. Glass sinter (usually porosity grade 3).
4. Cooling jacket.

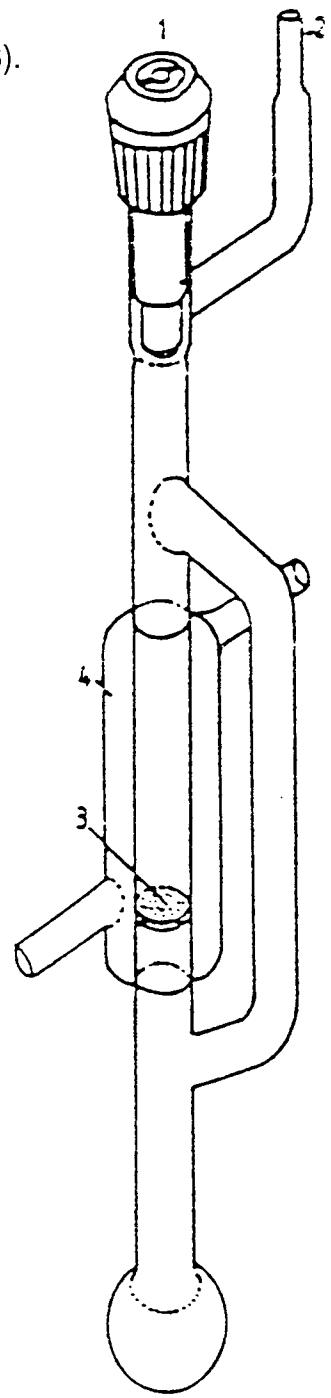

Differential Scanning Calorimetry

Differential scanning calorimetry was conducted using a Mettler FP85 thermal analysis cell coupled to a Mettler FP80 processing unit. Samples were sealed in aluminium capsules by cold welding. The lid of each capsule was pierced with a needle to produce a consistently sized hole which prevented pressure build up inside the capsule. Heating was carried out under a flow of argon (100±10ml/min). Data were recorded using either a Fisons y-t chart recorder (or later) on an Opus PCIII microcomputer (software written by Dr. J.M. Rawson, Chemistry Department, University of Durham) coupled to an Epson LQ-850+ dot-matrix printer.

Other Thermolysis Studies

The six experiments A-F descibed in Chapter 5 were designed as a scaled up simulation of the d.s.c. experiments discussed in Chapter 4. A pyrex crucible was used instead of an aluminium one, and white-spot nitrogen was used instead of argon as the flow gas (rate 400ml/min). The cylindrical coiled-wire furnace (built by Dr. Z.V. Hauptman) was connected to a Eurotherm 818 temperature controller.

2.3 Spray Pyrolysis Experiments

The Spray Kit

The spray kit was housed in a cabinet consisting of two compartments. The lower compartment contained the temperature controller, bottled spray solutions pneumatically-powered feed pump and extractor fans. The upper chamber, fitted with transparent plastic doors, contained the substrate support, heating elements, thermocouple and spray gun. The upper compartment was connected to the extraction flue via carbon filters.

The ceramic substrate support (approximately 18"x18") was heated by means of seven quartz halogen heating lamps, five directly underneath, with a further two lamps (each housed in an aluminium shade) either side and 12" above the plane of the substrate support. The lamps were all connected to the same Eurotherm 815

temperature controller.

The solutions were pumped to the spray gun using a Wagner 9-40 pneumatically powered feed pump operating on 'in-house' compressed air (2 bar). The spray gun was a Wagner Automatic Air-Coat Gun A 100 AC with a sintered tungsten carbide tip and was situated 18" above the centre of the substrate. Its gas shroud was white spot nitrogen (1 bar).

2.4 Specialised Techniques for Analysis of ZnO films

Thickness Measurements

Film thicknesses were measured using an α-step machine (model 200, Tencor Instruments) which used a mechanical stylus profileometer. The samples were step-edged using hydrochloric acid.

Optical Transmittance Measurements

Optical transmittance measurements were carried out in the range 300-1000nm using a Pye Unicam SP6-350 spectrophotometer.

X-Ray Analysis

Wide angle ($5° \leq \theta \leq 180°$) X-ray scattering was carried out on a Siemens D5000 diffractometer using Kβ filtered CuKα radiation (λ = 1.54Å).

Chapter 3:

Synthesis of possible precursors to semiconducting zinc oxide films

3.1. Mono aquo bis (2,4- pentanedionato) zinc - $Zn(acac)_2.H_2O$

3.1.1 Synthesis and identification

The literature is well documented with preparations of $Zn(acac)_2.H_2O$. This was a modified version of the synthesis of Rudolph and Henry[1]. Instead of adding $ZnSO_4.7H_2O_{(aq)}$ to a solution of $NaOH_{(aq)}$ and acetylacetone, the following procedure was used to minimise the effect of any side reactions between the β - diketone and the base.

Acetylacetone (50g, 0.5mol) was stirred in water (200ml). To this was added a solution of zinc sulphate heptahydrate (72g, 0.25mol) in water (250ml). On addition of 0.88 ammonia solution (30 ml) a white solid was precipitated which was filtered, washed successively with water (50ml) and 40-60° petroleum ether (50ml), and dried *in vacuo* (0.01 torr, room temp.) for eight hours. The crude product (61.5g, 87.4%) was dissolved in hot (50°C) ethyl acetate (500ml) to which acetylacetone (25ml) had been added. After filtering through a hot (50°C) glass sinter the resulting solution was allowed to cool and the solvent slowly evaporated in a fume cupboard. Subsequent drying *in vacuo* (0.01 torr, room temp.) yielded a white, crystalline product (57.65g, 81.9%).

Carbon and hydrogen analyses were as follows: found C 42.71%, H 5.66%, required C 42.65%, H 5.73%. The infra-red and mass spectra confirmed that the compound was $Zn(acac)_2.H_2O$ and these methods of analysing the monohydrate are discussed in greater detail in later sections of this thesis.

3.1.2. Impurities in the synthesis of $Zn(acac)_2.H_2O$

In all the preparations of $Zn(acac)_2.H_2O$ a brown impurity was present as a greasy coating on the $Zn(acac)_2.H_2O$ crystals, particularly at the evaporation

points. Chromatographic studies concluded that the amount of impurity was very small relative to the product (estimated at not greater than 0.1%).

As there was a possibility that the impurity may have been related to the thermal decomposition of the monohydrate (recrystallisation involved heating to 50°C in solution) its identification was attempted. The investigation was based on several peaks in the mass spectrum of the product that did not fit the breakdown pattern and could have been due to the impurity. It was assumed that these peaks were due to genuine fragments and not to gaseous ion-neutral combinations because they occurred in relatively early spectra which was not the case for known products of gaseous ion-neutral reactions. There were four of these peaks which consistently appeared in the mass spectrum at m/e 155, 239, 254 and 417. Three methods were employed to attempt the identification of the fragments corresponding to the peaks.

Firstly, the distribution and size of neighbouring peaks were used to assess how many zinc atoms each fragment contained. This was possible because zinc's isotopic distribution means that fragments containing the metal give rise to a distinctive pattern of peaks in the mass spectra of its compounds. Using this information it was observed that the peak at m/e 417 contained one zinc atom and the other three contained none.

The second method used was an accurate mass study on the four peaks (plus two known peaks to assess the accuracy of the method). It was assumed that the fragments contained only C, H, O and Zn, and the values obtained are listed in table 3.1.

Table 3.1 Data from accurate mass study of $Zn(acac)_2.H_2O$

Peak(m/e)	Observed Exact Mass (amu)	Standard Deviation	Empirical Formula	Possible Structural Formula
155	154.99112	4.78	$C_8H_{11}O_3$	$(C_5H_7O_2)CH_3COCH$
239	238.99995	1.56	$C_{12}H_{15}O_5$	$(C_5H_7O_2)_2COCH$
254	254.01785	10.37	$C_{13}H_{18}O_5$	$(C_5H_7O_2)_2CH_3COCH$
417	416.97597	0.01	$C_{18}H_{25}O_7Zn$	$(C_5H_7O_2)_3CH_3COCHZn$
262	262.00110	6.15	$C_{10}H_{14}O_4Zn$	$(C_5H_7O_2)_2Zn$
425	424.96768	8.90	$C_{15}H_{21}O_6Zn_2$	$(C_5H_7O_2)_3Zn_2$

One of the most significant points regarding the empirical formulae was their close relationship with zinc acetylacetonate and, necessarily, each other. As would be expected the difference between the two peaks m/e 239 and m/e 254 was a methyl group. All the peaks had an empirical formula which could be expressed in terms of acetylacetonate ($C_5H_7O_2$), or fragments of it, and zinc.

In an attempt to strengthen the relationship between these peaks a parent - daughter study was performed for the peaks m/e 239 and 254. In this, breakdown fragments of specific peaks are identified. For the peak at m/e 254 fragments with m/e values of 239 and 155 were identified as 'daughters' (i.e. breakdown fragments) of $C_{13}H_{18}O_5$. However, the fragment with a m/e value of 155 was not identified as a 'daughter' of the peak at m/e 239.

Given the close relationship between the four fragments responsible for peaks m/e 155, 239, 254 and 417, and the empirical formulae indicated it seemed logical to deduce that the peaks were due to a polymerised form of

acetylacetone and its zinc salt.

According to the literature[2], acetylacetone undergoes an aldol condensation when exposed to light. It was with this in mind that the following reaction schemes were proposed.

Figure 3.1 Aldol condensation of acetylacetone

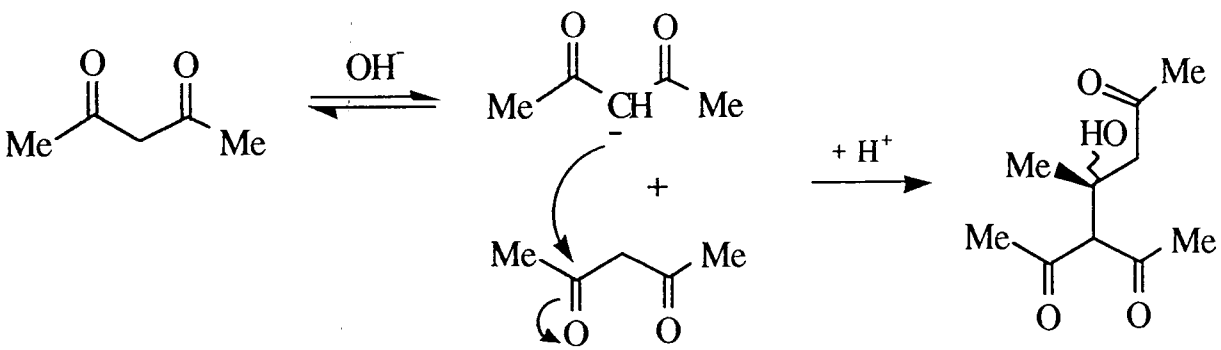

The use of freshly distilled acetylacetone in the preparation of $Zn(acac)_2.H_2O$ appeared not to reduce the amount of brown material in the product. This indicated that the acetylacetone oligomers were probably formed by the action of ammonia on the acetylacetone. It was for this reason that the base was added after rather than before mixing the acetylacetone and zinc sulphate, thereby minimizing the time for the formation of the impurity.

It was very likely that a polymer formed from acetylacetone would be a greasy brown substance. (Acetylacetone is observed to "yellow" on standing in light.) The brown material found on the crystals of $Zn(acac)_2.H_2O$ was likely to contain compounds with molecular weights in excess of 500 but these were probably too involatile to be detected in the mass spectrometer.

3.1.3 The reaction between alcoholic solutions of $Zn(acac)_2.H_2O$ and water

3.1.3.1 Introduction

In a paper[3] published in 1984, Kiichiro Kamata claimed that water reacts with a methanolic solution of $Zn(acac)_2$ to produce zinc oxide at room temperature. However, the samples were 'dried in a vacuum oven at 50°C, and it was this author's suspicion (that this process formed the ZnO) that led to a series of similar experiments using $Zn(acac)_2.H_2O$ with methanol and iso-propanol as solvents. It was also hoped that the experiments would give an indication as to the importance of water in the spray solutions of Mr. A.J.C. Fiddes, which were based on IPA.

3.1.3.2 Experimental

a) IPA as the solvent

$Zn(acac)_2.H_2O$ (5.62g, 20mmol) was dissolved in IPA (200ml) to give a 0.1 M solution. A thin stream of water (200mls) was added to this with vigorous stirring. The solution turned cloudy almost instantly and over a period of half an hour a gelatinous, white precipitate was formed. The mixture was left to stand for a further half an hour and then the solid material was filtered off using a Teflon membrane. All the samples were dried *in vacuo* (0.001 torr), one at room temperature, another at 50±5°C, and the final one at 100±5°C. The three dried samples (total weight 1.44g) were analysed for Zn, C and H and Debye-Scherrer X-ray photographs were obtained.

b) Methanol as the solvent

The procedure followed in this experiment was exactly the same as described previously, except that methanol was used instead of IPA. The observations were also identical, save that less dried product was obtained (1.06g). Analyses of Zn, C and H were carried out and the Debye-Scherrer X-ray photographs of the three samples were also recorded.

3.1.3.3 Results and discussion

In all cases the products were assumed to be mixtures of $Zn(acac)_2.H_2O$, $Zn(OH)_2$ and ZnO. The reduced amount of product obtained in the methanol experiment could be explained by $Zn(acac)_2.H_2O$'s greater solubility in that solvent than in IPA. The elemental analyses were used to gauge a rough idea of the composition of the mixtures and the Debye-Scherrer photographs identified the majority products of the compositions. The percentage of carbon in the sample was divided by 42.65%, the percentage of C in $Zn(acac)_2.H_2O$, to give the fraction of the sample which was $Zn(acac)_2.H_2O$. This figure was used to calculate the fraction of the hydrogen analysis that was due to $Zn(acac)_2.H_2O$. The difference was assumed to be due to $Zn(OH)_2$. Dividing the value for this difference by 2.03% (percentage of H in $Zn(OH)_2$) gave an approximate value for the fraction of $Zn(OH)_2$ in the sample. The remaining part of the sample was assumed to be zinc oxide.

The following rough percentages were calculated using this method:

IPA as solvent

	Drying Temperature		
	25°C	50°C	100°C
$Zn(acac)_2.H_2O$	60-65%	60-65%	10-25%
$Zn(OH)_2$	30-40%	30-40%	0-5%
ZnO	0-10%	0-10%	70-80%

MeOH as solvent

	Drying Temperature		
	25°C	50°C	100°C
$Zn(acac)_2.H_2O$	60-65%	60-65%	25-30%
$Zn(OH)_2$	25-35%	25-35%	10-15%
ZnO	0-10%	0-10%	55-65%

These results illustrated two important facts: firstly, that within the limits of experimental error there were virtually no differences between the IPA and methanol results and, secondly, somewhere between 50°C and 100°C the drying process alters the composition of the mixture. This second point was confirmed by the observation of $Zn(acac)_2.H_2O$ subliming out of the product mixture during drying at 100°C. The figures indicated that approximately two-thirds of the fresh precipitate was $Zn(acac)_2.H_2O$. However, this re-precipitated monohydrate represented only approximately 20-25% of the total $Zn(acac)_2.H_2O$ involved in the reaction - the rest remained in solution. The figures also indicated that less than ten percent of the monohydrate reacted with water to form $Zn(OH)_2$. There were probably two main factors that limited the reaction to that level. $Zn(acac)_2.H_2O$, being highly insoluble in water, was bound to be precipitated when water was added to its alcoholic solution. Solid $Zn(acac)_2.H_2O$ would react much more slowly with water than when in solution. Therefore, it was, in a sense, 'protected' by being precipitated out of solution. The second factor involved the strong absorbent properties of $Zn(OH)_2$. These ensured that some degree of co-precipitation was inevitable with a consequential hydrolysis rate.

The samples which were dried at 25°C and 50°C showed no evidence of ZnO in their X-ray powder photographs; this was not the case for the sample dried at 100°C. Unfortunately, the amorphous nature of $Zn(OH)_2$ meant that it was not possible to positively identify it in the X-ray photographs of any of the samples.

$Zn(OH)_2$ is known to decompose to ZnO at 125°C (760torr)[4] and this dehydration would take place at lower temperatures under reduced pressure i.e. below 100°C at 0.01 torr. Under these same conditions $Zn(acac)_2.H_2O$ is known to sublime[5] and the nature of the sublimate from the 100°C sample was confirmed by its infra-red spectrum[6].

It would seem, therefore, that Kamata misinterpreted his results, and this author concludes that it is not possible to produce ZnO from the reaction between $Zn(acac)_2.H_2O$ and water at room temperature unless the product is 'dried' under reduced pressure (0.01 torr) and at an elevated temperature (between 50°C and 100°C).

3.2 $Zn(acac)_2$ and $Zn_2(acac)_3(OAc)$

3.2.1 Synthesis of $Zn(acac)_2$ for d.s.c.

When a sample of anhydrous $Zn(acac)_2$ was required for d.s.c., it was decided to use the method outlined in the literature[1]. However, this author found that it was extremely difficult to eliminate $Zn(acac)_2.H_2O$ from the finished product so a slight modification to the original preparation was made. This entailed using a 'dog' (see Section 2.2) to provide a totally closed system.

A solution of 1.5g of $Zn(acac)_2.H_2O$ in 10ml of methanol was filtered into one leg of a 'dog'. This was cooled to -50°C using an acetone/dry-ice bath. The resulting precipitate was filtered off and dried *in vacuo* (room temperature, 0.01 torr) to yield 0.98g (70%) of white material. Carbon (found 45.07%, calc. 45.57%) and hydrogen (found 5.45%, calc. 5.35%) elemental analyses indicated $Zn(acac)_2$ and the infra-red spectrum confirmed no moisture was present. It was expected, given the meta-stable nature of the product[7] , that trimerisation would occur over a period of time.

The d.s.c. study of this product is recorded in Chapter 4.

3.2.2 $Zn_2(acac)_3(OAc)$

3.2.2.1 Introduction

Whilst studying the thermal decomposition of $Zn(acac)_2.H_2O$, Rudolph and Henry[8] discovered a compound with the empirical formula $Zn_2(acac)_3(OAc)$. The compound appeared to be an intermediate to the formation of zinc acetate. However, the authors were unable to determine its molecular weight and its structure remained open, although the authors favoured a six-coordinate tris(acetylacetonato) zincate anion giving the formula $Zn[CH_3CO_2][Zn(acac)_3]$.

The same paper also noted that the same compound was formed when $Zn(OAc)_2.2H_2O$ was heated in acetylacetone. In a subsequent paper[9], further molecular weight determinations appeared to confirm the molecular formula as $Zn_2(acac)_3(OAc)$ and the authors cited the compound's poor solubility in organic solvents as evidence of a salt-like structure. The low stability of the $[Zn(acac)_3]$ anion in ionising solvents was also noted[10].

3.2.2.2 Synthesis and analysis

$Zn_2(acac)_3OAc$ was synthesised according to the second method of Rudolph and Henry[8]. 50ml of acetylacetone were heated to 90°C. To this was added, with stirring, 21.9g (0.1mol) of $Zn(OAc)_2.2H_2O$. The acetate did not appear to dissolve, rather, a milky suspension was formed. This was filtered hot, leaving a white compound which was dried in a desiccator. On cooling of the filtered acetylacetone solution, further precipitation took place, but this compound was identified by infra-red as $Zn(OAc)_2.2H_2O$, indicating that despite the excess of acetylacetone, not all the $Zn(OAc)_2.2H_2O$ had reacted. It was also noted that when the experiment was repeated without stirring $Zn(OAc)_2.2H_2O$ was simply precipitated on cooling, thereby illustrating the need for thorough mixing of reactants.

After drying, 9.7g (19.9% yield) of white material were obtained. Elemental analyses (C: found 41.73%, calc 41.92%,; H: found 4.86%, calc. 4.97%; Zn: found 27.10%, calc. 26.84%) confirmed the formula $Zn_2(acac)_3(OAc)$. Infra-red studies showed that the compound did not pick up moisture even after 24h exposure to the atmosphere. This author was unable to recover the compound from any solvent without decomposition having occurred - the resulting products being zinc acetate and zinc acetylacetonate.

Studying the thermal stability of the compound by differential scanning calorimetry (see Figure 3.2) showed that the compound was stable up to

195°C. At this temperature a sharp endotherm was noted, which observations confirmed to be melting. After this, the d.s.c. trace indicated many processes, both endo- and exothermic, taking place, and the tarry residue observed at the end of heating (400°C) was testimony to significant decomposition.

Figure 3.2 D.s.c. of $Zn_2(acac)_3(OAc)$ (4°C/min)

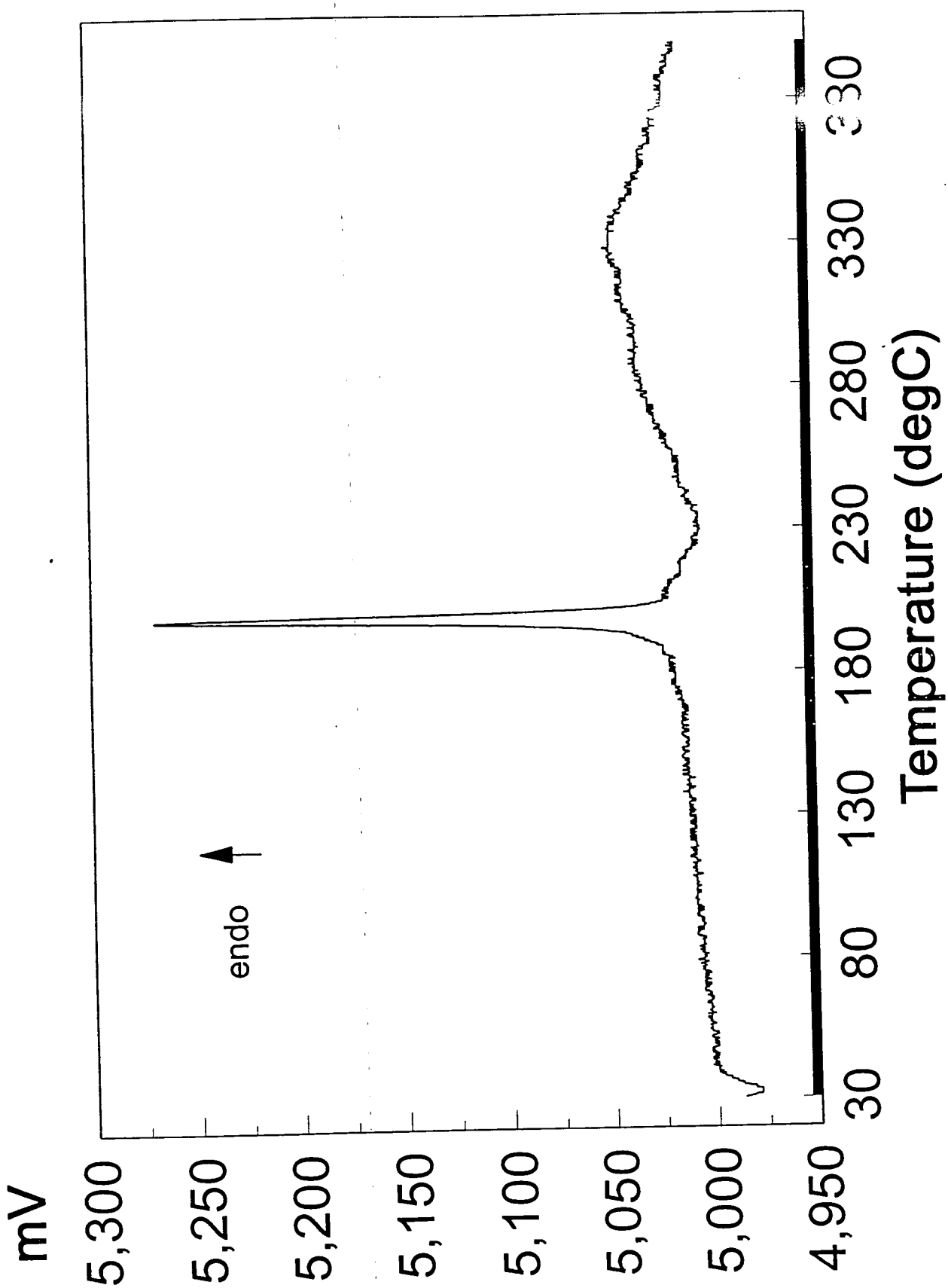

3.2.3 Crystal Structure of $Zn(acac)_2$

3.2.3.1 Introduction

This author made several attempts to produce single crystals of $Zn_2(acac)_3(OAc)$ for the purpose of crystal structure determination. Earlier attempts using solvents proved entirely unsuccessful due to the compound's instability in solvents. Subsequent attempts focused on sublimation under very high vacuum. One such attempt (see below for details) yielded a few colourless crystals. However, X-ray structure analysis identified these as $Zn(acac)_2$ monomer - a known compound for which the crystal structure had not previously been identified. This was not entirely unexpected as a break down such as:

$$2\ Zn_2(acac)_3(OAc) \text{ ------> } 3\ Zn(acac)_2 + Zn(OAc)_2$$

does not seem unlikely under elevated temperatures and high vacuum.

3.2.3.2 Preparation of Crystals of $Zn(acac)_2$

0.5g of $Zn_2(acac)_3(OAc)$ were placed in a Pyrex crucible and covered with glass wool. The crucible was placed at the bottom of a pyrex tube (internal diameter 12mm). Two constrictions (internal diameter 3mm) divided the tube into three sections - top, middle and bottom (containing the crucible). The tube was placed under a high vacuum ($2x10^{-7}$ torr) for 24h. Then, whilst still under vacuum, the middle (95°C) and bottom (105°C) sections were heated. After 24h small crystals had formed in the middle section. This section was then sealed off and placed in a cylindrical coiled-wire furnace and exposed to a heating cycle (65 to 105°C, 30 min per cycle, 90 cycles). The crystal structure was obtained from the resulting colourless crystals by Prof. W. Clegg of the University of Newcastle upon Tyne (see Chapter 2 for further details).

3.2.3.3 Description of solid state crystal structure of $Zn(acac)_2$

The solid state crystal structure of $Zn(acac)_2$ is shown in Figure 3.3 and the associated data is in shown below.

Bond lengths (Å) and angles (°)

Zn(1)-O(11)	1.930(4)	Zn(1)-O(12)	1.930(4)
O(11)-C(11)	1.261(7)	O(12)-C(12)	1.322(6)
C(11)-C(13)	1.405(7)	C(11)-C(14)	1.551(10)
C(12)-C(13)	1.381(7)	C(12)-C(15)	1.431(9)
Zn(2)-O(21)	1.935(4)	Zn(2)-O(22)	1.945(4)
O(21)-C(21)	1.261(8)	O(22)-C(22)	1.282(8)
C(21)-C(23)	1.373(7)	C(21)-C(24)	1.576(9)
C(22)-C(23)	1.388(7)	C(22)-C(25)	1.440(12)
O(11)-Zn(1)-O(12)	98.4(2)	O(11)-Zn(1)-O(11a)	110.2(2)
O(11)-Zn(1)-O(12a)	119.8(2)	O(12)-Zn(1)-O(12a)	111.6(2)
Zn(1)-O(11)-C(11)	121.7(3)	Zn(1)-O(12)-C(12)	120.9(3)
O(11)-C(11)-C(13)	125.9(5)	O(11)-C(11)-C(14)	113.5(5)
C(13)-C(11)-C(14)	120.4(6)	O(12)-C(12)-C(13)	124.7(4)
O(12)-C(12)-C(15)	117.0(5)	C(13)-C(12)-C(15)	118.3(5)
C(11)-C(13)-C(12)	127.9(5)	O(21)-Zn(2)-O(22)	96.0(2)
O(21)-Zn(2)-O(2lb)	115.6(2)	O(21)-Zn(2)-O(22b)	119.5(1)
O(22)-Zn(2)-O(22b)	112.1(2)	Zn(2)-O(21)-C(21)	121.6(3)
Zn(2)-O(22)-C(22)	122.7(3)	O(21)-C(21)-C(23)	128.3(5)
O(21)-C(21)-C(24)	112.2(5)	C(23)-C(21)-C(24)	119.5(6)
O(22)-C(22)-C(23)	125.4(5)	O(22)-C(22)-C(25)	117.6(6)
C(23)-C(22)-C(25)	116.9(6)	C(21)-C(23)-C(22)	125.5(6)

Figure 3.3 Solid state crystal structure of $Zn(acac)_2$

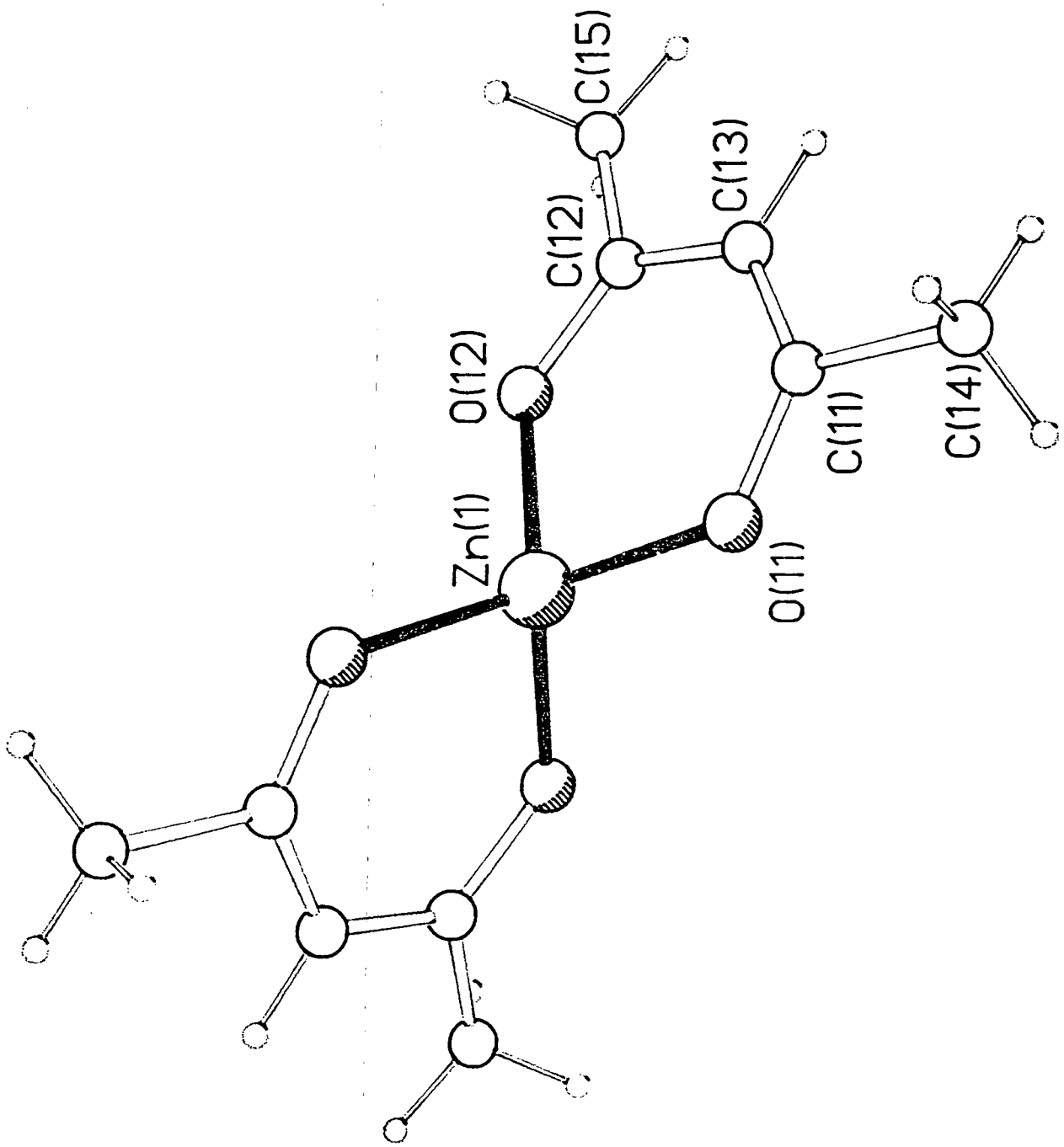

The crystal structures of $[Zn(acac)_2]_3$[5] and $Zn(acac)_2.H_2O$[12] are already known, as well as the gaseous molecular structure of $Zn(acac)_2$ [13].

The closest comparison to this crystal structure was the one for $Zn(acac)_2$ in the gas phase [13]. Also of interest were those for the monohydrate [11, 12] and the trimer [5]. This existing literature showed $Zn(acac)_2$ (g) to have the shortest Zn-O bond length [1.942(6)Å][13] compared with 2.00(3)Å for the trimer [5] and 2.02(2)Å for the monohydrate [12]. This was due to the coordination numbers of the zinc atoms involved. $Zn(acac)_2$ was four-coordinate, and the monohydrate and trimer had five-coordinate zinc atoms, (the trimer also had a six-coordinate zinc atom with Zn-O distances of approximately 2.10[5]). It was therefore unsurprising to find that the Zn-O bond length for $Zn(acac)_2$ (s) was 1.930(4)Å as this compound also has only four oxygen atoms around each zinc atom. This figure was much closer to the sum of the covalent radii, 1.91Å, rather than the sum of the ionic radii, 2.14Å[13].

The OZnO bond angles are very similar for both the gas[13] and solid phase structures: both structures are very close to a tetrahedral arrangement of oxygen atoms about the zinc atom. As the gas phase structure is completely free of packing forces it can be deduced that very little of the same forces exist in the solid state structure.

3.3 $Zn(acac)_2.H_2O$: Reactions with 2,6- and 3,5-lutidine

3.3.1 Introduction

Reactions between zinc β-diketonate complexes and N-donor bases are well documented [10,14-16]. It was, therefore, of little surprise to find that $Zn(acac)_2.H_2O$ reacted with 2,6- and 3,5- lutidine (2,6- and 3,5 -dimethylpyridine). However, what was of interest was the number of ligands per molecule of $Zn(acac)_2$. If possible, zinc prefers hexa-coordination, as is seen by the

tendency of $Zn(acac)_2$ to form the trimer, $[Zn(acac)_2]_3$, which contains one six-coordinate and two five-coordinate zinc atoms[5]. When water is the donor ligand (i.e. $Zn(acac)_2.H_2O$) a five-coordinate structure is preferred[12]. With pyridine complexes the coordination depends on the steric hindrance caused by other groups on the pyridine ring[15]. Complexes of 2,6- and 3,5- lutidine with $Zn(acac)_2$ were synthesised and their coordination numbers (for zinc) were determined by ^{1}H.n.m.r. studies.

3.3.2 Synthesis and general characterisation

The synthesis was based on that used by Graddon and Weeden[15] to produce monomethyl pyridine complexes of $Zn(acac)_2$.

28.3g (0.1 mol) of $Zn(acac)_2 H_2O$ (see 3.1 for synthesis) were dissolved in 200 ml of the appropriate lutidine by heating (80°C) and stirring, giving rise to a clear yellow tinted solution. This was placed in a refridgerator (2°C) overnight, upon which the solution yielded large, colourless crystals. The crystals were filtered off, washed with 50ml of petrol and dried *in vacuo* (25°C, 0.01 torr).

C, H and N analyses for the product of the reaction with 2,6- lutidine were : found C 54.80%, H 6.39%, N 3.63%; theory for $Zn(acac)_2$.(2,6-lutidine) C 55.07%, H 6.25%, N 3.78%. This indicated a straight exchange between the coordinated water and 2,6- lutidine. However, analyses for the product of the 3,5- lutidine reaction (C 58.08%, H 6.82%, N 4.63%) did not correspond with any exact combination of $Zn(acac)_2$ and 3,5- lutidine.

3.3.3 'H n.m.r.

The 'H n.m.r. spectrum of $Zn(acac)_2$. (2,6-lutidine) contained five peaks in the exact ratios required to reaffirm the formula and confirm the zinc atom as five-coordinate. The 'H n.m.r. spectrum for the 3,5-lutidine compound also contained five very similarly positioned peaks (see figure 3.4). However, the

ratios were different to those for the spectrum of $Zn(acac)_2$. 2,6-lutidine. The peaks were positioned at (relative ratio in parenthesis) 1.99ppm (9.2), 2.29ppm (6), 5.32ppm (1.55), 7.41ppm (1) and 8.15ppm (2), and these corresponded, respectively, to : methyl proton on acac ring (1.99ppm); methyl proton on lutidine ring (2.29ppm); C-H proton on acac ring (5.32ppm); C-4 proton on pyridine ring (7.41); and C-2 + C-6 protons on pyridine ring (8.15ppm).

Using the ratio of these five peaks it was possible to calculate that the product was a mixture of approximately 25% $Zn(acac)_2$. $(3,5\text{-lutidine})_2$ and 75% $Zn(acac)_2$. (3,5-lutidine).

Figure 3.4 'H n.m.r. of $Zn(acac)_2$.(3.5-lutidine)x adduct in $CDCl_3$

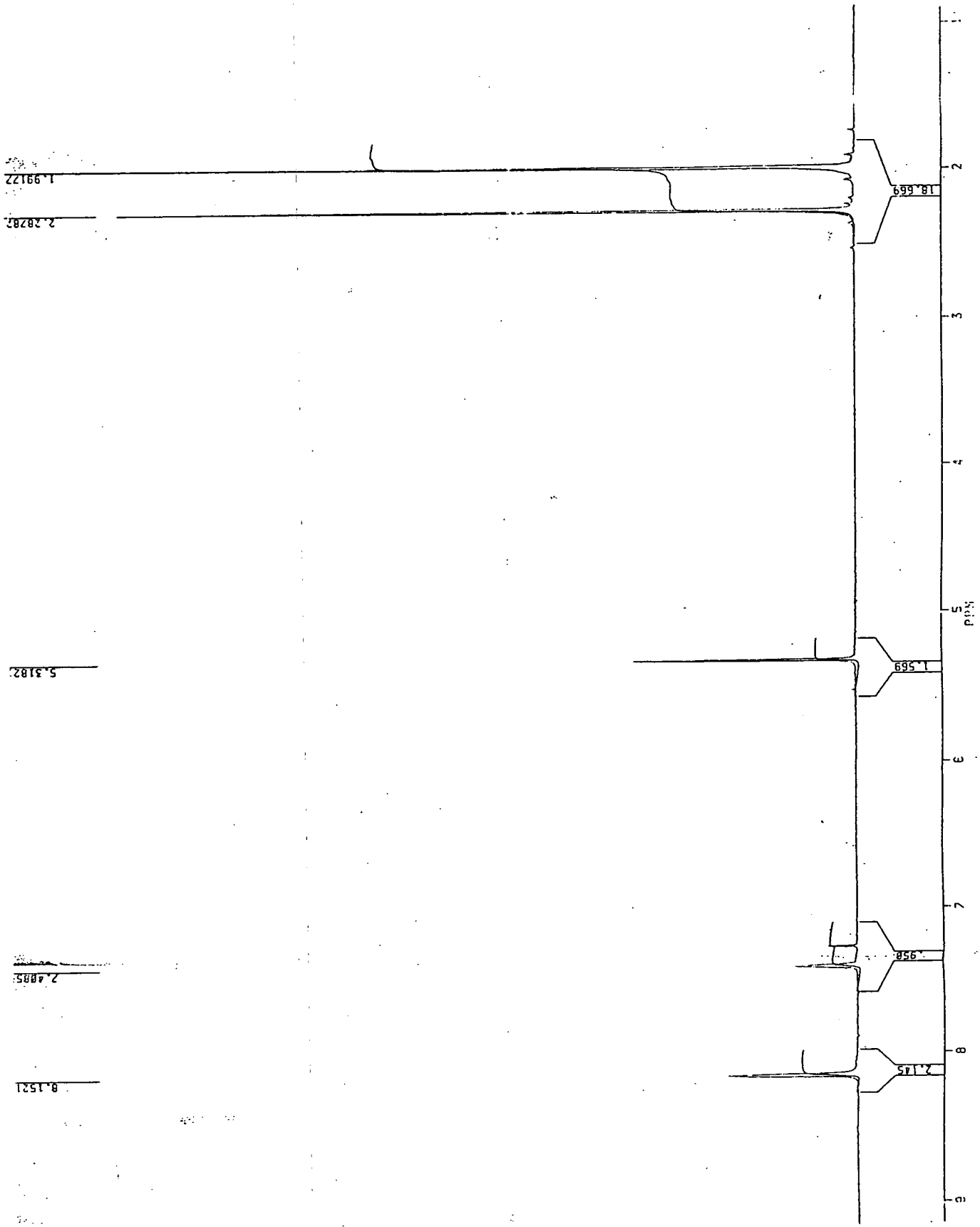

Obviously, the extra steric hindrance created by having the methyls placed on the C-2 and C-6 carbon atoms, rather than the C-3 and C-5 carbon atoms, restricts the 2,6-lutidine compound to a 1:1 complex. However, the extra "freedom" of the 3,5-lutidine does not permit a completely 1:2 complex (six-coordinate zinc), rather, an equilibrium exists between the two forms. A low temperature 'H n.m.r. study of the 3,5-lutidine complex showed no peak splitting, indicating that fast exchange of ligands was taking place between the two adducts.

3.3.4 Synthesis of $Zn(acac)_2$. (3,5-lutidine)

Synthesis of the 1:1 adduct, without contamination by the 2:1 adduct, was achieved by the following method.

14.08g of $Zn(acac)_2.H_2O$ (50mmol) were dissolved in 100ml of warmed (50°C) methanol to form a clear solution. To this was added 11.4ml (100mmol) of 3,5-lutidine (i.e. exact 1:2 ratio). The resulting clear solution was left to stand at room temperature overnight. The resulting colourless crystalline material was filtered off, washed with petrol (30ml) and dried *in vacuo* (25°C, 0.1torr, 18hrs) to give 16.50g (89%) of product. C,H and N analysis (found : C 54.79%, H 6.18%, N 3.60%; theory for 1:1 adduct : C 55.07%, H 6.25%, N 3.78%) indicated that the 1:1 adduct had been formed exclusively. This was confirmed by the peak ratio in the 'H n.m.r. spectrum (in $CDCl_3$) of the compound. It would appear that diluting the ligand concentration, by using a separate solvent, limits the complex formation to the 1:1 adduct. The 2:1 adduct is only formed in the extreme case where no independent solvent is present.

3.4 Zinc ethylacetoacetonate - $Zn(etaa)_2$

3.4.1 Synthesis and identification

Two preparations of $Zn(etaa)_2$ were found in the literature. Grummitt *et al.*[17] repeated the preparation of Backus and Wood[18] and also quoted a method of purification.

The preparation of Backus and Wood was followed, with a few modifications, as was the purification of Grummitt et. al., however, a few discrepancies were found.

$ZnCl_2$ (5.03g, 37mmol) was dissolved in methanol (25mls). To this was added a solution of NaOMe (4.00g, 74mmol) in methanol (25mls). A white precipitate was formed immediately, stirred at room temperature for fifteen minutes, and then filtered off. To the remaining solution was added a solution of ethylacetoacetate (10mls, 78mmol) in methanol (30mls). The resulting white precipitate was filtered off, washed with methanol, and dried for four hours *in vacuo* (0.001 torr, room temperature) to yield 8.9g (75%) of crude product.

Although the Backus and Wood preparation used sodium metal in methanol instead of sodium methoxide the original precipitate was still identified as sodium chloride. Despite the fact that $Zn(OMe)_2$ is known to have a polymeric structure[19] which renders it totally insoluble in methanol, both sets of authors claimed that the remaining solution contained this compound! This author's

isolation of the dissolved intermediate yielded a white material. Zinc, carbon and hydrogen analyses indicated that the product contained a much higher percentage of zinc (and lower carbon and hydrogen) than would be expected for zinc methoxide. The material exhibited no visible change on heating to 300°C and its mass spectra showed no peaks due to zinc containing fragments, indicating that the material was involatile. The infra-red spectrum of the product showed a large absorption in the region of 3500cm^{-1} indicating the presence of O-H in the compound. This information leant favour to two major possibilities. Either co-ordinated methanol, present during the formation of the methoxide, prevented polymerisation and allowed solubility, or the compound is the basic methoxide with a general formula $[Zn(OMe)_2]_x.[Zn(OH)_2]_y$ [19]. However, if the first possibility were accurate a low value for the zinc analysis would be expected, and the basic compound is unlikely to be very stable in methanol.

$Zn(etaa)_2$ was recrystallised according to the method of Grummitt *et al.* [17] Approximately half a gramme of the crude material was stirred at room temperature in 200mls of ethylacetate to which 10mls of ethylacetoacetate had been added. The cloudy solution was filtered and then cooled to 0°C, yielding fine, white needles, the purity of which was indicated by carbon and hydrogen elemental analysis.

3.4.2 Further analysis and structural studies

The d.s.c. trace of $Zn(etaa)_2$ (see fig. 3.5) between 30°C and 400°C exhibited two major endotherms: one relatively small, broad peak (onset temperature ~ 90°C), which was probably due to absorbed moisture (c.f. work on $Zn(acac)_2$ in chapter 4), and a larger, sharp peak (onset temperature 148.5°C) associated with the melting of the product (literature melting point [17] 147-150°C).

At approximately 350°C the trace indicates exothermic activity probably due

to the beginning of a decomposition process. The black, tarry residue observed after heating at 400°C implied that this was the case.

The infra-red spectrum of $Zn(etaa)_2$ showed no bands due to O-H bonds indicating that the compound was free from co-ordinated solvent. An attempt to synthesise the unknown compound $Zn(etaa)_2.H_2O$, by a method exactly analogous to the one described in 3.1.1, succeeded only in precipitating $ZnSO_4.7H_2O$. This was because the pK_a value for ethylacetoacetate (10.1)[20] was higher than that for acetylacetone (8.8)[20]. The salts of high pK_a (i.e. weak) acids are more likely to hydrolyse, which would appear to be the

Figure 3.5 D.s.c. of $Zn(etaa)_2$ (4°C/min)

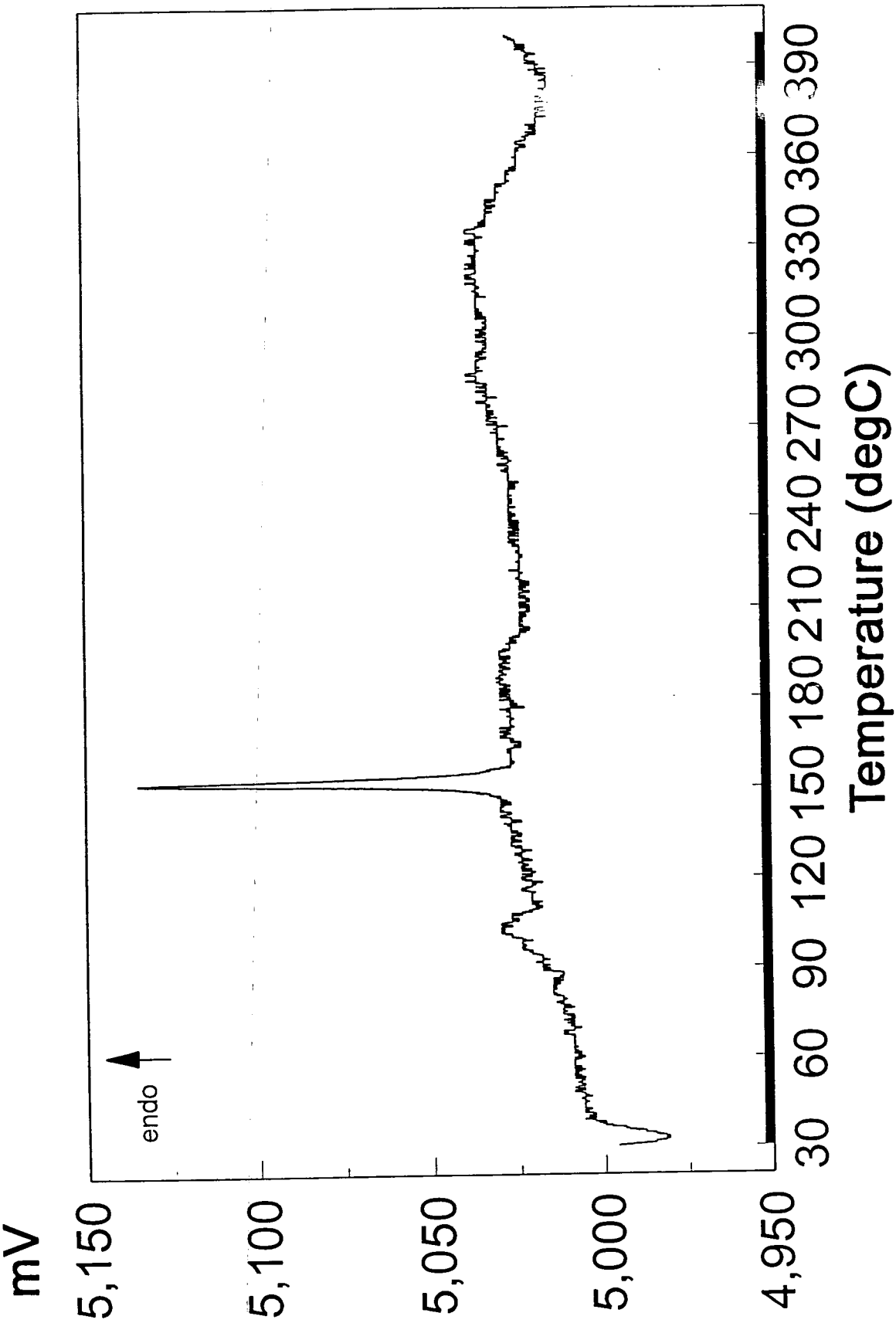

A couple of points should be noted in the mass spectrum of $Zn(etaa)_2$. Firstly, the existence of a molecular ion peak (m/e 322) helped confirm the identity of the product. Secondly, the spectrum contained peaks due to species with higher molecular weights than the supposed molecular ion e.g. $Zn_2(etaa)_3$ at m/e 515. These peaks did not prove that the compound exists as an oligomer (they could have been the product of gaseous ion-neutral reactions), they merely indicated the possibility.

Takegoshi *et al.*[7] demonstrated that solid state ^{13}C n.m.r. was capable of distinguishing between structurally different cabon atoms. It was hoped that the solid state ^{13}C n.m.r. spectrum of zinc ethylacetoacetate might provide a more definitive answer as to its structure (i.e. whether it was monomeric or oligomeric). The obtained spectrum (see Figure 3.6) exhibited six major peaks. The proposed assignments are shown below.

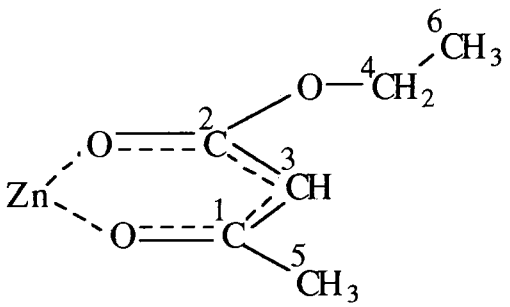

C atom	shift (ppm)
1	186.5
2	173.5
3	87.4
4	59.8
5	28.1
6	14.6

Figure 3.6 ^{13}C n.m.r. of zinc ethylacetoacetate

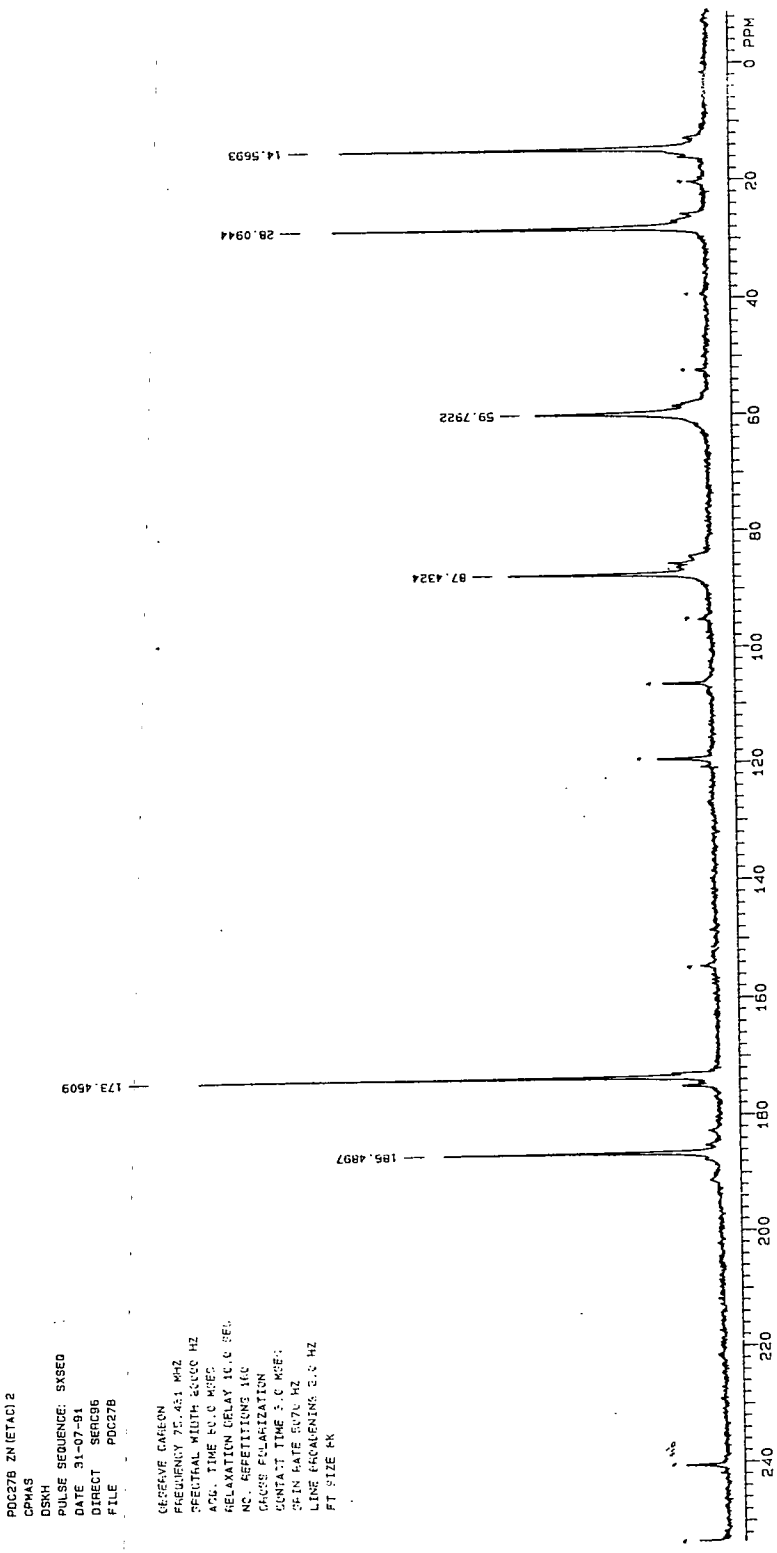

The existence of only six major peaks indicated that this was also the number of chemically and structurally inequivalent carbon atoms. This suggested that there was only one type of etaa ligand in the structure, and coupled with the good solubility, implied $Zn(etaa)_2$ was a monomer, with a regular tetrahedral arrangement of oxygen atoms around the zinc, in the solid state.

Several very small peaks, just either side of the major ones, may have indicated the presence of a compound with more than six inequivalent carbon atoms, for example an oligomer. The existence of $Zn(etaa)_2$ as a stable monomer was not a surprise as this is the case for $Zn(DPM)_2$ [21] which is also sterically more crowded than $Zn(acac)_2$ preventing the zinc atom from attaining a coordination number greater than four.

3.5 Tris (2,4- pentanedionato) aluminium (III)

3.5.1 Tris (2,4- pentanedionato) aluminium (III) - synthesis and identification

This compound (and its Ga and In equivalents) were synthesised as possible dopant precursors.

The compound was synthesised according to one of the methods in the literature [22], although this author found it unnecessary to use an elevated temperature during any part of the reaction.

Aluminium nitrate nonohydrate (18.75g, 50mmol) was dissolved, by stirring, in water (100mls). To this solution, with continuous stirring, was added, firstly, acetylacetone (15g, 150mmol) and, secondly, 0.88 ammonia solution (20mls). On addition of the ammonia an off-white precipitate was immediately formed. This was filtered off, washed with acetone, and dried *in vacuo.* (0.01 torr, room temperature) for three hours to give a pale yellow product (13.59g,

80%). Recrystallisation from cold chloroform gave an off-white compound (13.38g, 78%).

Elemental analyses (required C 55.55%, H 6.53%, found C 55.37%, H 6.43%) gave a strong indication that the product was $Al(acac)_3$ and this was confirmed by its EI mass spectrum, which showed a molecular ion peak at m/e 324.

The melting point of the material (within 2°C of the literature melting point for $Al(acac)_3$ [23]), determined by dsc (see below), also confirmed its identity.

3.5.2 Tris (2,4- pentanedionato) aluminium (III) - differential scanning calorimetry

The dsc trace of $Al(acac)_3$ (see fig. 3.7) exhibited two main features: a sharp endotherm (onset temperature 195.5°C), which observation confirmed to be the melting of the sample (literature value 192-4°C[23]), and a broad endotherm beginning immediately after the sharp peak, peaking at 289°C, and ending at approximately 294°C. Observations, backed-up by weight-loss measurements (over 95% of mass lost by 400°C), indicated that this feature was due to the evaporation of the material. The remaining residue was pale in colour, indicating, along with its small size, little decomposition.

3.6 Tris (2,4- pentanedionato) gallium (III)

3.6.1 Tris (2,4- pentanedionato) gallium (III) - synthesis and identification

This compound was synthesised using a virtually identical method to that for $Al(acac)_3$ i.e. one slightly modified from the literature [22].

Gallium (III) nitrate hexa-hydrate (5.27g, 20mmol) was dissolved by stirring, in

Figure 3.7 D.s.c. of $Al(acac)_3$ (5°C/min)

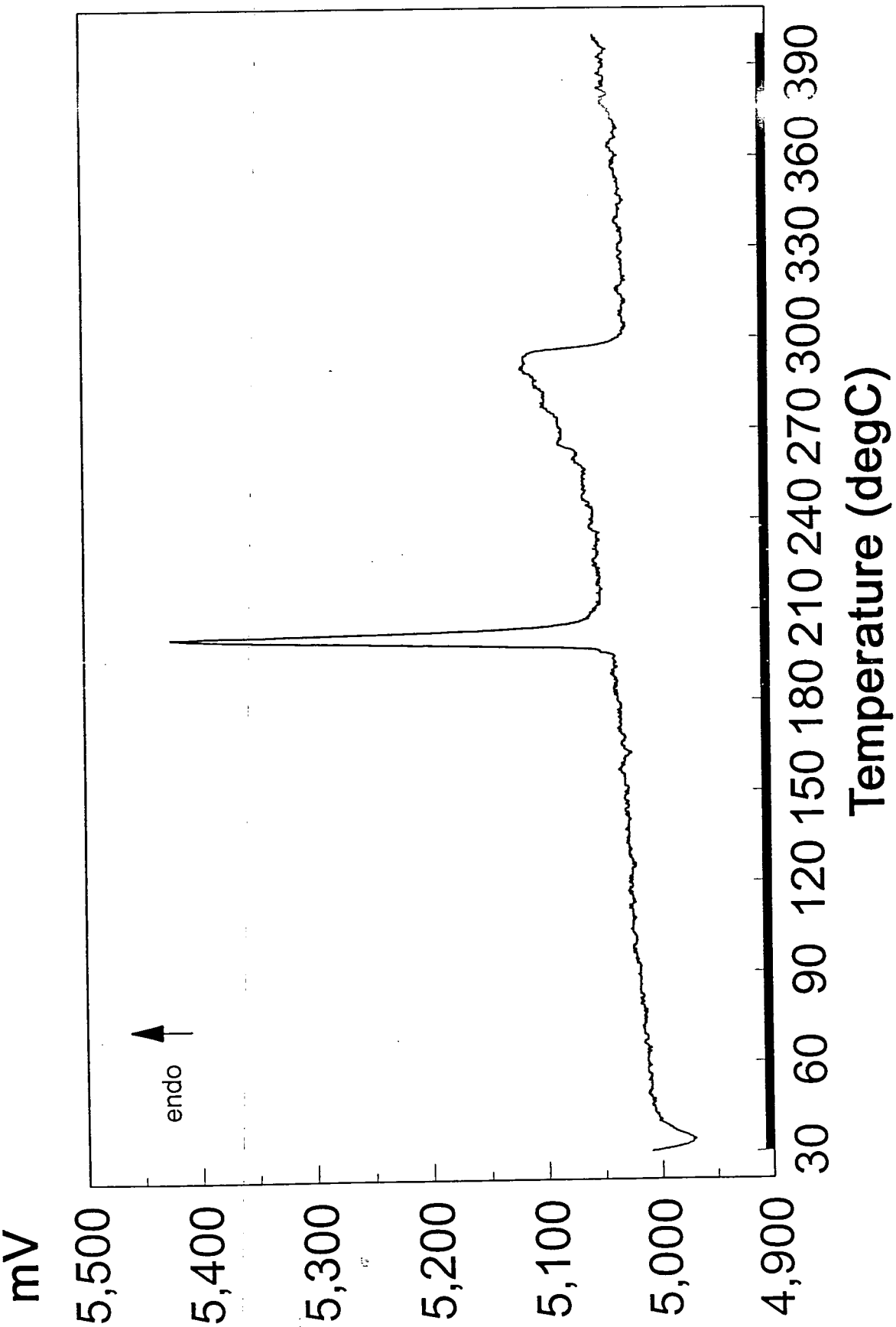

water (40ml). Stirring continued whilst, firstly, acetylacetone (6g, 60mmol) was added, and then 0.88 ammonia solution (3.5ml). The addition of the ammonia precipitated a white solid which was filtered, washed with water, and dried for two hours *in vacuo* (0.001 torr, room temperature) to give a white product (3.96g, 70%). This was dissolved in toluene (50ml, 35°C), filtered, and the solvent evaporated (room temperature) in a fume cupboard yielding a white, crystalline material (3.65g, 65%).

Elemental analyses (required C 49.09%, H 5.72%, found C 48.88%, H 5.77%) indicated that the product was $Ga(acac)_3$ and this was confirmed by its EI mass spectrum which exhibited a molecular ion peak at m/e 366. The melting point, which was within 2.5°C of the literature melting point [23] for $Ga(acac)_3$, also confirmed the nature of the sample.

3.6.2 Tris (2,4- pentanedionato) gallium (III) - differential scanning calorimetry

The dsc trace for $Ga(acac)_3$ (see fig. 3.8) was very similar to that for $Al(acac)_3$ exhibiting two major features. These were a sharp endotherm (onset temperature 197-8°C) due to the melting of the sample (literature value 194-5°C [23]), and a very broad and unsymmetrical endotherm beginning almost immediately after the sharp peak, having a maximum at 301-2°C, and ending at approximately 315°C. Observations, which confirmed that the first peak was due to melting, also indicated that the second one was due to evaporation. A weight-loss of 88% at 400°C confirmed this.

3.7 Tris (2,4- pentanedionato) indium (III)

3.7.1 Tris (2,4- pentanedionato) indium (III) - synthesis and identification

The synthesis of this compound was based on the literature method[22], the major difference being the absence of heating during the preparation. Indium

Figure 3.8 D.s.c. of $Ga(acac)_3$ (5°C/min)

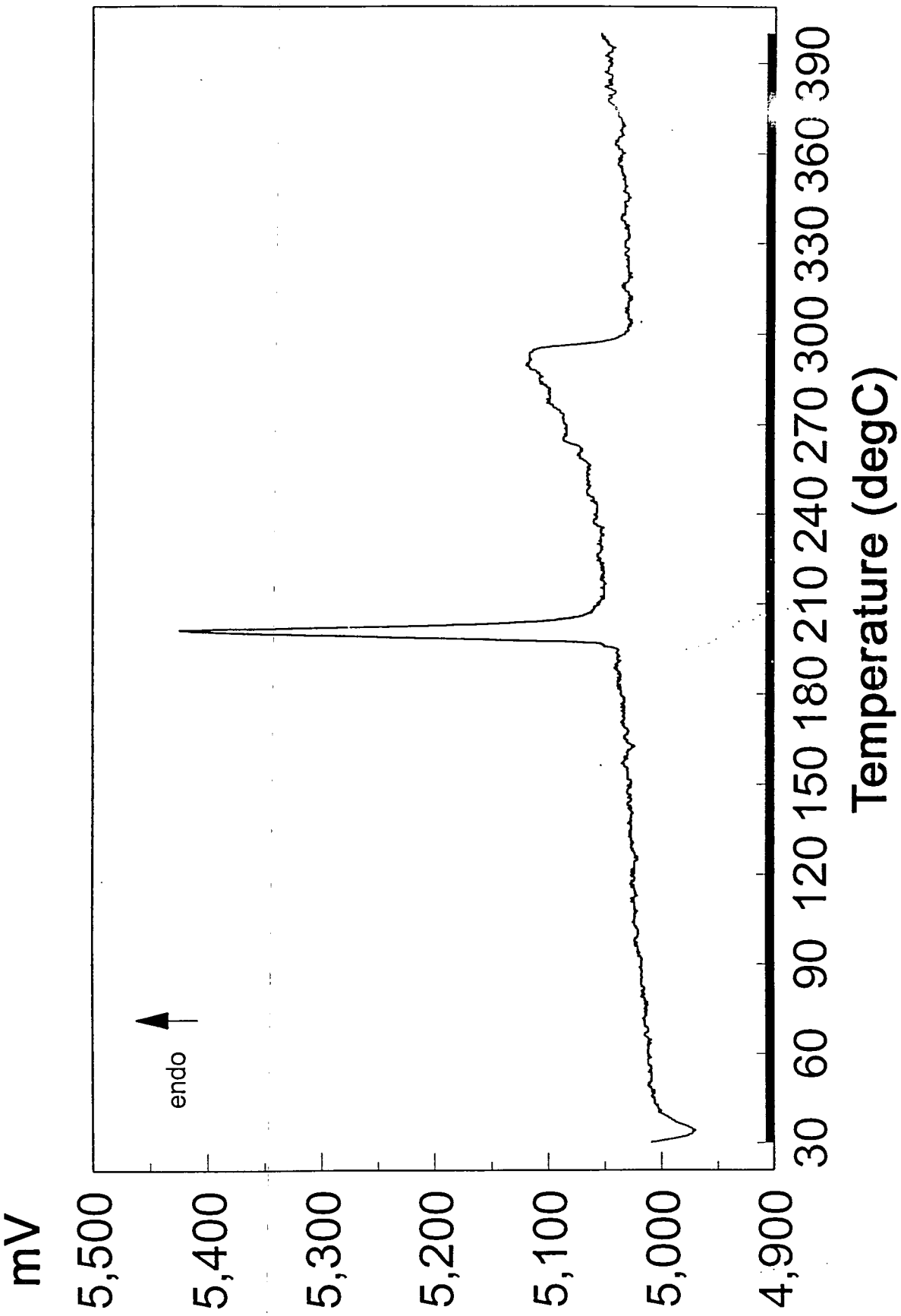

nitrate pentahydrate (9.8g, 25mmol) was dissolved in water (50ml) by stirring. To this was added, with continuous stirring, acetylacetone (7.5g, 75mmol) followed by 0.88 ammonia solution (10ml). The precipitate formed on the addition of the ammonia was left to stand for five minutes and then filtered off. It was washed, firstly, with water and, secondly with diethyl ether. Drying *in vacuo* (0.01 torr, room temperature) for three hours gave a pale yellow product (4.38g, 44%). This was dissolved in warm toluene (35°C, 40ml), filtered, cooled, and partially evaporated to give off-white crystals, which were removed by filtering and dried in air (3.71g, 38%).

Elemental analyses for the first sample (required C 43.71%, H 5.14%, found C 43.49%, 4.99%) indicated that it was $In(acac)_3$. This was confirmed by its EI mass spectrum (molecular ion peak m/e 412). This data was backed-up by the melting point, which was less than 1°C away from the literature value[23].

3.7.2 Tris (2,4- pentanedionato) indium (III) - differential scanning calorimetry

Unsurprisingly, the dsc trace of $In(acac)_3$ (see fig. 3.9) exhibited the same basic features as those of $Al(acac)_3$ and $Ga(acac)_3$. The sharp endotherm (onset temperature 187.5°C) was again verified as the melting (literature value 186-7°C [23]) of the sample by observation in a melting point tube. The unsymmetrical, broad endotherm (peak maximum approx. 296°C, end temperature 302°C), which followed immediately, was thought to be due to evaporation from the melt on the basis of observations in conventional melting point apparatus and the near 80% weight-loss by 400°C. However, upwards of 350°C the $In(acac)_3$ sample showed a significantly unsettled baseline indicating probable slow decomposition. This was not observed with $Al(acac)_3$ or $Ga(acac)_3$.

Figure 3.9 D.s.c. of $In(acac)_3$ (5°C/min)

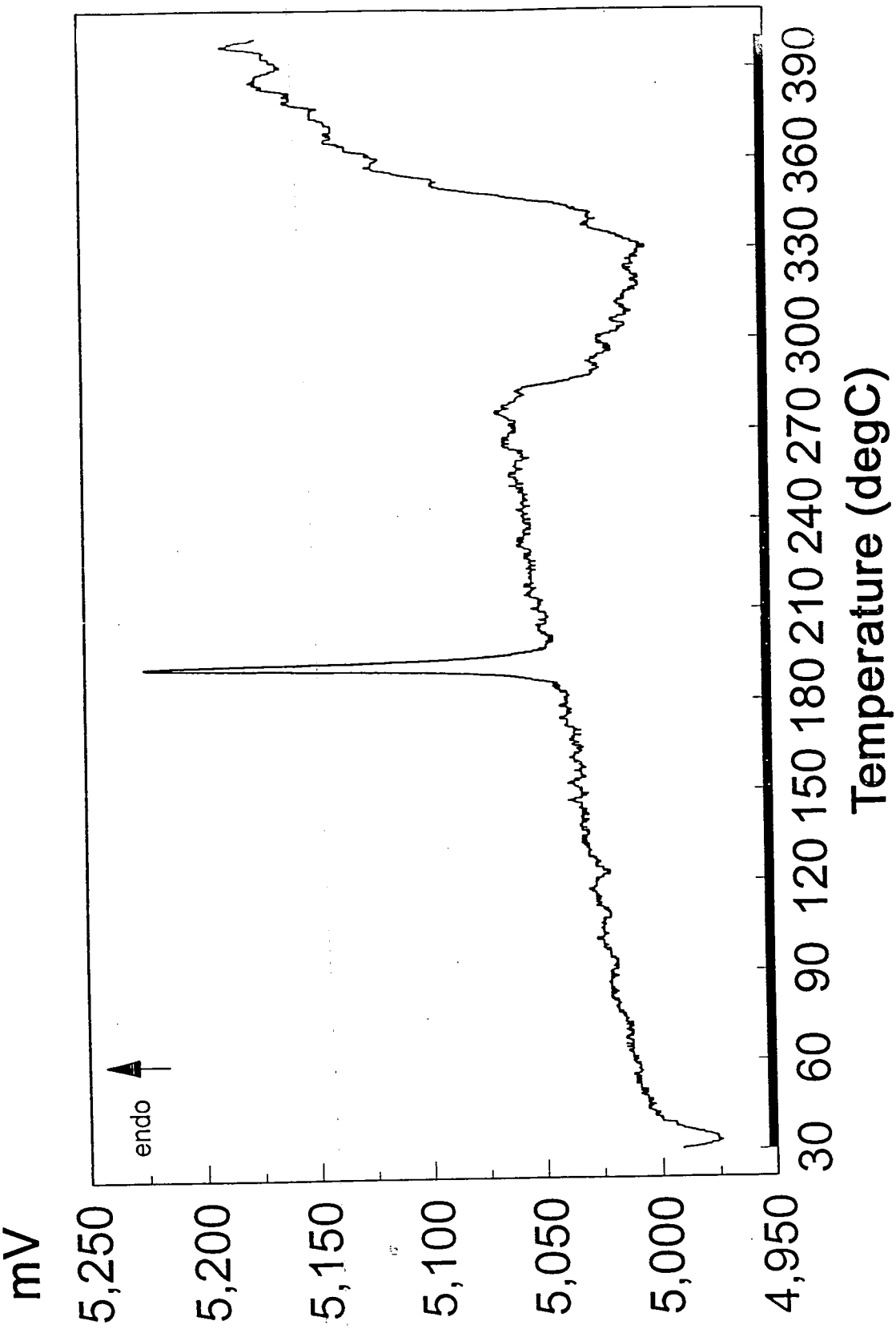

References

1 G. Rudolph and M.C. Henry, *Inorg. Synth.*, 1967, **10**, 74.

2 L.H. Finar, Organic Chemistry Vol. 1, 1957, 184.

3 K. Mamala, H. Hosono, Y. Maeda and K. Miyokawa, *Chem. Lett.*, 1984, **12**, 2021.

4 N.W. Sidgwick, Chemical elements and their compounds, 1950, 283.

5 M.J. Bennett, F.A. Cotton and R. Eiss, *Acta Cryst.*, 1968, **B24**, 904.

6 M.L. Niven and D.A. Thornton, *Spectrose. Lett.*, 1980, **13**, 419.

7 K. Takegoshi, K.J. Schenk and C.A. McDowell, *Inorg. Chem.*, 1978, **26**, 2552.

8 G. Rudolph and M.C. Henry, *Inorg. Chem.*, 1964, **3**, 1317.

9 G. Rudolph and M.C. Henry, *ibid.*, 1965, **4**, 1076.

10 F.P. Dwyer and A.M. Sargeson, *J. Proc. Roy. Soc. N.S.W.*, 1956, **90**, 29.

11 E.L. Lippert and M.R. Trutter, *J. Chem. Soc.*, 1960, 4996.

12 H. Montgomery and E.C. Lingafelter, *Acta Cryst.*, 1963, **16**, 748.

13 S. Shibata and M. Ohta, *J. Mol. Struct.*, 1981, **77**, 265.

14 M.L. Niven and D.A. Thornton, *S. Afr. J. Chem.*, 1979, **32**, 135.

15 D.P. Graddon and D.G. Weeden, *Aust. J. Chem.*, 1963, **16**, 980.

16 M.L. Niven and G.C. Percy, *Transition Met. Chem.*, 1978, **3**, 267.

17 O. Grummitt, J. Perz and J. Mehaffey, *Org. Prep. Proced. Int.*, 1972, **4**, 299.

18 J. Backus and F. Wood, U.S. Pat. 3, 453, 300.

19 R.C. Mehrotra and M. Arora, *Z. Anorg. Allg. Chem.*, 1969, **370**, 300.

20 K. Ashby, P. Willard and *J. Goel, J. Org. Chem.* 1979, **44**, 1221.

21 F.A. Cotton and *J.S. Wood, Inorg. Chem.*, 1964, **3**, 245.

22 G.T. Morgan and H.D.K. Drew., *J. Chem. Soc.*, 1921, **119**, 1058.

23 CRC Handbook of Chemistry and Physics, 60th Edition, edited by R.C. Weast.

Chapter 4

Differential Scanning Calorimetry of $Zn(acac)_2.H_2O$ and $Zn(acac)_2$

4.1 Introduction

Following the successful spray pyrolysis of $Zn(acac)_2.H_2O$ (to form ZnO) in the experiments of Mr. A.J.C. Fiddes, this author decided, for comparison, to investigate the static thermal properties of the compound and its anhydride. Mr.Fiddes' most interesting results concerned the decomposition of $Zn(acac)_2.H_2O$ to zinc oxide when the substrate temperature was only 96°C[1] [$Zn(acac)_2.H_2O$ is quoted[2] as melting with decomposition at 138°C]. Unfortunately, no cheap method was available to the author to study the spray *in situ.* so it was decided to use differential scanning calorimetry (d.s.c.) to perform a static, solid state investigation.

The literature contains little work on the thermal behaviour of zinc acetylacetonate and its hydrate. One of the first studies was carried out by Charles and Pawlikowski[3] who measured the increase in pressure resulting from the formation of volatiles when various acetylacetonates were heated in a closed system. Anhydrous zinc acetylacetonate was used and the measurements showed that the volatile material was produced when the sample was continuously heated at 191°C for fifty hours. When later readings were taken, after cooling to 27°C, they indicated that gaseous material was still present, demonstrating that decomposition, and not vaporisation of the starting material, had taken place. A subsequent paper by Von Hoene *et al.*[4] identified the gaseous products produced by a variety of β-diketonates (but not zinc) as carbon dioxide, acetone, methane and acetylacetone.

Rudolph and Henry[5,6] observed an interesting difference in the thermal behaviours of $Zn(acac)_2$ and $Zn(acac)_2.H_2O$; the monohydrate yielded a new compound of empirical formula $Zn_2(acac)_3OAc$, when it was refluxed in an inert solvent[5]. When this experiment was carried out in a sealed system, thereby preventing the escape of water, only zinc acetate was formed[5]. In comparison, only $Zn(acac)_2$ was recovered unchanged when it was used in analogous experiments[5]. Although unable to elucidate the structure of $Zn_2(acac)_3OAc$, the authors proposed that it was a salt-like structure involving the $[Zn(acac)_3]$- anion[5,6].

Four papers[7-10] discussed, albeit briefly, the differential thermal analysis (D.T.A.) of "zinc acetylacetonate". Ohrbach *et al.*[7] studied the anhydrous compound in an oxygen atmosphere, observing the major feature to be a broad exotherm due to the oxidative decomposition of the compound. Kido[8], who looked at the monohydrate, again in oxygen, measured an exotherm between 250°C and 500°C, and identified ZnO as the major product when heating was continued to 1000°C. Glavas *et al.*[9] claimed to have studied zinc acetylacetonate dihydrate but, as no firm evidence exists in the literature for the existence of a dihydrate, this author believes that the compound was a monohydrate. The experiments of Glavas *et al.* were conducted in air and the D.T.A. exhibited an endotherm (onset temperature ~ 120°C) and an exotherm (250-550°C) - probably due to melting followed by prolonged oxidative decomposition. Poston and Reisman[10] recorded the D.T.A. of purchased $Zn(acac)_2$ (2°C/min) up to 500°C in oxygen and in argon. They noted significant vapour pressure below the decomposition temperature of approximately 200°C.

Two of the previous authors (i.e. Kido[8] and Glavas *et al.*[9]) looked at the thermogravimetric analysis of "hydrated" zinc acetylacetonate. They noticed that the greater rate of weight loss was seen between room temperature and 130°C, and observed nearly 100% weight loss by 200°C - probably due to evaporation of the starting material.

The relatively new technique of organoparticulate analysis has also been used to analyse metal acetylacetonates. Developed from thermoparticulate analysis, the method measured the temperature at which particulates were emitted from heated acetylacetonates. These particulates were 'condensation nuclei' capable of being measured by an ion chamber detector. Smith *et al.*[11] examined zinc acetylacetonate dihydrate (again thought by this author to be the monohydrate) and assigned it an organoparticulation range of 95-100°C when the heating rate was 6°C/min.

These rather scattered and, in some cases, brief studies illustrated the need for further in depth thermal analysis of $Zn(acac)_2$ and its monohydrate. Such work

would hopefully resolve the ambiguities in the literature and provide a more detailed picture of the thermal behaviour of both compounds.

4.2 Preliminary Work - ICI Wilton [$Zn(acac)_2.H_2O$].

4.2.1 Introduction

Because of practical problems, described later in this chapter (section 4.3.1), the initial thermal investigation of $Zn(acac)_2.H_2O$ was performed with a differential scanning calorimetry machine at I.C.I. Wilton. The experiments, supervised by Mr.I.D. Luscombe, were run using a sample synthesised by this author (see Chapter 3).[N.B temperatures quoted are for peak maxima and not onset temperatures].

4.2.2 Initial Work

Two d.s.c. experiments (A and B) were undertaken to investigate the thermal stability of $Zn(acac)_2.H_2O$; experiment A consisted of a primary scan [(i), 30-200°C] followed, after cooling each time, by three repeat scans [(ii), (iii) and (iv), 50-160°C] and used air as the purge gas. Experiment B was an exact repeat of experiment A, except that white spot nitrogen gas was used as the purge gas. In both experiments approximately 10mg of sample were heated in open pans at 20°C/min. It should be noted that the y-axis scale for the primary runs [Figures 4.1 and 4.2] was much larger than that used for the reheat scans.

Four endothermic processes (1-4) were noted in the primary scans [A(i) and B(i)] of both experiments [Figures 4.1 and 4.2] and the two traces were almost identical. This was not the case for the reheating scans; when the purge gas was air [Figure 4.3] all three [A(ii-iv)] showed negligible thermal activity, but when white spot nitrogen [Figure 4.4] was used, the first two [B(ii) and (iii)] displayed endothermic activity at approximately 130°C, the same temperature as in the primary scans.

Before assuming that the difference in these results was due to the only altered

variable, i.e. the purge gas, it was necessary to take a closer look at the experimental conditions.

Only one experiment was performed under each set of conditions and, as comparison of the scale shows, the reheat traces produced very small amounts of energy relative to the primary ones. This was probably because most of the sample evaporated out of the open pans during the primary scans (as Kido[8] also observed in his experiments). This suggests that the lack of thermal activity observed in A(ii)-(iv) may be due simply to a lack of sample! i.e. the difference in the two experimental results may not necessarily have been caused by the change in purge gas.

Such doubts meant that the only valid conclusion was that further experiments were required.

Figure 4.1 $Zn(acac)_2.H_2O$ in air - primary run A(i)

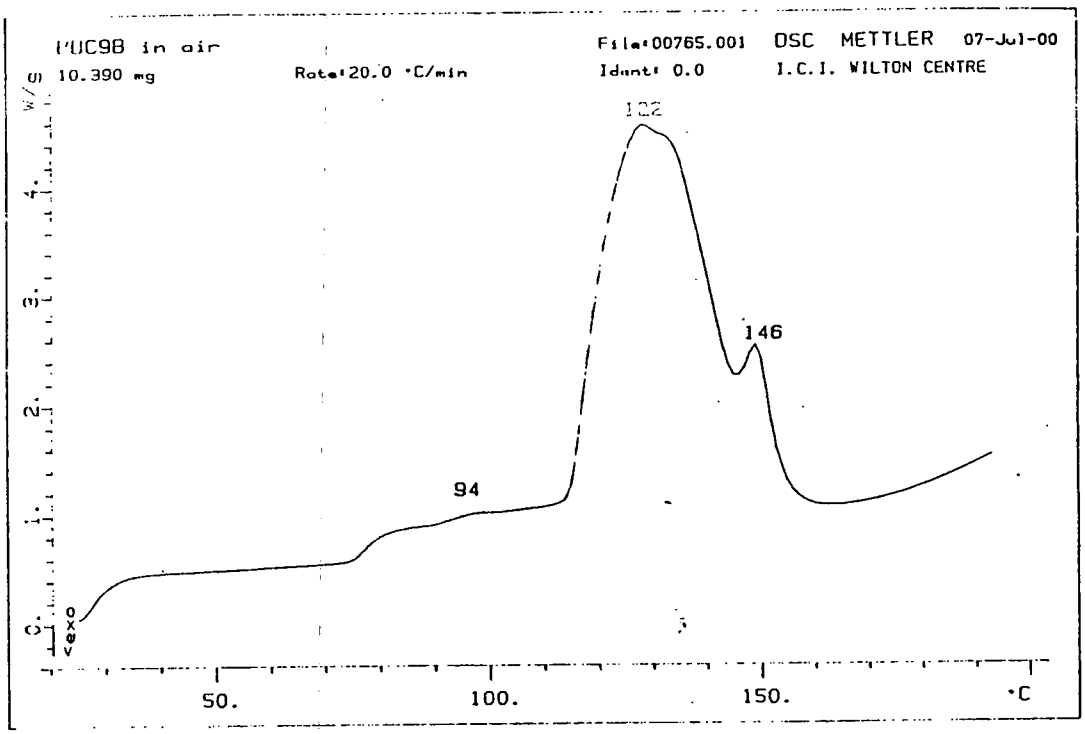

Figure 4.2 $Zn(acac)_2.H_2O$ in 'white spot' nitrogen - primary run, B(i)

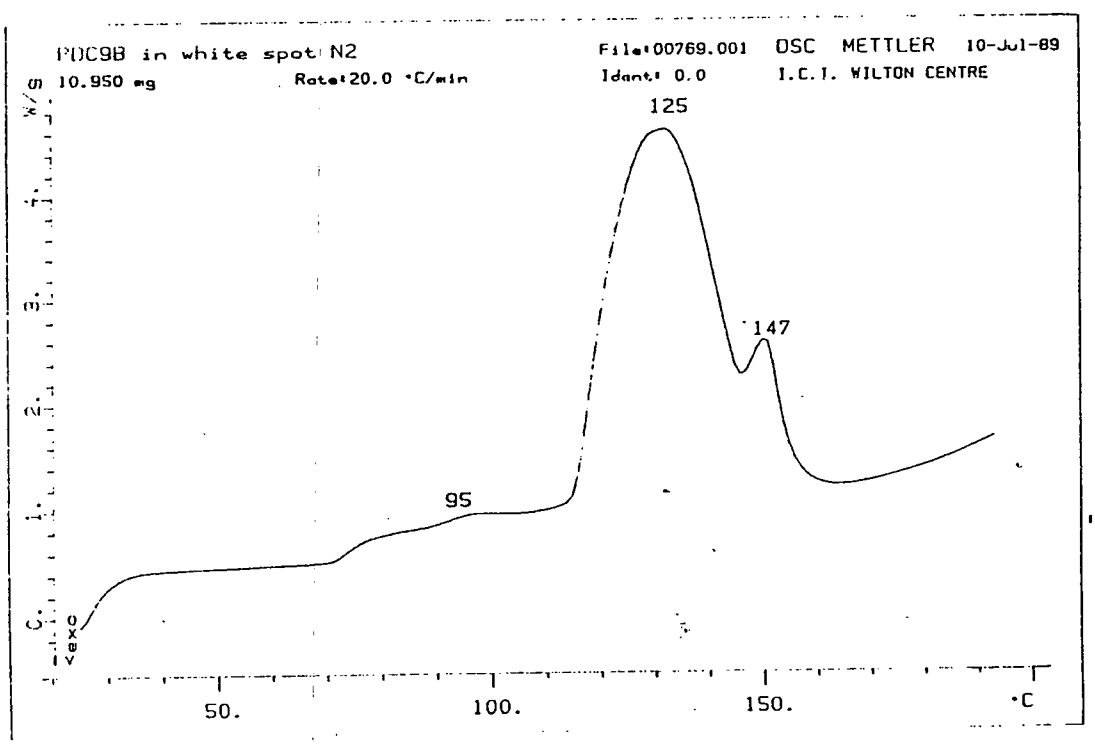

Figure 4.3 $Zn(acac)_2.H_2O$ in air - primary and reheat scans A(i)-(iv)

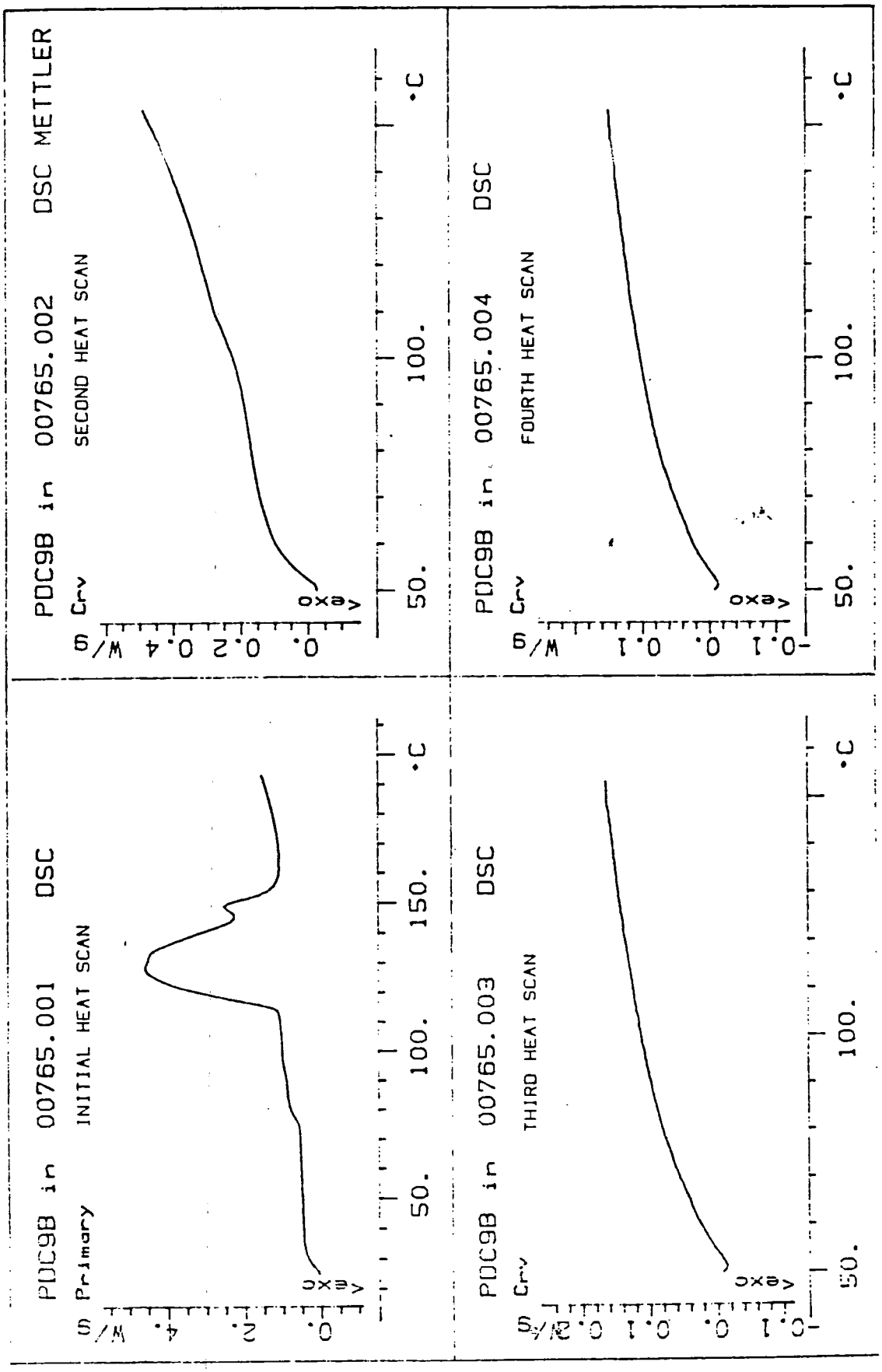

DSC SCANS CARRIED OUT IN OPEN PANS IN AN AIR ENVIRONMENT

Figure 4.4 $Zn(acac)_2.H_2O$ in 'white spot' nitrogen - primary and reheat scans B(i)-(iv)

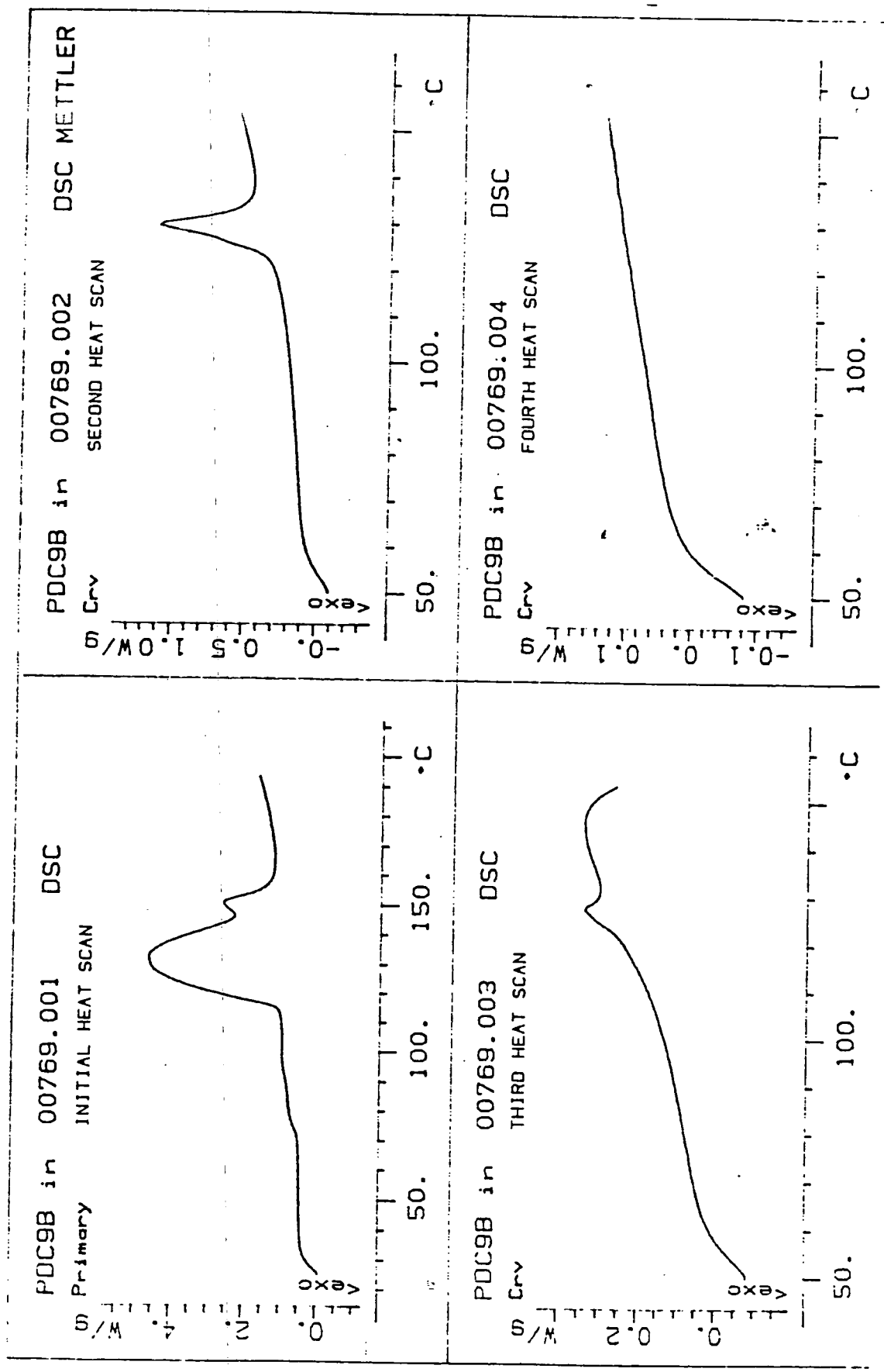

4.2.3 Further Experiments

The principal object of these experiments was to analyse the role of water, both ambient and coordinated, in the thermal behaviour of $Zn(acac)_2.H_2O$.

All the experiments discussed here were carried out in open pans and a heating rate of 20°C/min was used throughout. As with the 'initial' experiments (section 4.2.2), the same format was maintained i.e. a primary run (30-200°C) and, after cooling each time, three reheat scans (50-160°C). The purge gas was 'Zero Air' supplied by Air Products - claimed moisture content <2 ppm. Despite this figure, an in-line drier was used in the first and second experiments (C and D), but was dropped for the third (E) because it was thought to be introducing moisture into the system!

The major difference between the three runs was the pre-experiment treatment of the $Zn(acac)_2.H_2O$. in the first run the monohydrate was used directly; in the second it was dried in a vacuum oven (80°C) for two hours and in the third it was dried in the same oven for four hours.

The results [Figures 4.5, 4.6 and 4.7] showed that both these variables (in-line drier, vacuum oven drying) had an effect on the thermal behaviour of $Zn(acac)_2.H_2O$. The pre-oven dried samples markedly affected the primary runs; where no treatment was applied [Figure 4.5, C(i)] the primary trace was identical to those obtained in the initial experiments [Figures 4.1 and 4.2], indicating that the in-line drier was having no effect. However, when pre-experiment drying was used [Figures 4.6 and 4.7, D(i) and E(i)], the first (101/104°C) and fourth (144°C) peaks showed a decline in relative size. This reduction in relative intensity was more pronounced after the longer period of drying. Thus it is highly likely that the pre-experiment drying removed some of the coordinated water which caused a change in the d.s.c. trace and thereby established a connection between the nature of the primary runs and the amount of coordinated water.

Figure 4.5 $Zn(acac)_2.H_2O$ - No pre-experiment drying (C)

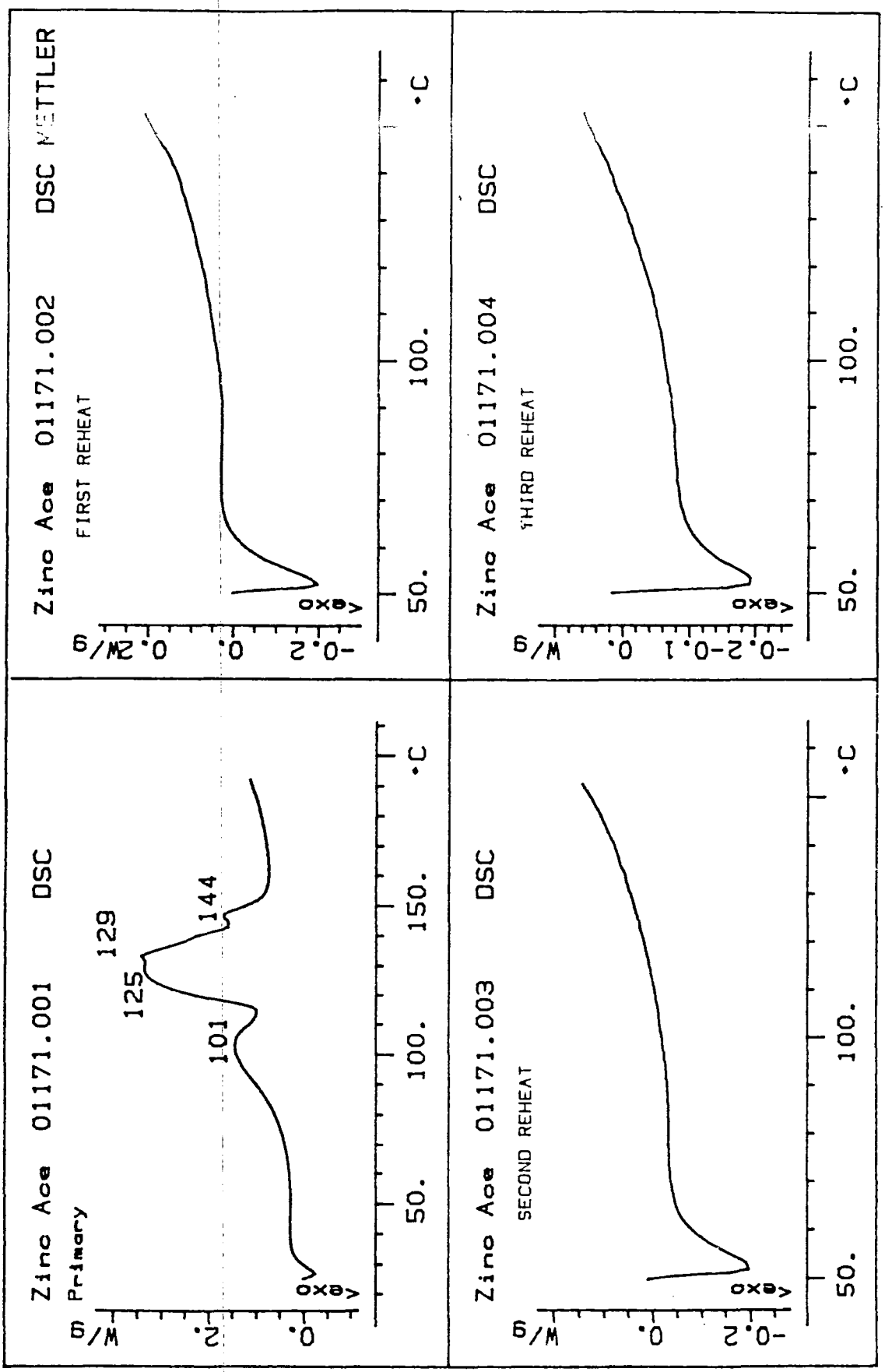

The lack of thermal activity in the reheat traces of experiments C (no drying, Figure 4.5) and D (two hours drying, Figure 4.6) indicated that there was no connection between the relative amount of water and the nature of the reheat traces (all coordinated water is probably removed in the primary scan, up to 200°C).

The exotherms produced in experiment E were totally unlike anything previously found in the d.s.c. of $Zn(acac)_2.H_2O$, but if it is accepted that in experiments C and D the in-line drier was introducing moisture, then the results show that thermal activity in the first and second reheat scans was observed because the purge gas was virtually dry.

In contrast to the pre-run drying , the presence of moisture (or lack of it) in the purge gas only appeared to affect the reheat scans, indicating that its presence had a significant effect during cooling after the primary run.

Following the interest generated by these preliminary studies this author decided that an in-depth 'hands-on' approach was desirable. With this in mind all future d.s.c. work was performed in Durham.

Figure 4.6 $Zn(acac)_2.H_2O$ - two hours drying (D)

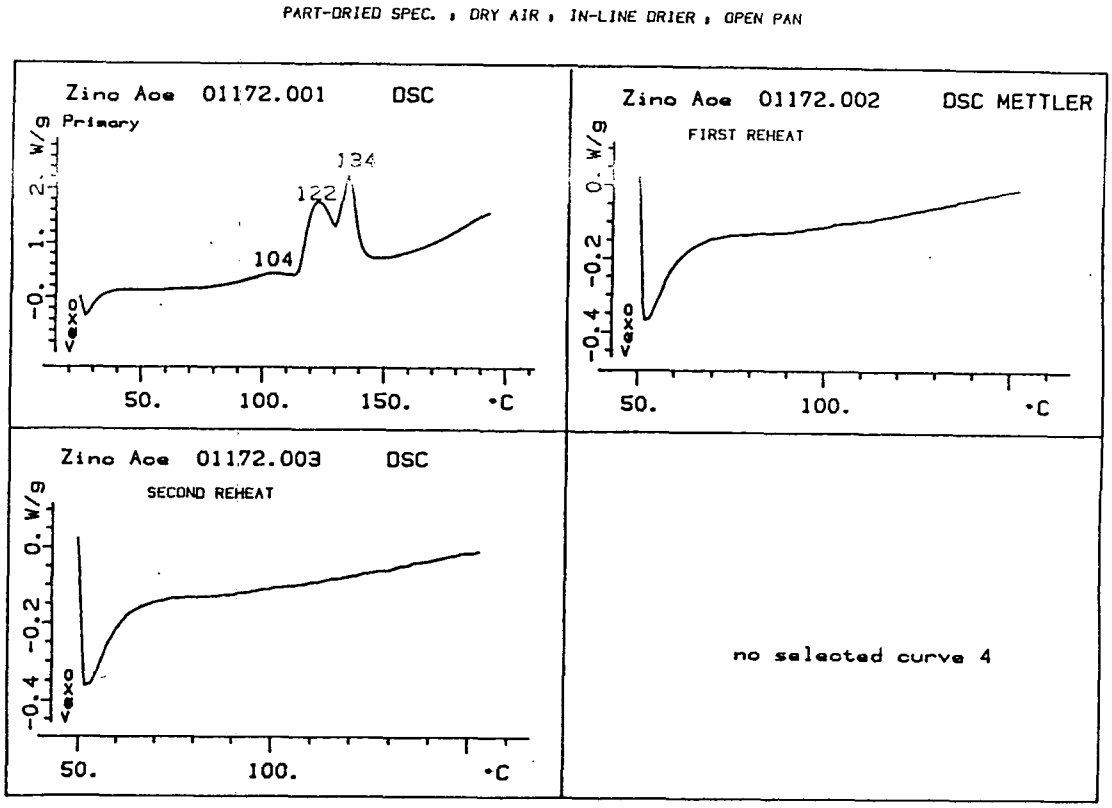

Figure 4.7 $Zn(acac)_2.H_2O$ - four hours drying (E)

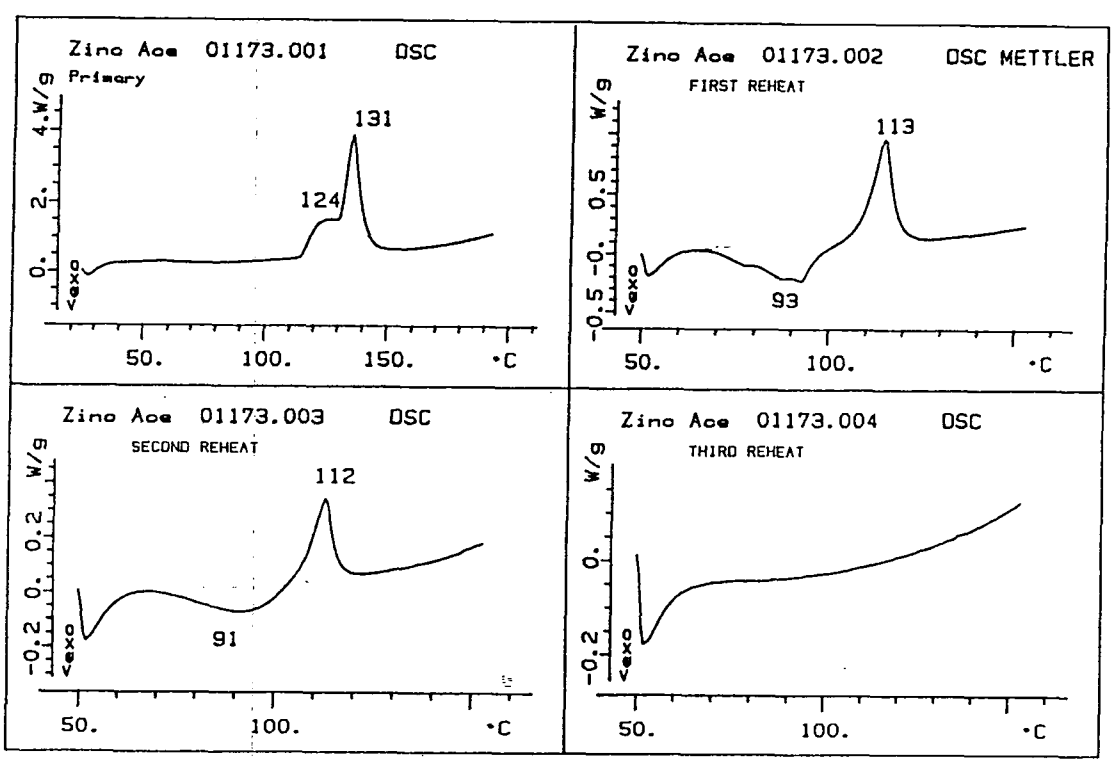

4.3 Differential Scanning Calorimetry - Durham - Initial Scans

4.3.1 Introduction

As mentioned previously, the preliminary results from I.C.I. Wilton led on to a more extensive study, performed in Durham, of the thermal behaviour of $Zn(acac)_2.H_2O$. It was decided to leave a further study of re-heat traces until later and concentrate on the initial ('primary') runs.

Because open-pan experiments were considered to be too great a risk to the d.s.c. equipment (through condensation of volatile matter) and hermetically sealed pans led to inconsistent results (as a result of pressure build up) a compromise was sought. Following the suggestion of Dr. Z.V. Hauptman a pin-hole of constant size was placed in the lid of all the sample capsules in order to prevent pressure build-up whilst minimising material loss through evaporation (see Chapter 2 for further experimental details). Dry argon was used as the purge gas.

The object of the first experiments was to study the effects on the traces of two variables, heating rate and sample particle size. Five heating rates were employed: 0.1°C/min, 0.4°C/min, 1.0°C/min, 4.0°C/min and 10°C/min. The two particle sizes used were less quantifiable; the larger one (hereafter referred to as 'coarse') was simply the 'as produced' sample i.e. white colourless needles. The smaller size was produced by grinding the coarse material with an agate pestle and mortar for *ca.* five minutes until it resembled an amorphous powder, referred to as 'fine'.

4.3.2 General Descriptions [$Zn(acac)_2.H_2O$]

All the observed thermal activity in the primary scans was endothermic and for the remainder of the chapter all peaks can be assumed to be endothermic unless stated otherwise.

Four different peaks were observed during these experiments (e.g. see Figure

4.16). All varied in size and/or position with respect to the heating rate and particle size. The first and third peaks were always observed, whereas certain conditions led to the absence of the second and fourth ones.

For ease of description the peaks have been assigned Roman numerals according to their order of appearance in the 10°C/min scan (see Figure 4.16) i.e. peak I occurs at the lowest temperature.

4.3.3 Detailed Descriptions of $[Zn(acac)_2.H_2O]$

4.3.3.1 Heating Rate: 0.1°C/min

The simplest traces were obtained when the heating rate was 0.1°C/min (see Figures 4.8 and 4.9). Both the 'coarse' and 'fine' samples showed two peaks; a broad endotherm, beginning at the onset of heating (65°C) and peaking between 75 and 80°C; and a sharp endotherm (onset temperature 127/8°C, peak temperature 130°C). The main difference between the two scans was the shape of peak I, *viz.* the fine sample displayed a sharper decline.

Figure 4.8 'Coarse' $Zn(acac)_2.H_2O$, 0.1°C/min

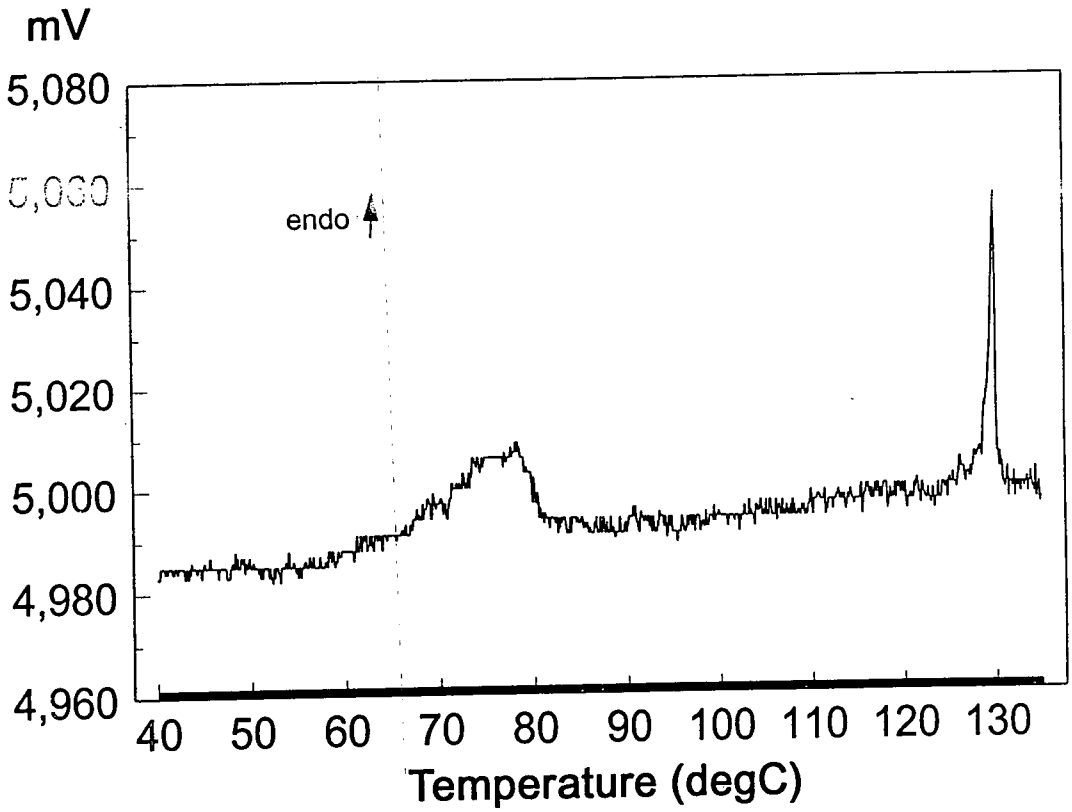

Figure 4.9 'Fine' $Zn(acac)_2.H_2O$, 0.1°C/min

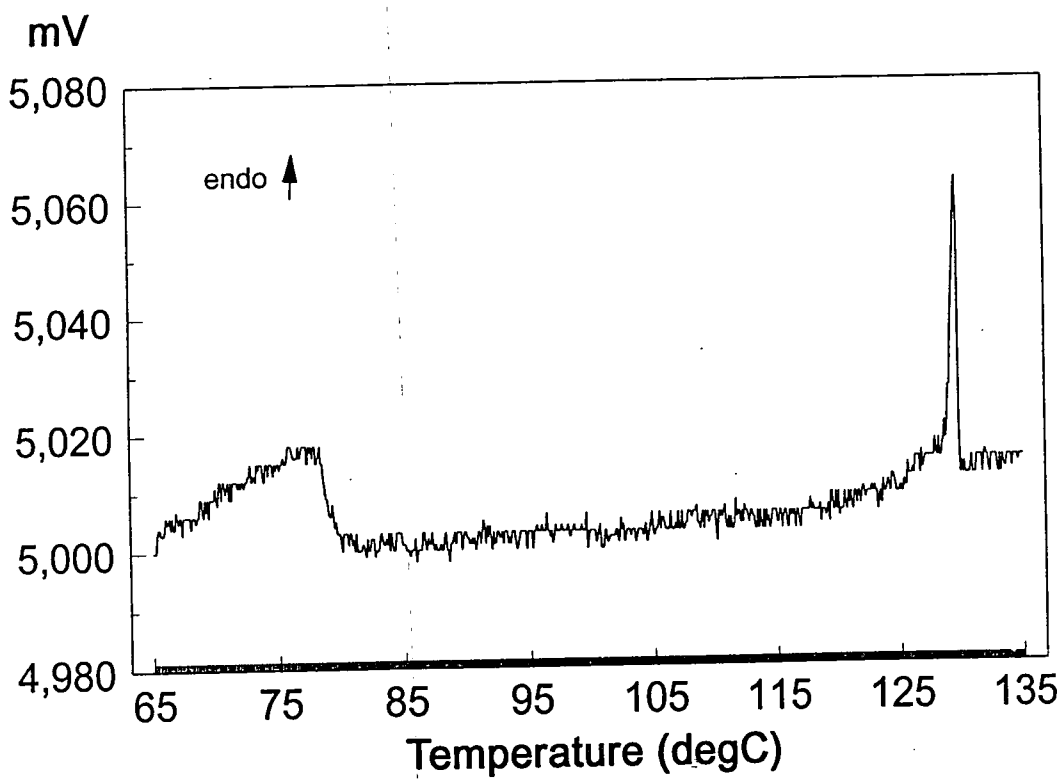

The marked difference in appearance of the two peaks (I and III) was a strong indication of the process behind them; in general broad and unsymmetrical peaks, such as I, are often associated with a relatively slow process such as vapour production. In the case of $Zn(acac)_2.H_2O$, such a vaporisation process would most likely be the loss of coordinated water (although sublimation of $Zn(acac)_2.H_2O$ could be a possibility).

Vaporisation can be described as a 'surface' process (i.e. this is where the process occurs from) and logically an increase in the ratio surface area/volume would lead to an increase in the rate of evaporation. This was observed at 0.1°C/min, where changing from a 'coarse' to a 'fine' sample (i.e. increasing the surface area/volume ratio) resulted in an earlier completion of peak I (i.e. increasing the rate of evaporation) when similar sample weights were used.

The discovery of a single lump of beige coloured residue deposited in the sample pans on completion of the two 0.1°C/min runs strongly indicated that fusion had taken place and this was supported by the sharp and symmetrical shape of the second endotherm (peak III) in the traces. If peak I were due to loss of coordinated water then the residue undergoing fusion would have been anhydrous $Zn(acac)_2$.

4.3.3.2 Heating Rate: 0.4°C/min

Given the neatness of the explanation above, it was quite a surprise to observe a third peak (peak II) appearing in traces run at 0.4°C/min (see Figures 4.10 and 4.11). The extra peak (onset temperature 111°C, peak temperature 113°C) was much more prominent when the sample was coarse and barely detectable for fine samples.

Figure 4.10 'Coarse' $Zn(acac)_2.H_2O$, 0.4°C/min

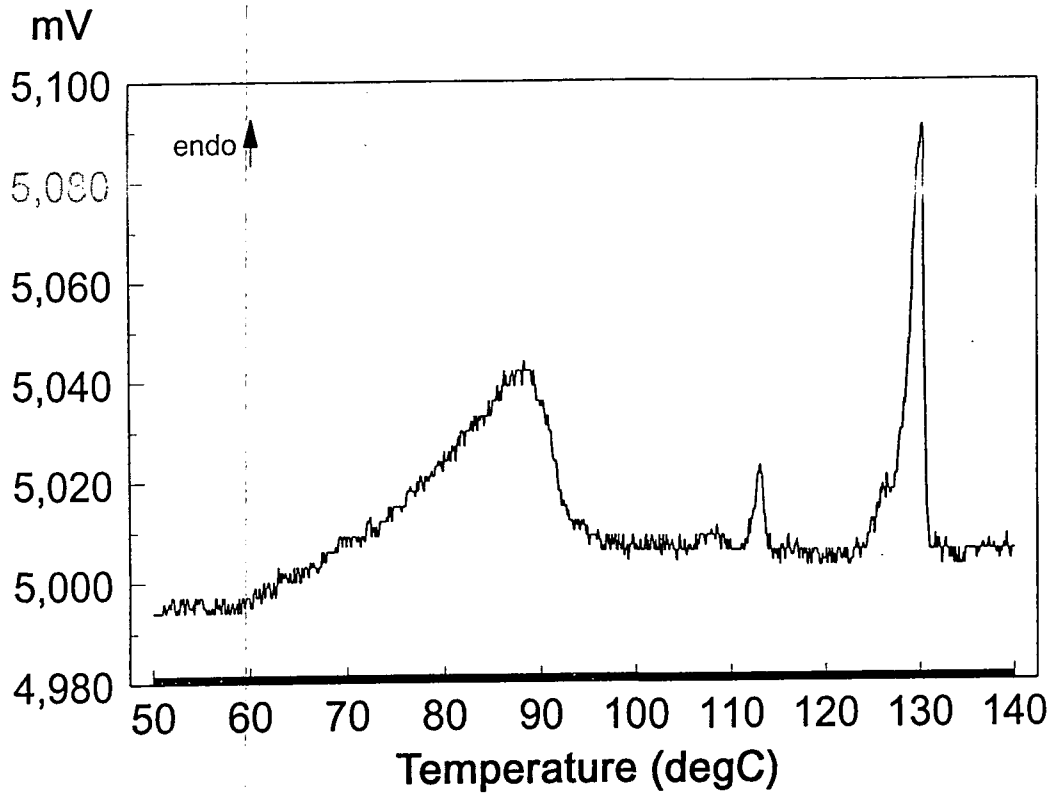

Figure 4.11 'Fine' $Zn(acac)_2.H_2O$, 0.4°C/min

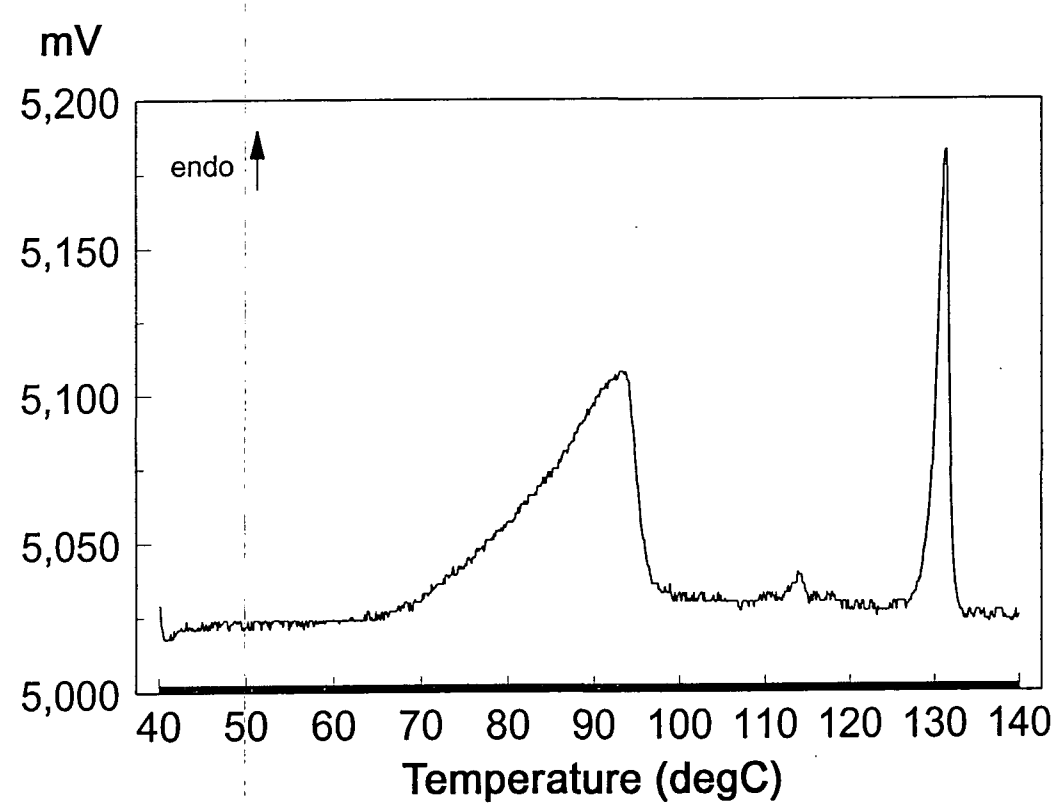

The positions of the peak I's observed in the 0.4°C/min traces (Figures 4.10 and 4.11) were markedly different to those seen in the 0.1°C/min traces (This was also true, to a much lesser extent, for the peak III's). These and other positional trends are discussed in Section 4.3.5 of this chapter.

It was also noted that the peak III's of the 0.4°C/min traces were less symmetrical, particularly when the sample was 'coarse' than those observed in the 0.1°C/min scans. This was the first indication that a fourth process could be taking place (discussed further in Section 4.4).

4.3.3.3 Heating Rate: 1.0°C/min

When a 'coarse' sample was heated at 1.0°C/min (Figure 4.12), the resulting peak II and peak III were roughly equal in size. This contrasted sharply with the 'fine' sample (fig. 4.13) where peak II was barely detectable.

The peak maxima temperatures for peaks I and III were higher than those for the previous heating rates (0.1°C/min 0.4°C/min) indicating a trend relating an increase in heating rate to an increase in peak maxima temperature.

Evidence for a further peak (IV), close to peak III, was obvious when the sample was 'coarse' (see Figure 4.12).

Figure 4.12 'Coarse' $Zn(acac)_2.H_2O$, 1.0°C/min

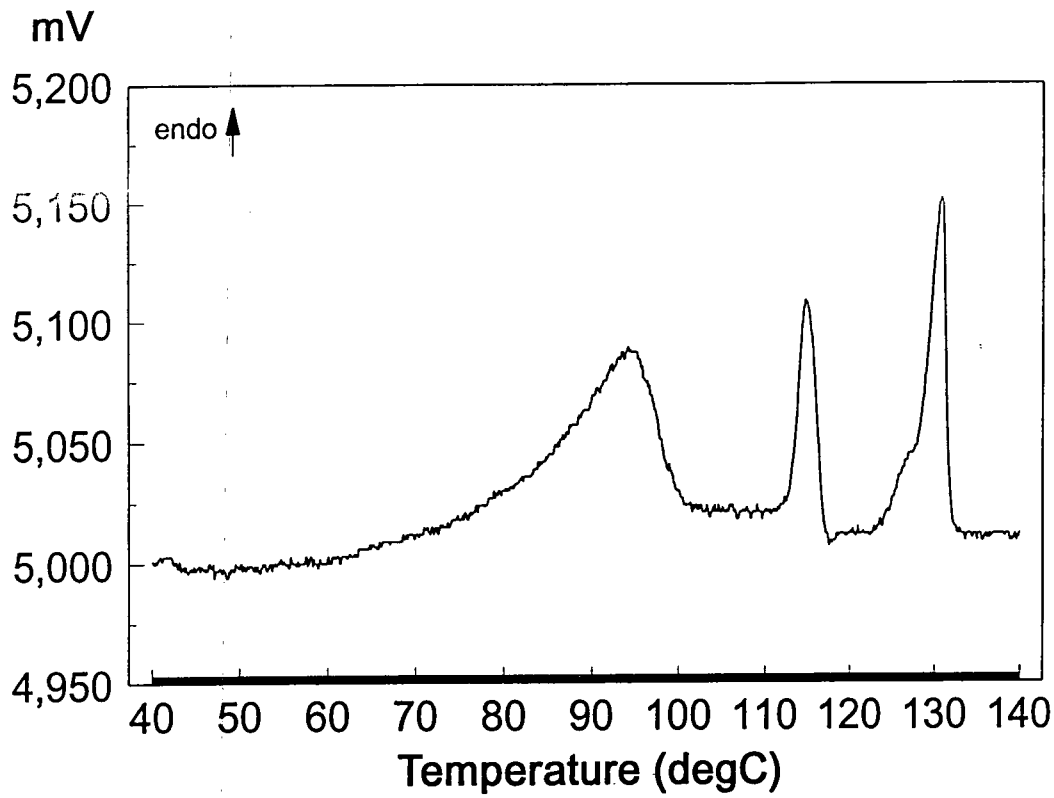

Figure 4.13 'Fine' $Zn(acac)_2.H_20$, 1.0°C/min

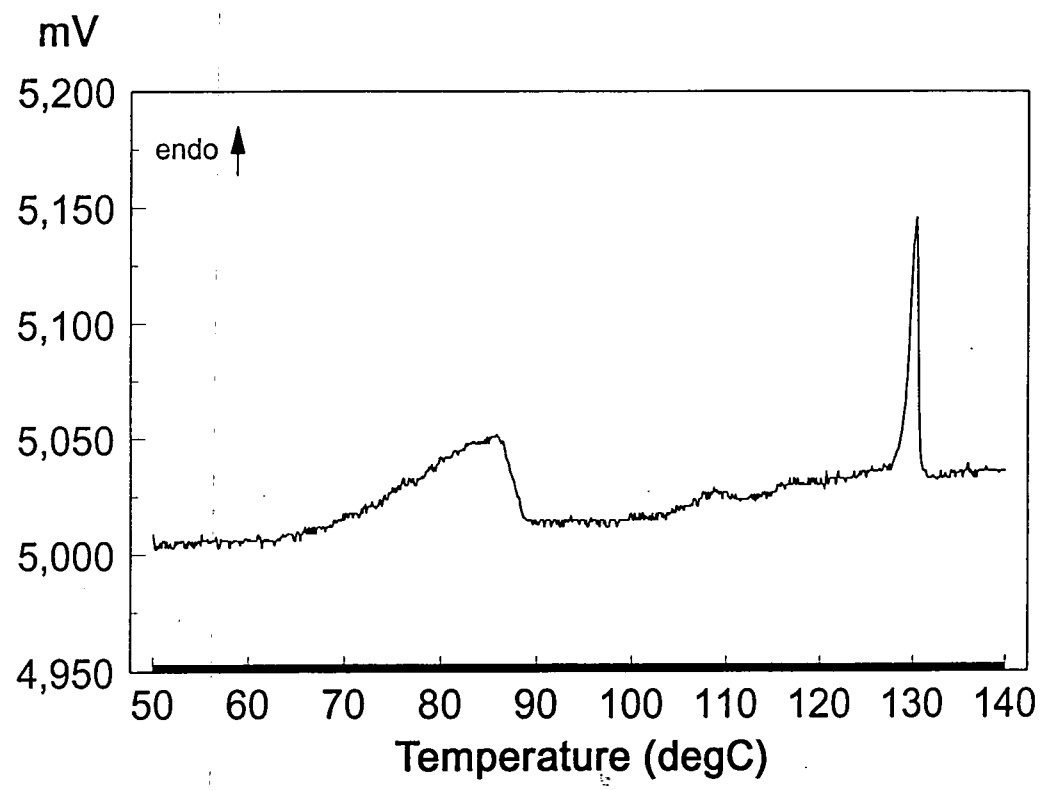

4.3.3.4 Heating Rate: 4°C/min

The trends observed (above) at the three lower rates of heating continued to be observed at 4.0°C/min; namely, the increasing relative size of peak II and the upward positional shifts of the peaks I - III (see Figures 4.14 and 4.15). No shoulder was observed at the lower temperature side of peak III (contrast the case for 1°C/min), but, as Figure 4.14 shows, a peak IV was present on the high temperature side of peak III when the sample was 'coarse'. A faint shoulder was also observed on the high temperature side of peak III when the sample was 'fine' (figure 4.15).

4.3.3.5 Heating Rate: 10°C/min

Unsurprisingly, the two traces (see Figure 4.16 and 4.17) obtained at this heating rate fitted both the position and magnitude trends which were observed at the other rates of heating. A fourth peak (peak IV) was clearly visible for both samples on the high temperature side of peak III.

Figure 4.14 'Coarse' $Zn(acac)_2.H_20$, 4.0°C/min

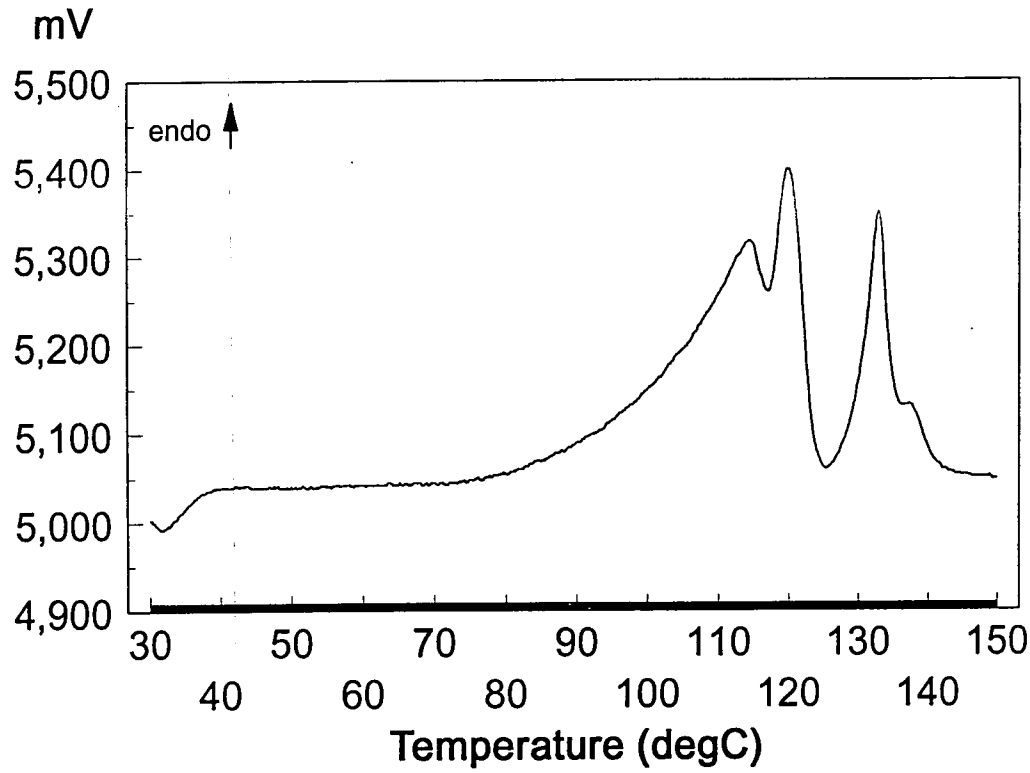

Figure 4.15 'Fine' $Zn(acac)_2.H_20$, 4.0°C/min

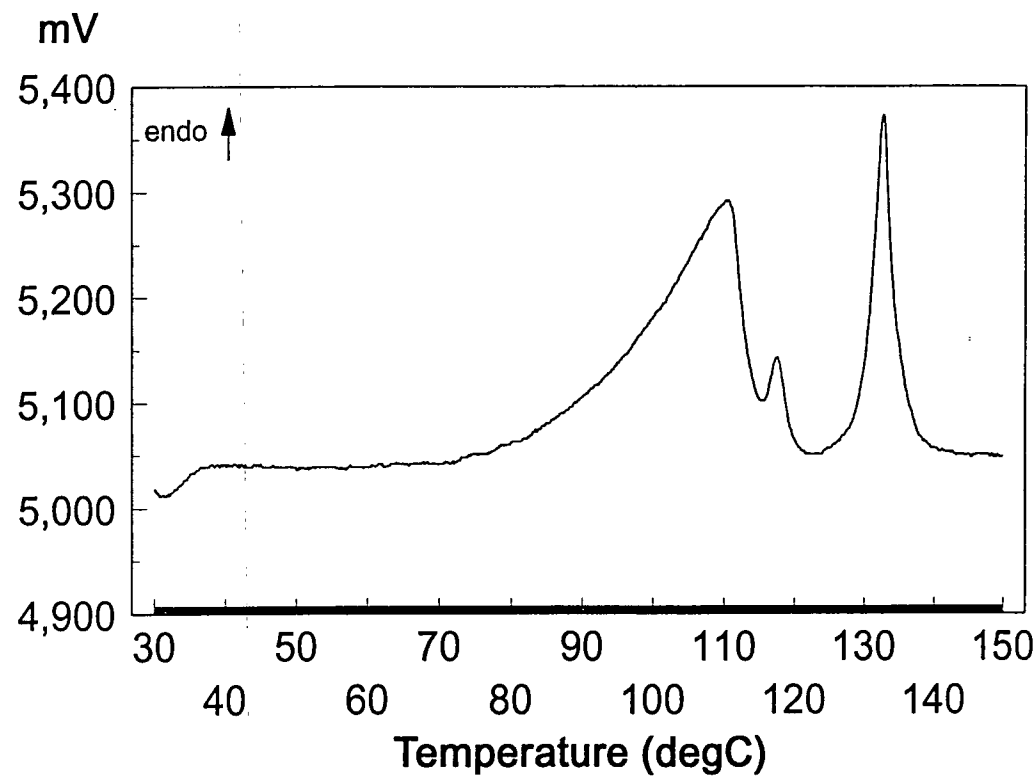

Figure 4.16 'Coarse' $Zn(acac)_2.H_20$, 10.0°C/min

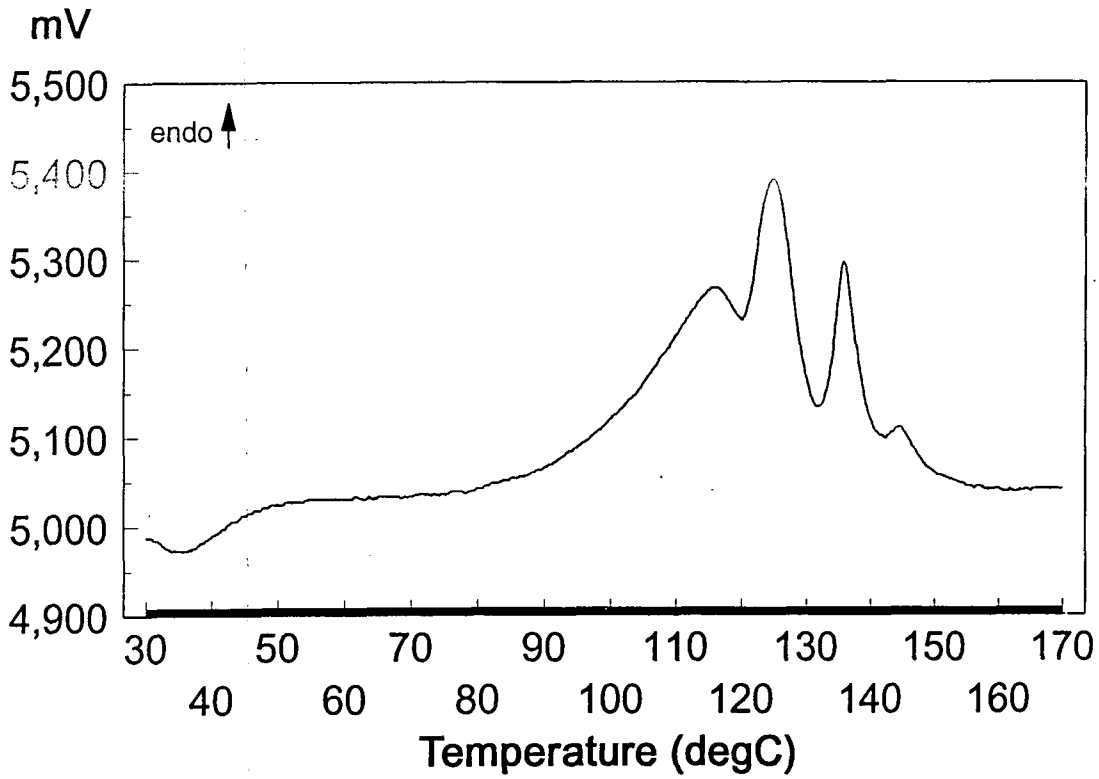

Figure 4.17 'Fine' $Zn(acac)_2.H_20$, 10.0°C/min

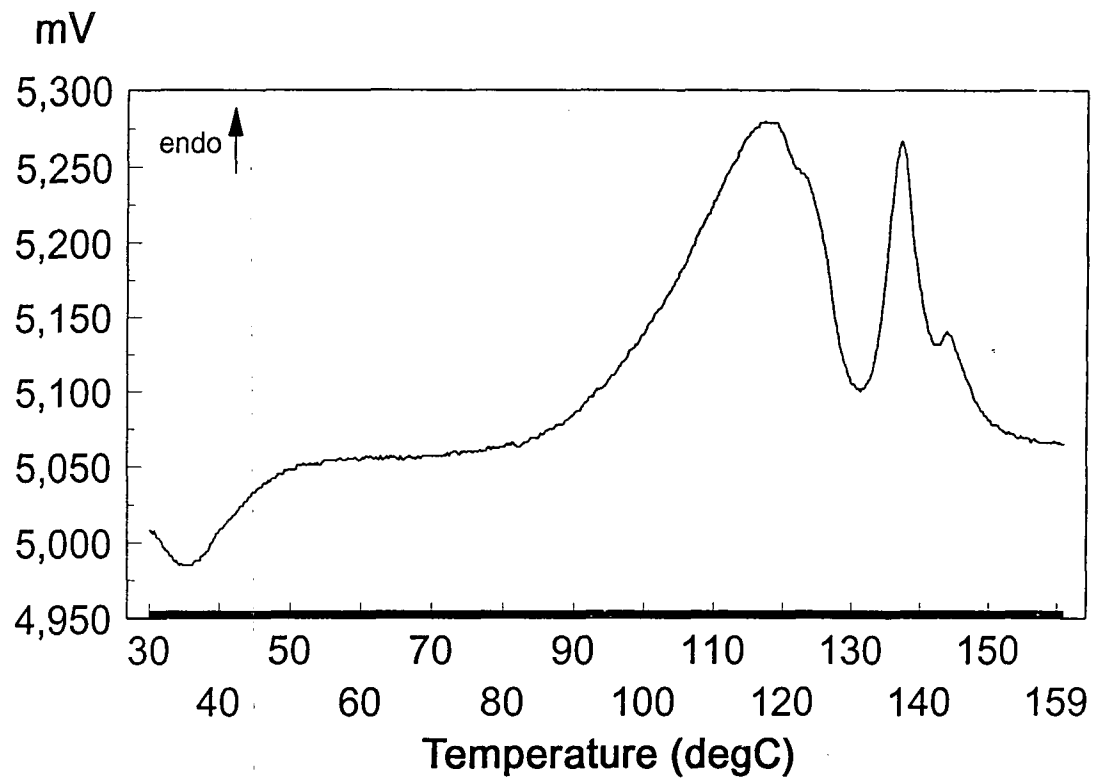

4.3.3.6 Conclusions

At the lowest rates of heating, the thermal behaviour of $Zn(acac)_2.H_2O$ appeared to be simple: the traces consisting of two peaks (peaks I and III) whose size and shape fitted an uncomplicated theory, *viz.* the coordinated water was evaporated before the anhydrous residue melted at III. However faster heating rates led to the observation of two other peaks (peaks II and IV) neither of which had an obvious explanation. Possible theories at this stage of the research included a molecular rearrangement [of $Zn(acac)_2$] , a reaction involving water vapour, and the involvement of residual $Zn(acac)_2.H_2O$ in reactions. Further discussion is given in Section 4.4.

4.3.4 Descriptions [$Zn(acac)_2$]

The synthesis of anhydrous $Zn(acac)_2$ is described in Chapter 3. Initially, four 'primary' scans were obtained using $Zn(acac)_2$. Two were run at a heating rate of 1°C/min and the others at 4°C/min. In the case of each heating rate one sample was used as produced and referred to as 'coarse' and the other was ground with an agate pestle and mortar for about five minutes until it resembled an amorphous powder - referred to as 'fine'.

All four traces (see Figures 4.18 - 4.21) consisted of two basic features. The first was a broad endotherm , similar in appearance to the peak I's of the $Zn(acac)_2.H_2O$ experiments but more variable in position. In fact it was not possible to reproduce this peak even when the exact conditions were repeated. This irreproducability, unique in these studies to this peak, led the author to believe that the peak was due to evaporation of adsorbed water. This was expected, as the practicalities of these experiments meant that exposure of this moisture-sensitive compound to the air was unavoidable.

The second feature was a sharp endotherm (onset temperature 129-30°C, peak temperature 130-2°C). It was virtually identical in size, shape and position to peak III in the $Zn(acac)_2.H_2O$ experiments and, as inspection of the sample pan contents after heating showed evidence of melting, fusion of $Zn(acac)_2$ was strongly favoured as the explanation of this peak. In addition, the onset temperature closely matched the melting point of $Zn(acac)_2$ (127°C) quoted by Rudolph and Henry[12]. (Bennett *et al.*[13] quoted a melting point of 129°C for the trimer $[Zn(acac)_2]_3$).

Figure 4.18 'Coarse' $Zn(acac)_2$, 1.0°C/min

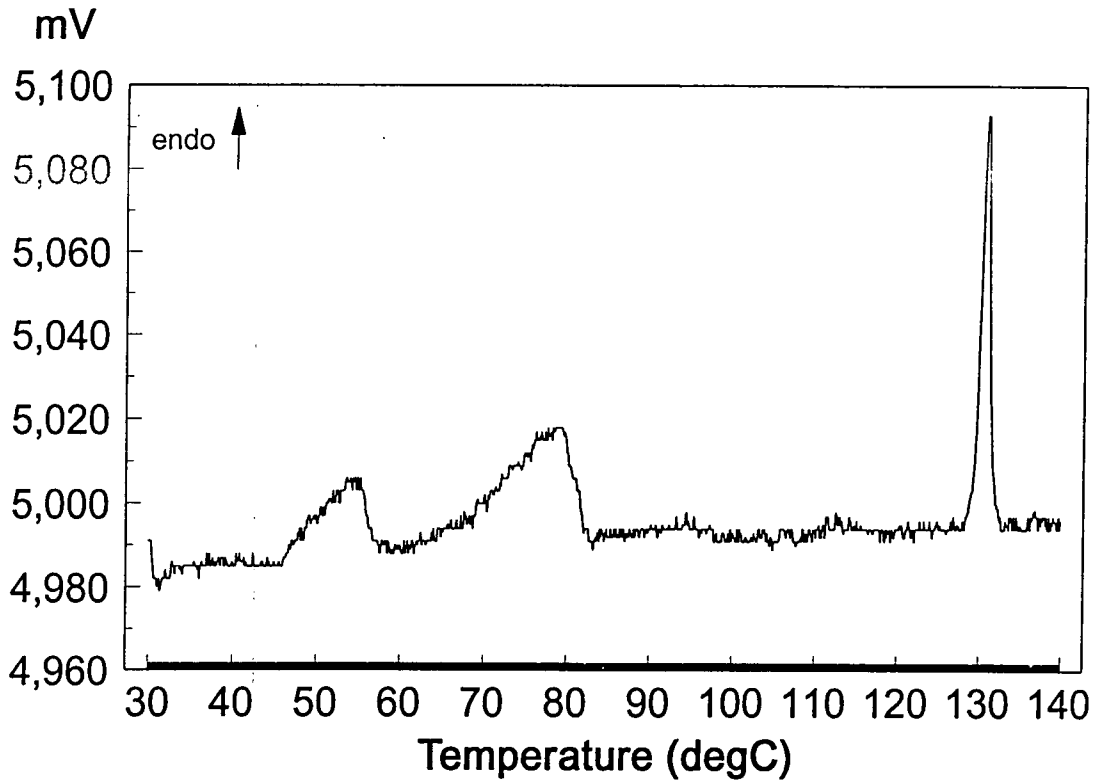

Figure 4.19 'Fine' $Zn(acac)_2$, 1.0°C/min

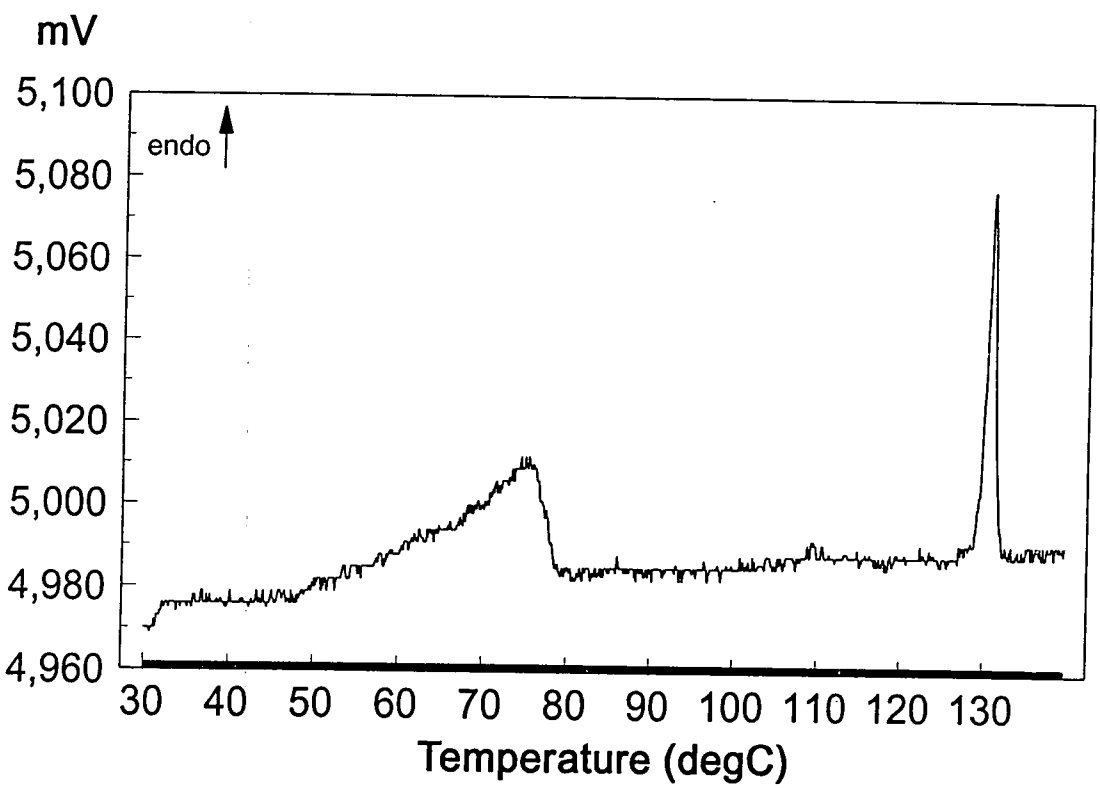

Figure 4.20 'Coarse' $Zn(acac)_2$, 4.0°C/min

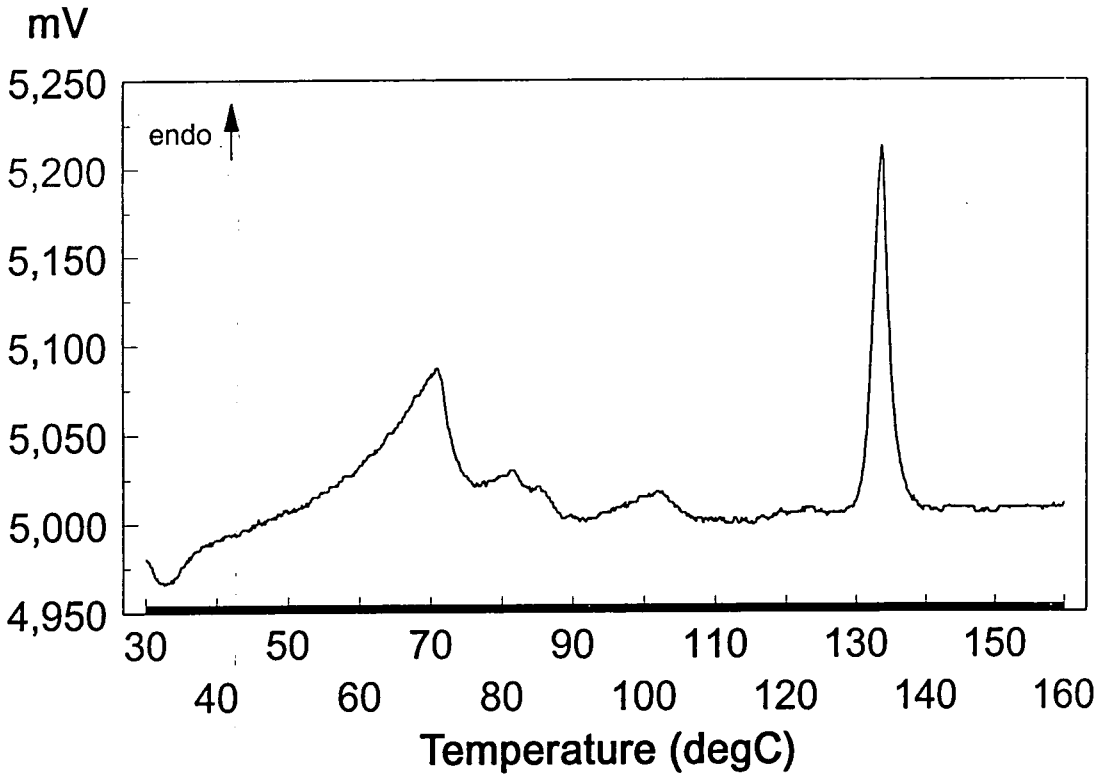

Figure 4.21 'Fine' $Zn(acac)_2$, 4.0°C/min

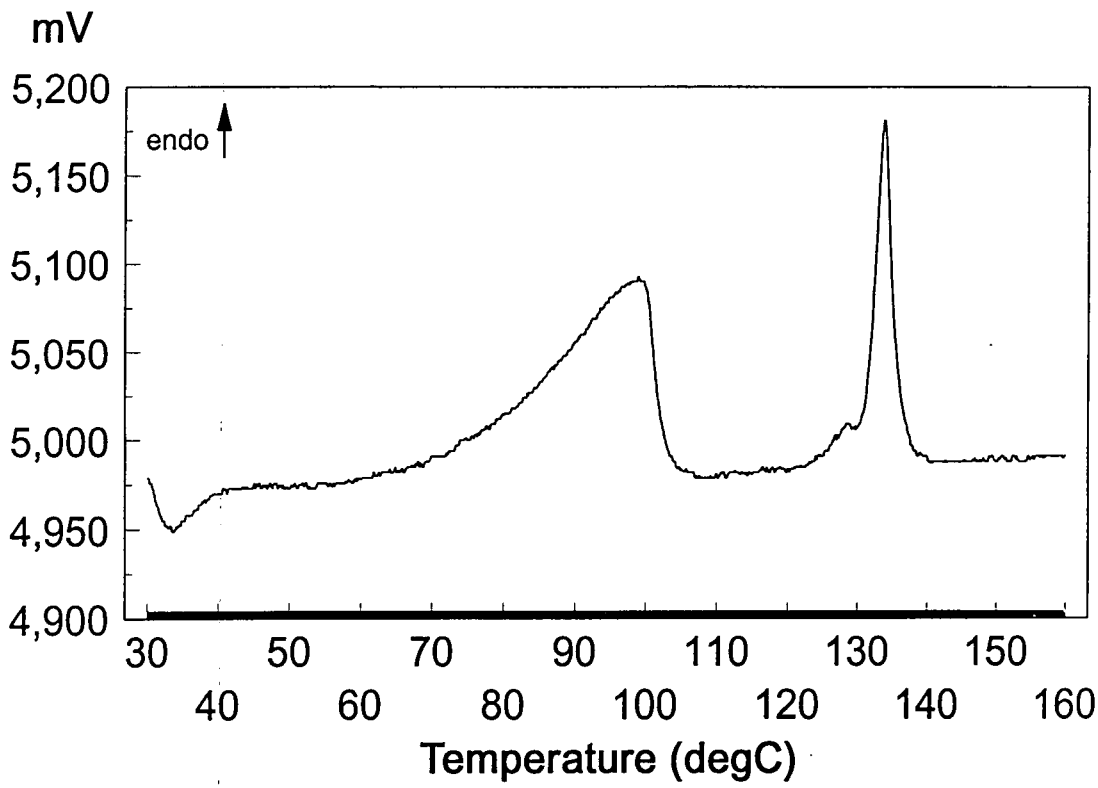

4.3.5 Numerical Analysis

4.3.5.1 A Note on the Measurements

As mentioned in Chapter 2, the d.s.c. data were analysed using software designed and written by Dr. J.M. Rawson. The two main purposes of these programs were to record accurate sample temperatures and to measure enthalpies for the various processes. The energy values were calculated using indium and benzoic acid standards (which were accurate within 2%), the figures quoted here are intended as comparative, not absolute values - especially as in some cases a degree of estimation was required. The sample temperatures were measured at the peak maxima rather than the onset temperature as these could be identified more accurately.

4.3.5.2 Analysis of Peak Maxima Temperatures [$Zn(acac)_2.H_2O$]

4.3.5.2.1 Peak I

Figure 4.22 shows the sample temperatures at the peak I maxima for different heating rates. The data confirmed the observations made in the previous section that the peak maximum temperature varied greatly with heating rate (from 78°C at 0.1°C/min to 114.6°C at 10°C/min!) and, at a given rate, the 'coarse' sample usually had its peak I maximum at a higher temperature. The lack of conformity to these trends, apparent at 4°C/min and 10°C/min, was probably due to a combination of two major factors; firstly, at these heating rates the degree of overlap between peaks is substantial. Such overlaps lead to the displacement of the maxima of the constituent peaks - the larger the overlap, the larger the displacement (see Figure 4.28). The second factor depends on the sample sizes. A relatively large sample size (e.g. 7.92mg) for the 'coarse' sample at 4°C/min (Figure 4.14) means a reduction in the gaseous volume of the sample pan. This restricts processes such as evaporation and this manifests itself in the d.s.c. traces by the associated peak 'shifting' to an elevated temperature.

Figure 4.22 Peak I maxima temperatures

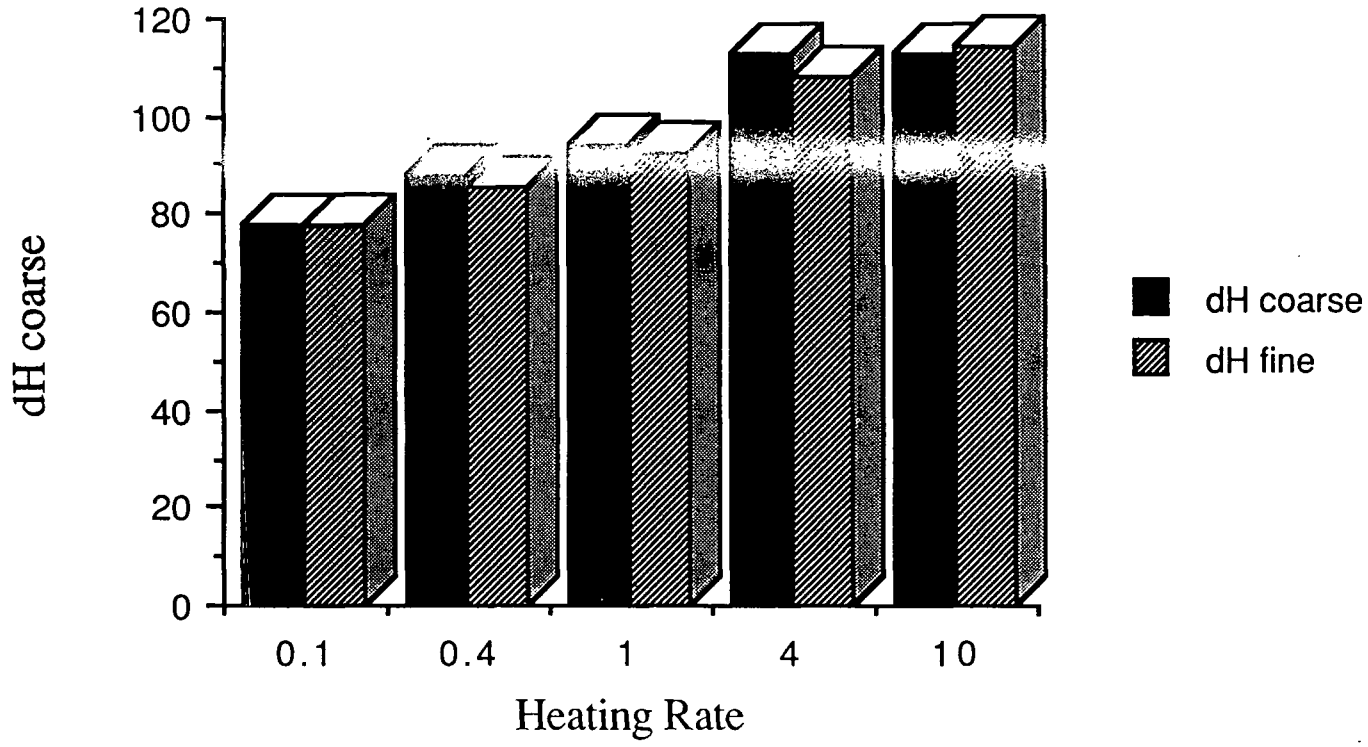

Figure 4.23 Peak II maxima temperatures

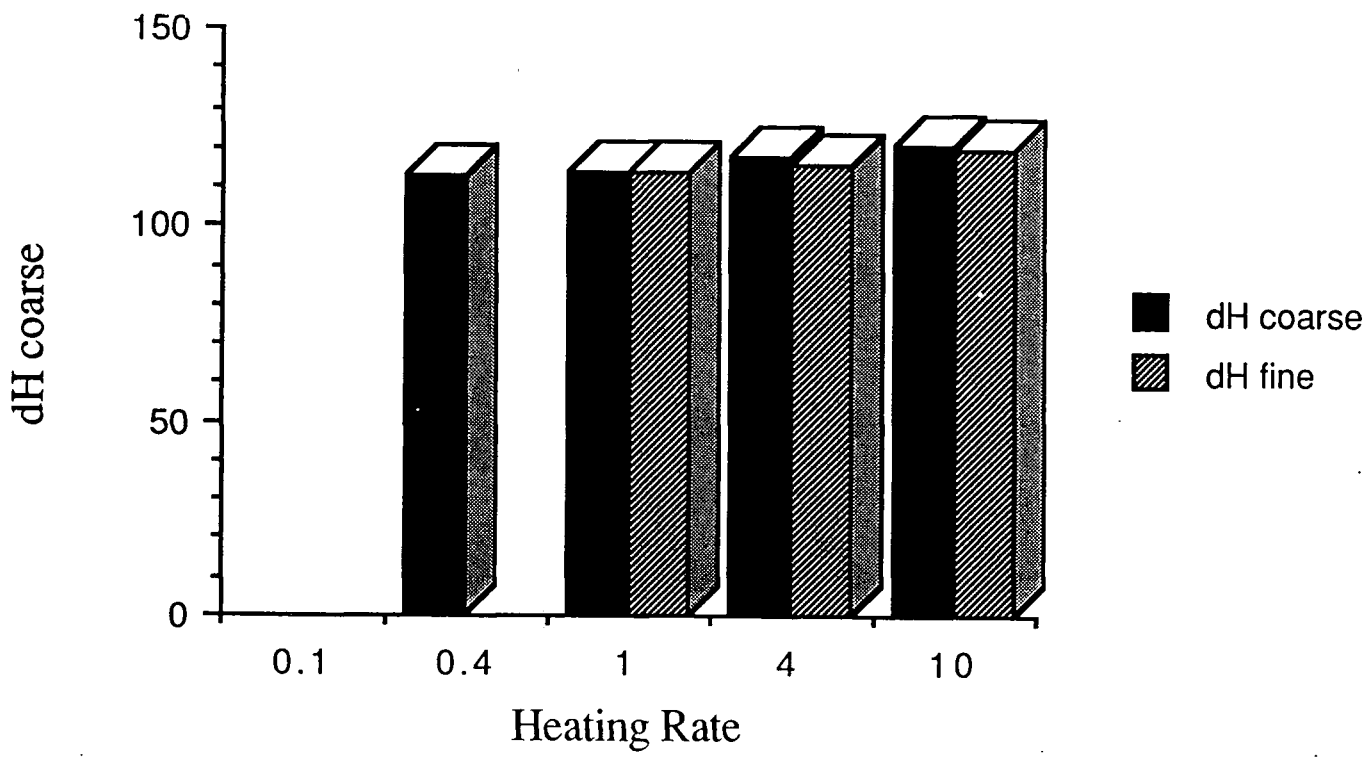

Conversely, the opposite is true for relatively small samples (e.g. 3.82mg) for the 'coarse' sample at 10°C/min (Figure 4.16).

4.3.5.2.2 Peak II

As Figure 4.26 shows, peak II exhibited a dramatic increase in size as the heating rate increased. This indicated that the conditions necessary for peak II were brought about by relatively high rates of heating e.g. incomplete breakdown of $Zn(acac)_2.H_2O$ or incomplete removal of breakdown products such as water.

In contrast to the set of peak I's , the range of peak II maxima was quite small (see Figure 4.23). In addition, the difference between 'coarse' and 'fine' samples at a given temperature was also slight for peak II. This implied that physical constraints, such as diffusion, had less of an effect on peak II than peak I.

4.3.5.2.3 Peak III

The peak maxima temperatures for all the peak III's were very similar (see Figure 4.24) - there was only 4°C difference between the highest and lowest values. Unlike peaks I and II there also appeared to be little difference between the 'coarse' and 'fine' samples. This compared favourably with the theory that the peak was due to fusion, as it is not significantly affected by particle size or heating rate (providing that the temperature lag is accounted for - see 4.3.5.4.3).

Figure 4.24 Peak III maxima temperatures

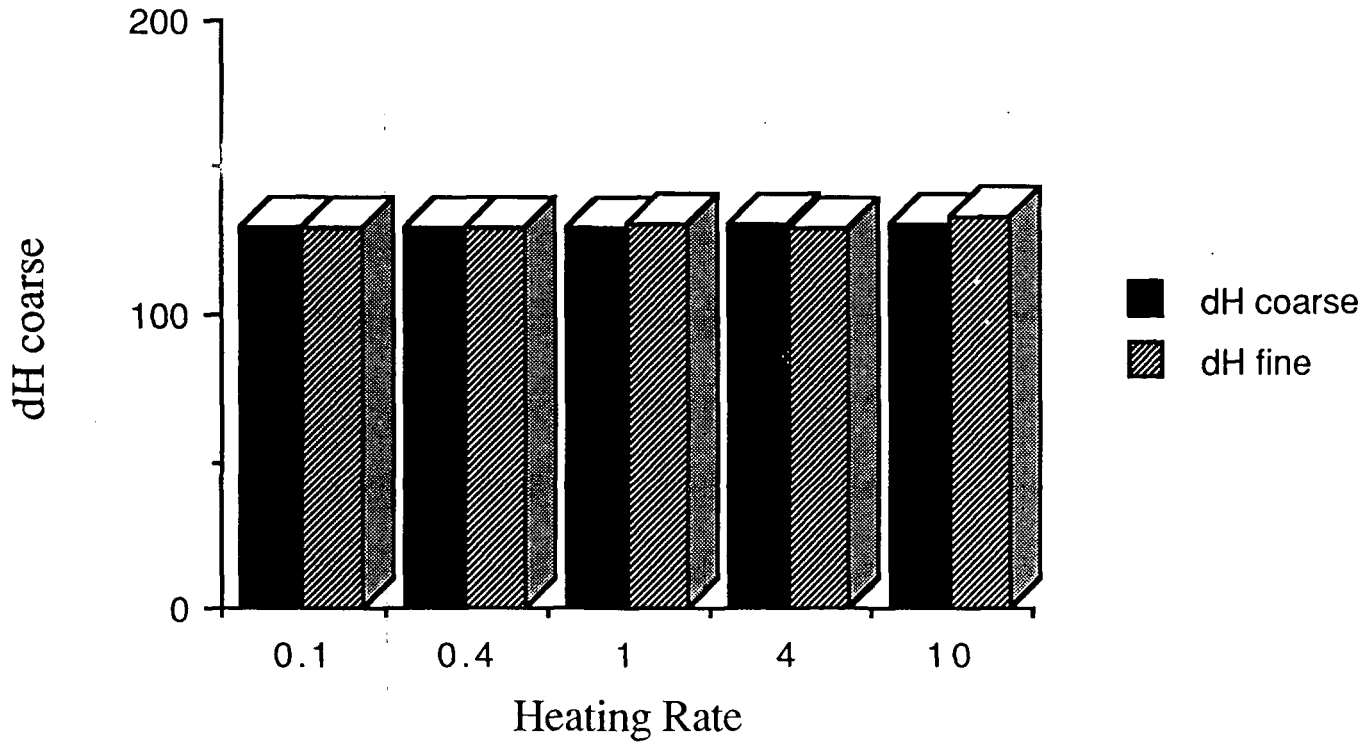

Figure 4.25 Peak I enthalpies

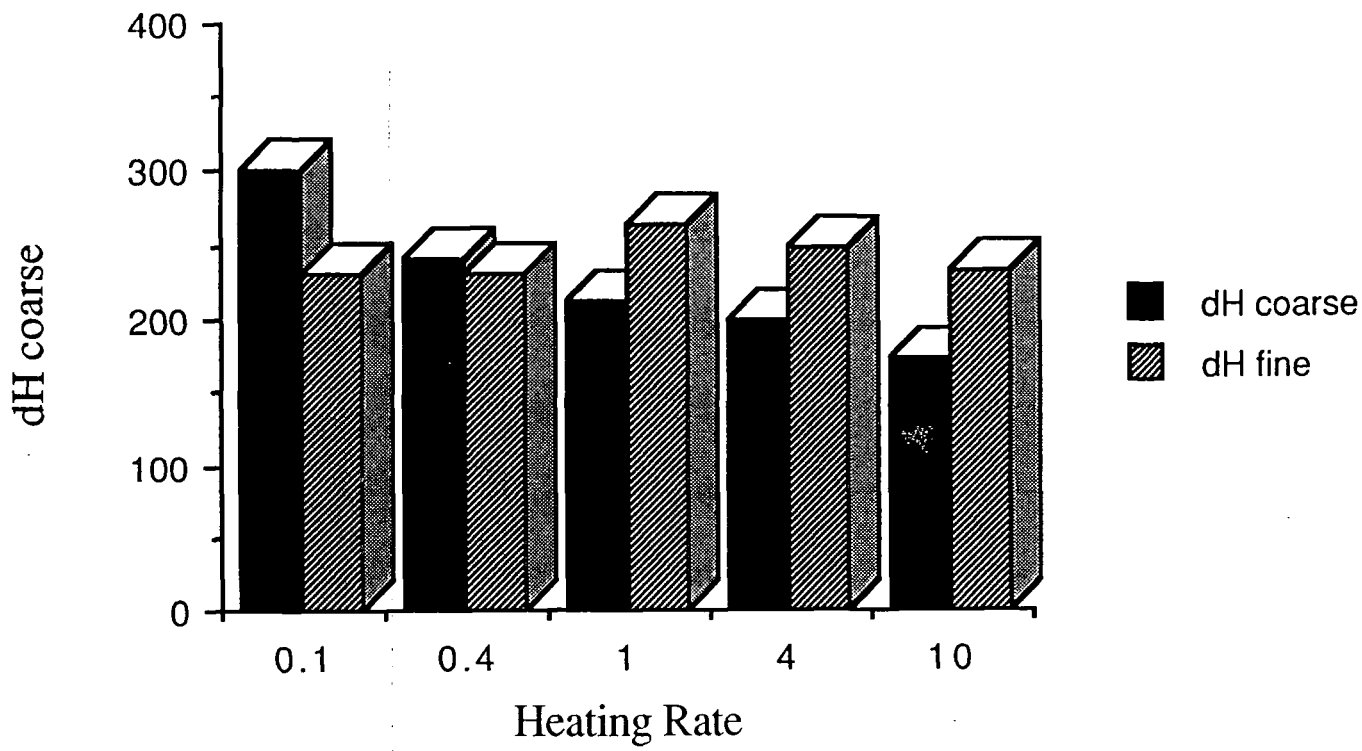

4.3.5.3 Analysis of Peak Maxima Temperatures for [$Zn(acac)_2$]

The first thermal feature seen in the traces of $Zn(acac)_2$ (see Figures 4.18-4.21) was too irregular in size and position to be meaningfully analysed in the same way as the peaks of $Zn(acac)_2.H_2O$. There were no such problems with the second feature, and analysis of the peak maxima temperatures showed that the figures closely matched those of peak III for $Zn(acac)_2.H_2O$ (see Figure 4.24), strengthening the theory that both peaks were due to the melting of $Zn(acac)_2$.

4.3.5.4 Enthalpies [$Zn(acac)_2.H_2O$]

4.3.5.4.1 Peak I

Figure 4.25 shows the ΔH values recorded for peak I. The 'coarse' samples show a clearly decreasing trend with increasing heating rate. Although the differences between some of the values for the 'fine' samples were just as obvious, a distinct trend could not be identified. This was probably due to errors in the enthalpy measuring methods; it was often difficult to pinpoint the baseline position at the onset of peak I because it was difficult to assess exactly where peak I began. This also made it difficult to decide on a starting temperature for the runs, and in some cases, part of peak I may not have been recorded. This would have been most likely at the lower rates of heating, which began at higher temperatures. Compensating for such errors gives a trend of decreasing peak I enthalpy values as the heating rate was increased, and, at a given heating rate, enthalpy values were higher for the 'fine' samples.

Taking the enthalpy value to be a measure of the fraction of the sample which has undergone the peak I process (probably evaporation) then it follows that the 'fine' sample heated at 0.1°C/min was nearest to completion and the 'coarse' one heated at 10°C/min was the furthest. This would be expected if the process were evaporation (of water of crystallisation) as it is governed by diffusion which is favoured by slow heating rates and small particle sizes.

The great disparity in the figures indicates that in many circumstances a sizeable

proportion of $Zn(acac)_2.H_2O$ does not undergo the peak I process. Presumably a competing process, favoured by quick heating rates and large particle size, is taking place.

4.3.5.4.2 Peak II

Figure 4.26 shows two clear trends in the enthalpy values for peak II; the first was a rapid increase in the size of the peak with an increase in heating rate, and the second was the greater size of the 'coarse' sample's peak (in comparison to the 'fine' sample) at a given heating rate. These trends were completely opposite to those observed for peak I, implying that there is a direct relationship between the two processes e.g. some $Zn(acac)_2.H_2O$ lost its coordinated water (giving rise to peak I) whilst the remainder of the $Zn(acac)_2.H_2O$ was involved in some other process resulting in peak III. Alternatively peak II could have involved 'lingering' volatiles from the peak I process.

4.3.5.4.3 Peak III

A general decline in the magnitude of peak III with an increase in heating rate can be observed in Figure 4.27. The only value that disagreed with this pattern was the one obtained from the 'fine' sample heated at 4°C/min. This discrepancy was probably due to the inclusion of a fourth peak, eclipsed by peak III. This error was not made for the other calculations because the fourth peak was clearly identifiable as a shoulder.

Figure 4.26 Peak II enthalpies

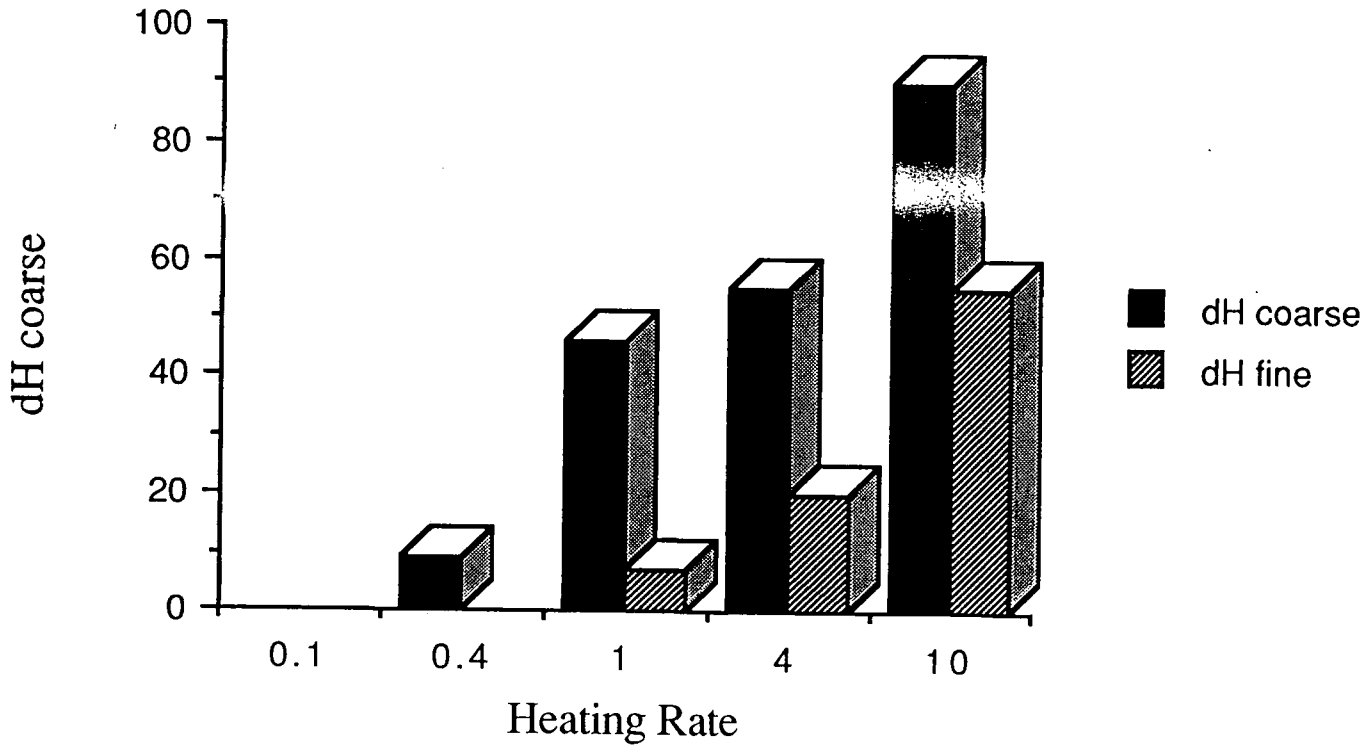

Figure 4.27 Peak III enthalpies

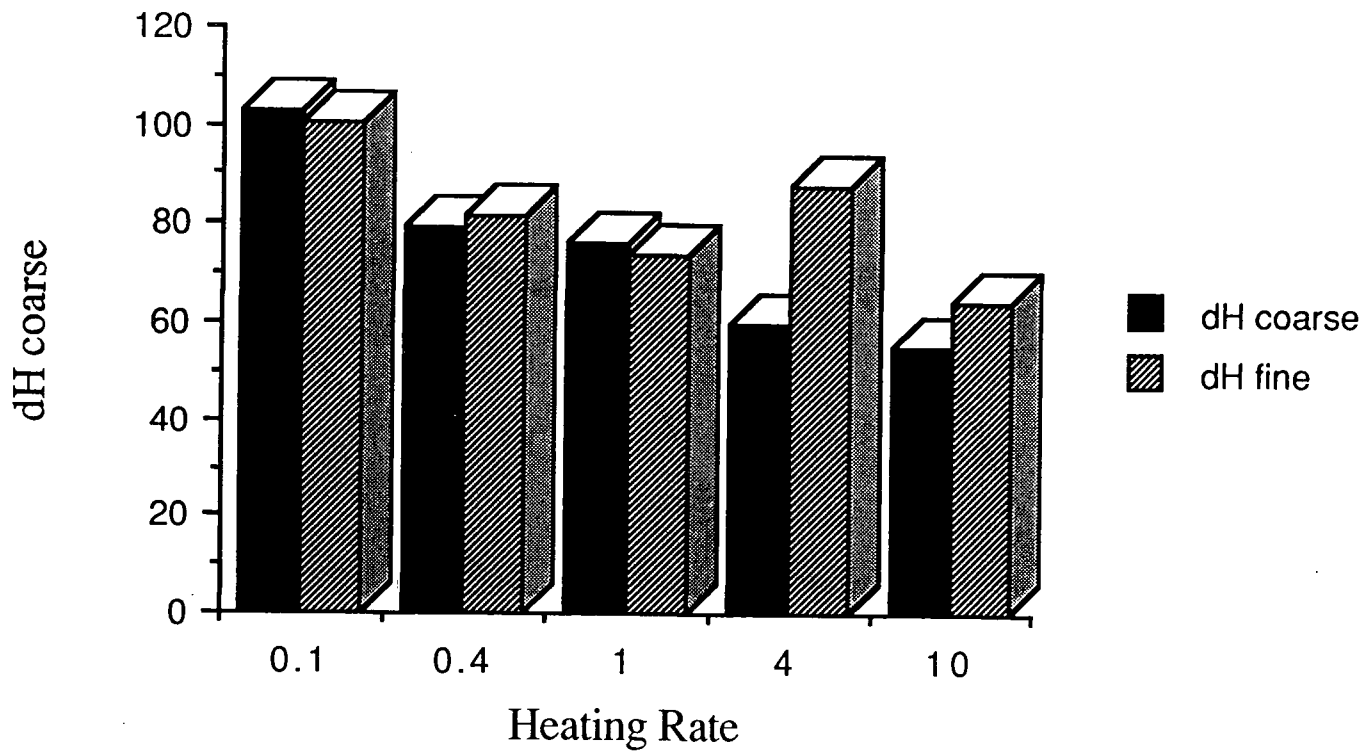

Figure 4.28 'Fine' $Zn(acac)_2.H_2O$, 10.0°C/min

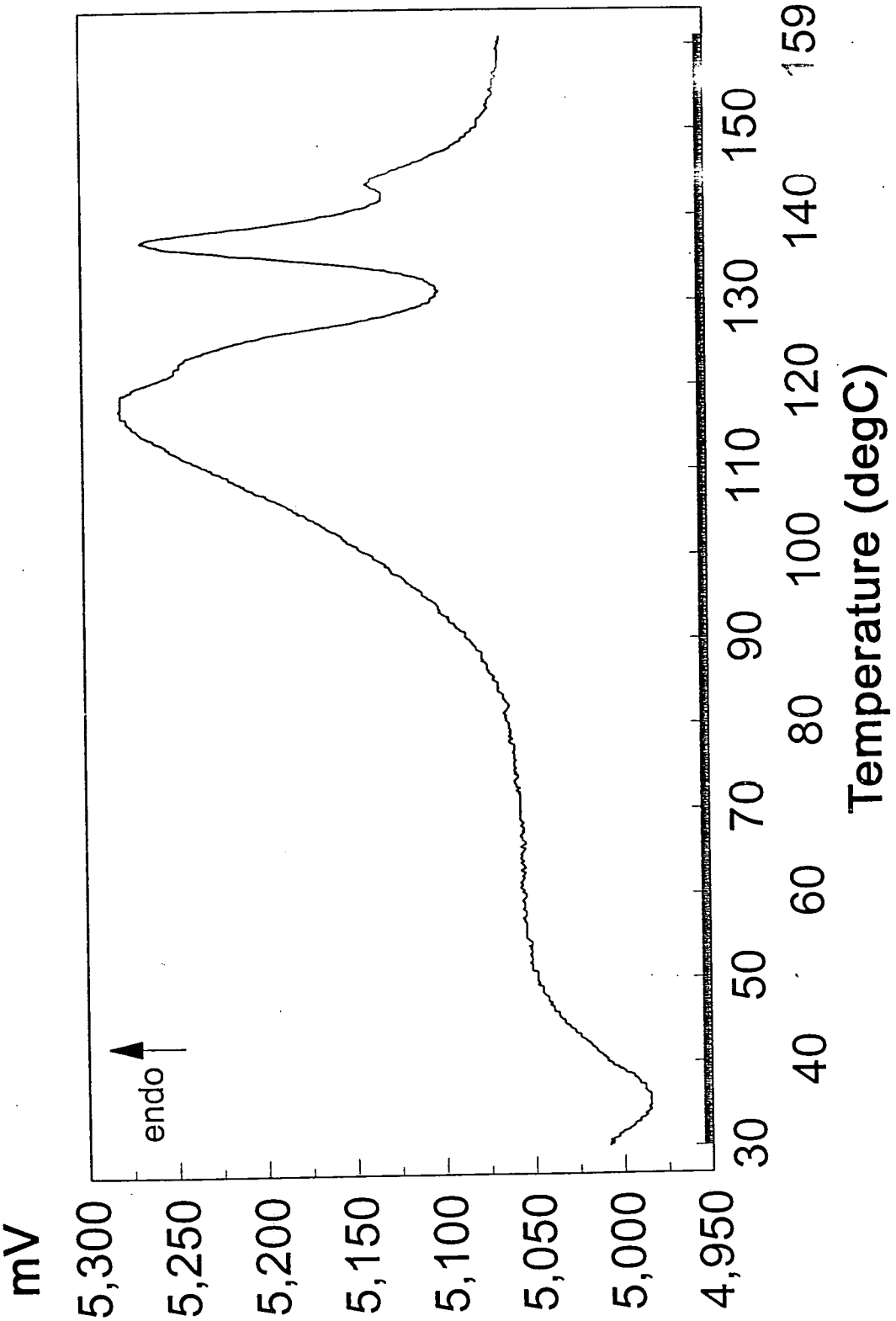

At first glance, the declining magnitude of peak III fitted well with the similar trend observed for peak I. However analysis of the enthalpy calculation method revealed a more complicated situation.

The calculations were performed using the sample weight as the denominator. This type of analysis therefore works well for peak I processes, and the trend associated with peak II was too clear to be worried about small errors. However, for peak III measurements, the real sample weight would have been lower than the original sample weight used in the calculations (due to the loss of volatiles). Such an error would have led to a falsely high enthalpy value. A larger weight loss for a sample would have led to a greater error in the enthalpy value. For $Zn(acac)_2.H_2O$, low heating rates and particle size gave the greatest reductions in sample weight, after heating. Adjusting for these observations emphasises the trends observed for peak III, backing the theory that peak III was due to the fusion of $Zn(acac)_2$ i.e. more water loss from $Zn(acac)_2.H_2O$ rendered more $Zn(acac)_2$ to melt.

4.3.5.5 Enthalpies [$Zn(acac)_2$]

Only the enthalpies associated with the sharp endotherm (III), situated at approximately 130°C, were calculated, as the other feature in these traces was too irregular. The figures calculated were 81 J/g (1°C/min) and 73 J/g (4°C/min) for the 'coarse' samples and 65 J/g (1°C/min) and 65J/g (4°C/min) for the 'fine' samples (Error: +/- 5 J/g). However, work in the next section of this chapter shows that a larger percentage weight-loss was observed for samples with 'fine' particle size, resulting in relatively smaller sample sizes (compared with the 'coarse' material) and consequently lower enthalpy values.

4.3.6 Weight Loss Measurements

4.3.6.1 Introduction

All the d.s.c. samples described above were weighed accurately on a five figure balance (see Chapter 2) before and after heating. These figures were used to calculate the percentage weight loss of the samples. In addition to the measurements made at the end of the traces, some readings were taken at various points during the scan (see Figure 4.29) to try and ascertain the contribution to weight loss of each peak process.

The accuracy of the weighing balance meant that the weight-loss percentages could be reliably quoted to the nearest 1%. However the residues displayed a tendency to reabsorb moisture when removed from the argon flow. This was necessary when weighing the samples and led to slightly variable results. Nevertheless, over the course of many scans, some trends were observable.

4.3.6.2 Results

The majority of the data collected was for 'coarse' samples. It was interesting to note the large reduction in weight, which occurred at higher temperatures after the distinct peaks (I-IV) in the scans had occurred. For example, when the heating rate was 2°C/min, 10% of the weight was lost up to 150°C, compared with 75% up to 400°C (instrument maximum). Although the region 150-400°C lacked any identifiable peaks, it did show a 'wandering baseline' indicating some thermal activity. The black tarry deposit recovered at 400°C indicated the complete break up of the acetylacetonate ligand.

As expected, samples heated at the slower rates exhibited a larger percentage weight loss at the end of the scan (140-160°C) than those heated more quickly. This was due to the increased time available (at slower heating rates) for the loss of volatiles from the sample pan.
Using a heating rate of 1°C/min, which gave three distinguishable peaks,

Figure 4.29 'Coarse' $Zn(acac)_2.H_2O$, 1.0°C/min

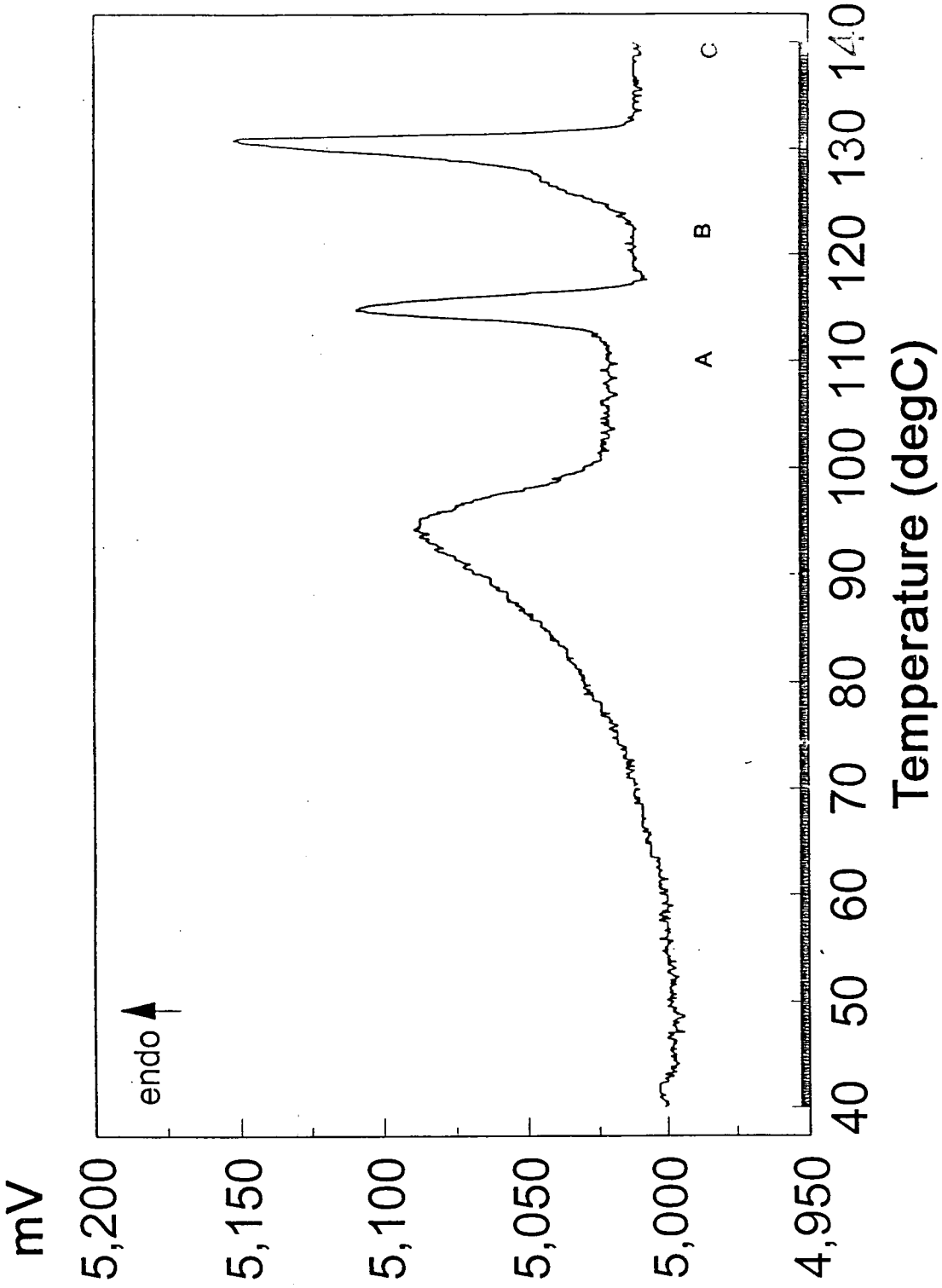

measurements were made after each peak i.e. at 110°C (A), 122°C (B) and 140°C (C) and at the end point, 160°C (D) (see Figure 4.29). The figures obtained were 3-4% at point A, ~8% at B, 9-11% at C, and at point D, ~14%. The calculated weight loss for the dehydration reaction (below) - the proposed peak I process- is 6.4%. The value obtained at point A (i.e. 3-4%) indicated that incomplete water loss had occurred, assuming that the peak I process was as proposed. It should be noted that the inevitable reabsorption of moisture during weighing will have contributed to the apparently low value obtained at point A but the ΔH measurements discussed earlier (section 4.3.5.4) confirmed that incomplete dehydration was the significant factor.

The values obtained for points B,C and D showed that weight loss was associated with peaks II and III. However this could have been misleading as it was thought that steady sublimation of $Zn(acac)_2$ and/or $Zn(acac)_2.H_2O$ from the capsule could have been contributing to weight loss.

Weight loss values for 'fine' samples were consistently higher than those for the corresponding 'coarse' sample. This was expected, as section 4.3.3 and 4.3.5 had shown, since 'fine' samples led to the earlier completion of all the peaks, compared to 'coarse' samples. The high values supported the theory that readsorption of moisture, which would be higher for 'fine' samples because of the greater surface area, was not greatly significant.

4.3.7 Reheating Experiments

4.3.7.1 Introduction

The most interesting results obtained at I.C.I. Wilton (see Section 4.2) were those for samples which were heated , cooled and then re-heated. Following the detailed study of primary scans, it was decided that the Durham work should proceed onto reheating experiments with the hope that this would shed further light on the intriguing thermal behaviour of $Zn(acac)_2.H_2O$.

4.3.7.2 $Zn(acac)_2.H_2O$

All three experiments, conducted with 'coarse' $Zn(acac)_2.H_2O$, consisted of a 1°C/min primary scan, cooling (>-10°C/min), and a re-heating scan at 4°C/min. The primary scans were run to points A (110°C), B (122°C) and C (140°C) (see Figure 4.30); all three reheat scans were run between 30°C and 200°C. The object of the three experiments was to try and ascertain whether the processes responsible for peaks I, II and III were reversible. It was hoped that the experiments would show the difference between an irreversible process in a dry atmosphere such as loss of coordinated water, and a reversible one such as fusion.

In the first experiment, the sample was heated past peak I (110°C, point A), cooled back to room temperature and then reheated to 160°C. The reheat trace (not shown) exhibited peaks II and III, but no trace of peak I, indicative that peak I was an irreversible process (when conducted in a dry atmosphere) and could be attributed to water loss.

A similar result was obtained for the second experiment (point B) in which the primary scan contained both peaks I and II and the reheat scan showed peak III only. In both the first two experiments, cooling and reheating during the thermal activity of $Zn(acac)_2.H_2O$ appeared to have no effect on the overall outcome. This was not the case when the primary scan covered all three peaks (see Figure 4.30). As the reheat trace (Figure 4.31) shows, peak III was repeated, adding weight to the theory that fusion was responsible for the peak. However the trace also, unexpectedly, exhibited two other peaks: a small endotherm (onset 97°C)

Figure 4.30 'Coarse' $Zn(acac)_2.H_2O$, 1.0˚C/min

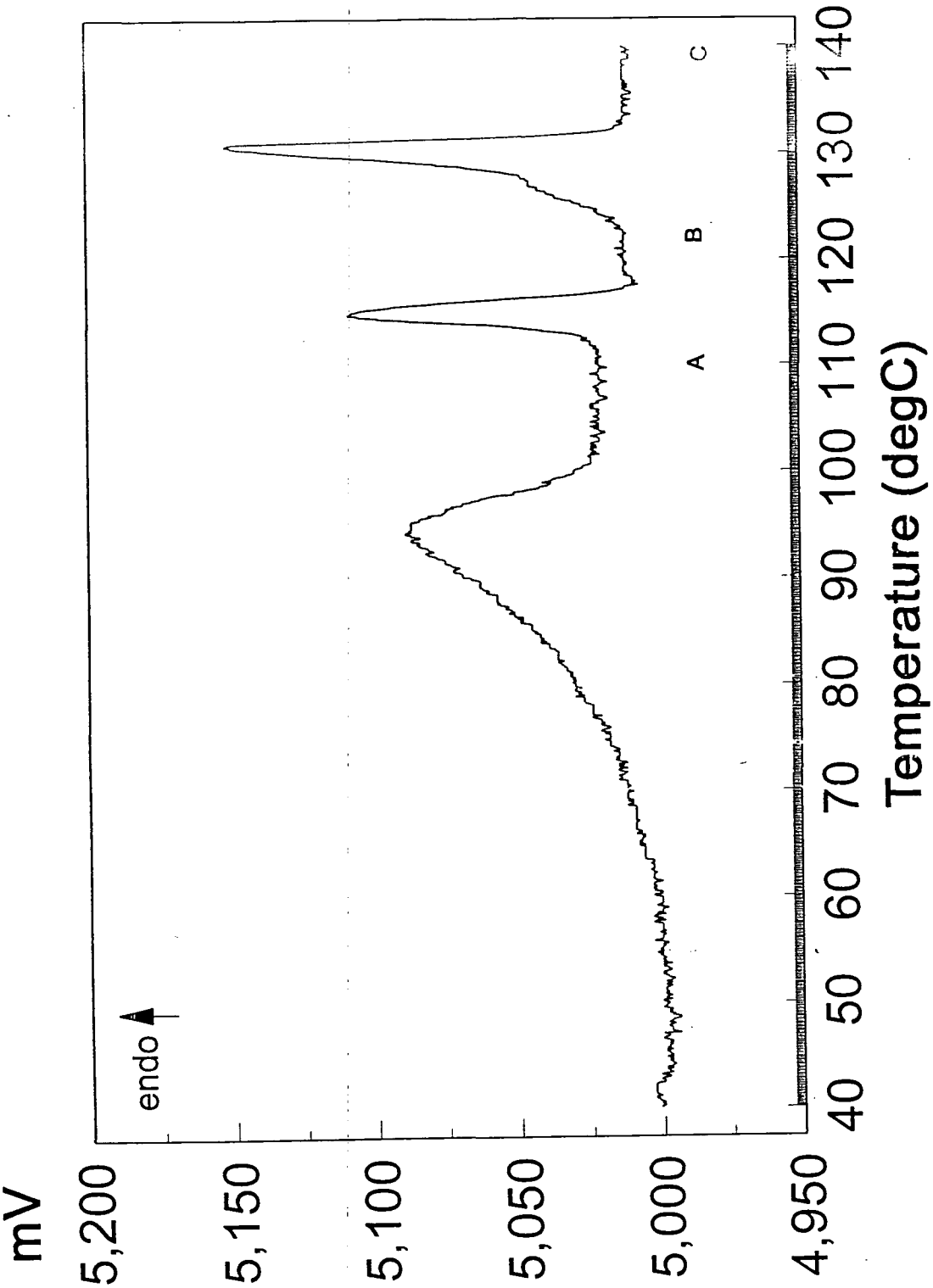

Figure 4.31 Reheating - 4°C/min

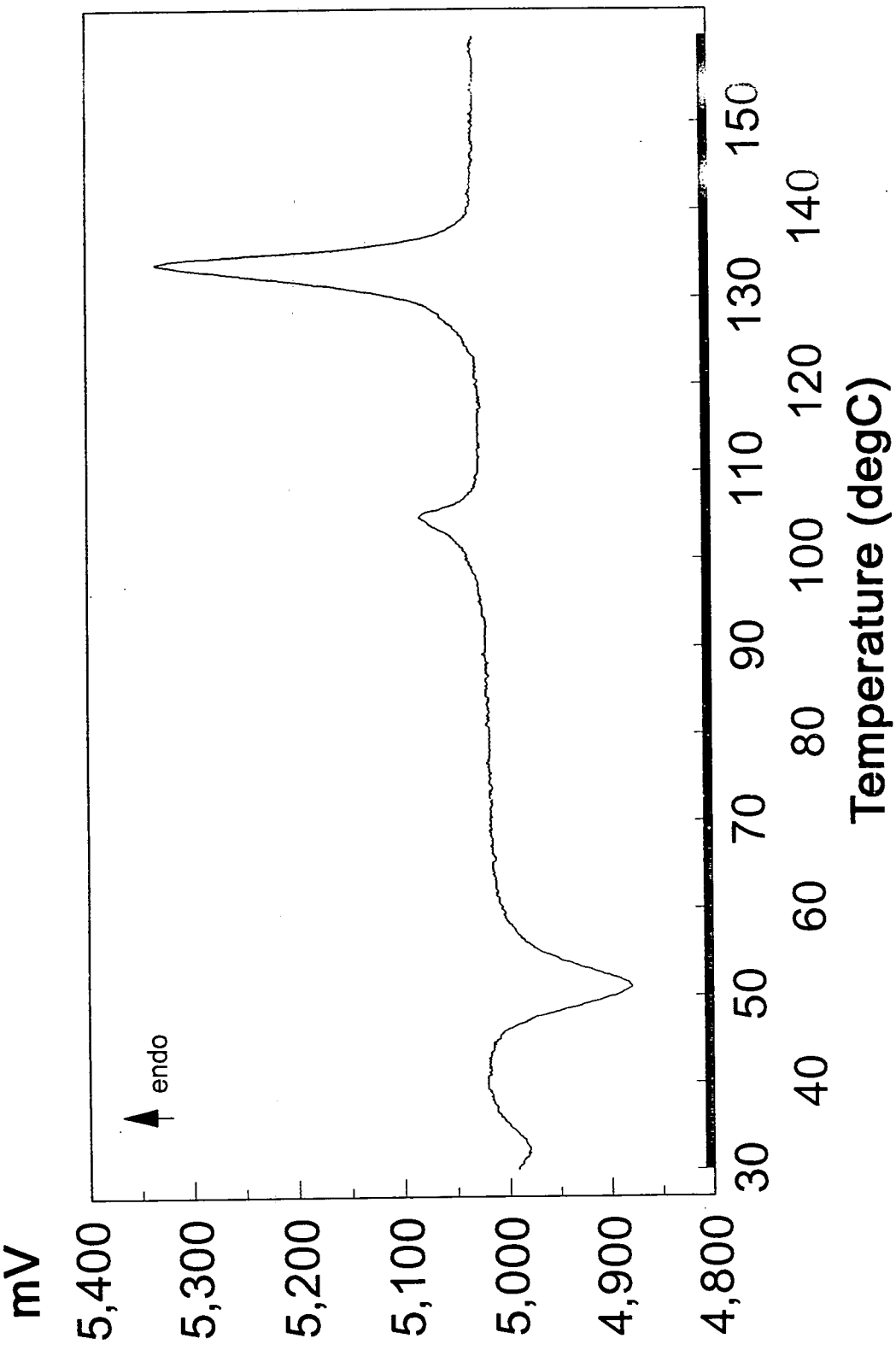

and an exotherm (onset ~45°C). In subsequent repeats of this experiment, the small endotherm was not observed. The exotherm could have been the result of energy released during a rearrangement of the sample to a less energetic form. The higher energy form could have been 'trapped' by rapid cooling.

When a sample of anhydrous $Zn(acac)_2$ was heated to 140°C, cooled and then reheated (i.e. using the same conditions as the 'point C' experiment above) the reheat scan was almost identical to the reheat scan in the third (point C) $Zn(acac)_2.H_2O$ experiment, indicating that after heating both $Zn(acac)_2.H_2O$ and $Zn(acac)_2$ both the final residues are the same.

4.4 Conclusions

At low rates of heating (<0.4°C/min) the d.s.c. trace of $Zn(acac)_2.H_2O$ showed a simple process involving only two peaks (I and III). Peak I was almost certainly due to the loss of coordinated water, and peak III due to the melting of anhydrous $Zn(acac)_2$. At higher heating rates the picture became more complex, with the appearance of two additional peaks (II and IV). Peak II's tremendous variation with heating rate and particle size indicated that it was connected with un-dehydrated $Zn(acac)_2.H_2O$, possibly a rearrangement to a higher energy form, or an interaction requiring both residual water and a high enough temperature. Peak IV looked to be directly related to peak II e.g. volatilisation of a compound formed by the process resposible for peak II. Further conclusions on the thermal behaviour of $Zn(acac)_2.H_2O$ including the possible identity of any products of a reaction involving residual water are included in Section 5.5.

Anhydrous $Zn(acac)_2$ presented a similar picture. Two peaks were observed; one irregular one, due to the vaporisation of absorbed moisture, and one due to the melting of $Zn(acac)_2$, identical to peak III of the $Zn(acac)_2.H_2O$ scans.

Although much of the basic thermal behaviour of $Zn(acac)_2.H_2O$ was identified using differential scanning calorimetry, the more complex scans of $Zn(acac)_2.H_2O$ were still unclear. For this reason it was decided to use alternative forms of

thermal analysis, described in Chapter 5.

References

1. A.J.C. Fiddes, personal communication.
2. Aldrich Catalogue, Handbook of Fine Chemicals, 1992-3, 1342.
3. R.G. Charles and M.A. Pawlikowski, *J. Phys. Chem.*,1958, **62**, 440.
4. J. Von Hoene, R.G. Charles and W.M. Hickam, *J. Phys. Chem.*, 1958, **62**, 1098.
5. G. Rudolph and M.C. Henry, *Inorg. Chem.*, 1964, **3**, 1317.
6. G. Rudolph and M.C. Henry, *Inorg. Chem.*, 1965, **4**, 1076.
7. K.-H. Ohrbach, G. Radhoff and A. Kettrup, *Themochim. Acta*, 1983, **67**, 189.
8. H. Kido, *Ariake Kogyo Koto Senmon Gakko Kiyo*, 1986, **22**, 17.
9. M.J. Glavas and T.J. Ribar, *Glas. Hem. Dms. Beograd*, 1967, **32**, 229.
10. S. Poston and A. Reisman, *J. Electron. Mater.*, 1989, **18**, 553.
11. J.D.B. Smith, J.F. Meier and D.C. Phillips, *J. Therm. Anal.*, 1977, **11**, 423.
12. G. Rudolph and M.C. Henry, *Inorg. Synth.*, 1967, **10**, 74.
13. M.J. Bennett, F.A. Cotton and R. Eiss, *Acta Cryst.*, 1968, **B24**, 904.

Chapter 5

Further Studies of the Thermal Behaviour of $Zn(acac)_2.H_2O$

5.1: Introduction and Background

The experiments about to be described came about as a result of Mr. A.J.C. Fiddes' discovery that ZnO was formed when an alcoholic solution of $Zn(acac)_2.H_2O$ was sprayed onto a glass substrate heated to 96°C[1]. Despite the unusual experimental conditions, decomposition at such a low temperature was a surprise. The static thermal study - by differential scanning calorimetry (Chapter 4) - indicated a complicated thermal behaviour for $Zn(acac)_2.H_2O$. The d.s.c. method was chosen because it was the most practical way of studying the thermolysis; however, it was not possible to obtain a complete rationalisation of the decomposition using this method.

At this point very little attention had been paid to the residues formed in the d.s.c. experiments. One exception to this was one of the very first scans of $Zn(acac)_2.H_2O$ at Durham; the sample was heated to 150°C at 5°C/min and the resulting residue was analysed. Infra-red and mass spectroscopy only showed the presence of $Zn(acac)_2$ (anhydrous). However, the elemental analysis indicated that the residue contained 40.5% carbon [n.b. 42.65% C in pure $Zn(acac)_2.H_2O$ and 45.57% C in the anhydride, $Zn(acac)_2$]. The reduction in the percentage carbon could only have occurred if volatilisation of a compound (or compounds) containing more than 45.57% carbon had taken place. Such a volatilisation would necessarily have been preceded by decomposition , which would have produced at least one volatile 'carbon-rich' compound and at least one involatile 'carbon-deficient compound'. Both infra-red and mass spectroscopy of the residue failed to identify anything other than $Zn(acac)_2$. This indicated that the residual decomposition product(s) were probably present in low concentrations, had low volatility, and were relatively infra-red inactive, e.g. ZnO.

This author felt that the residues of d.s.c. experiments required further study. However, the scale of the average experiment meant that it was usually only possible to obtain 3 or 4mg of residue - clearly insufficient if any decomposition

products were to be isolated. With this in mind, the author decided to use conventional apparatus to mimic conditions in the calorimeter and thereby provide larger quantities of the products of heating $Zn(acac)_2.H_2O$ (see below).

5.2: The Experiments

The studies can be neatly divided into six experiments (A-F). These were all conducted in a pyrex tube through which a constant flow of nitrogen was maintained. The pyrex crucible, containing the $Zn(acac)_2.H_2O$ sample, was situated in the half of the pyrex tube that was housed in an electric furnace. The other half of the tube was cooled by means of a water jacket. Experimental details can be found in Chapter 2 (Section 2.2). The variables particular to each experiment are outlined below.

5.2.1: Themolysis Experiment A (0.4°C/min, 105°C, 12 min. dwell).

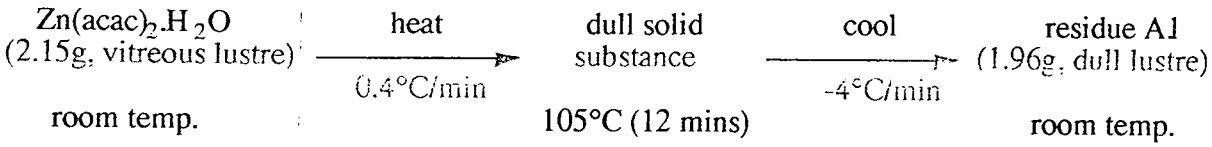

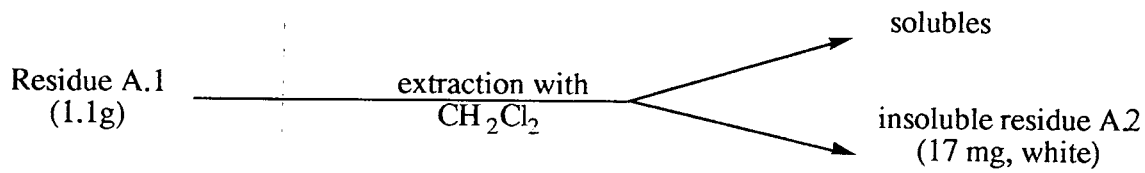

Analysis methods:

Residue A.1: C,H elemental analysis, i.r., ^{1}H n.m.r.

Residue A.2: X-ray diffraction

5.2.2: Thermolysis Experiment B (0.4°C/min, 120°C, 12 min dwell).

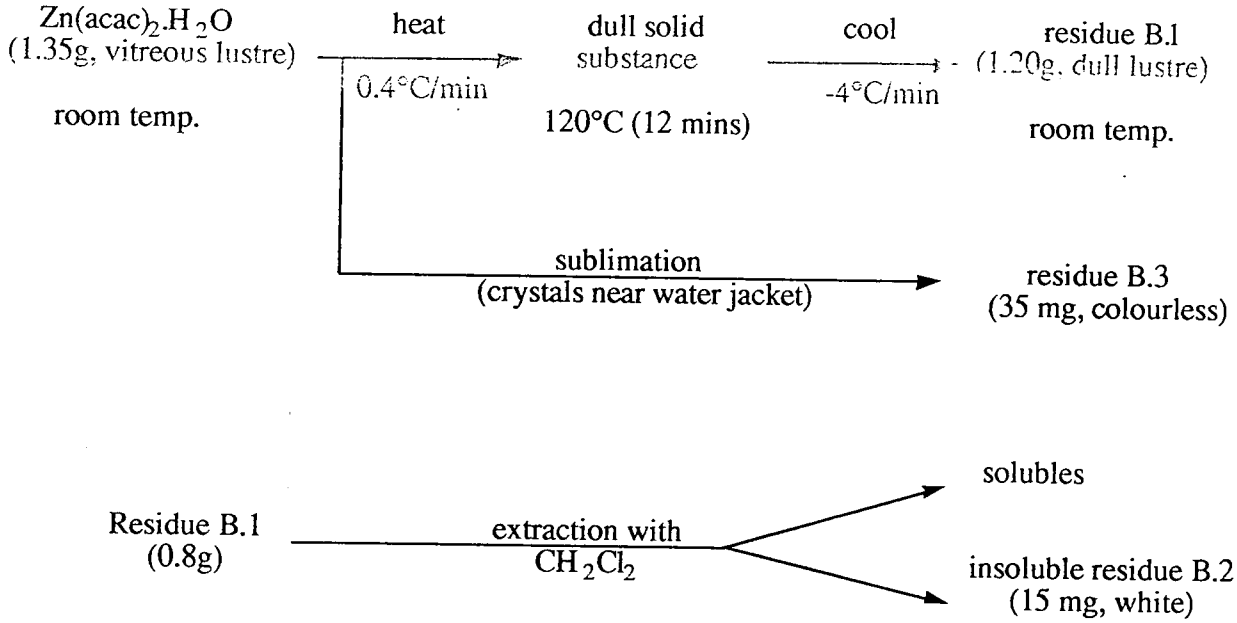

Analysis methods:

Residue B.1: C,H analysis, i.r., ^{1}H n.m.r.

Residue B.2: X-ray diffraction

Residue B.3: i.r.

5.2.3: Thermolysis Experiment C (0.4°C/min, 140°C, 12 min dwell).

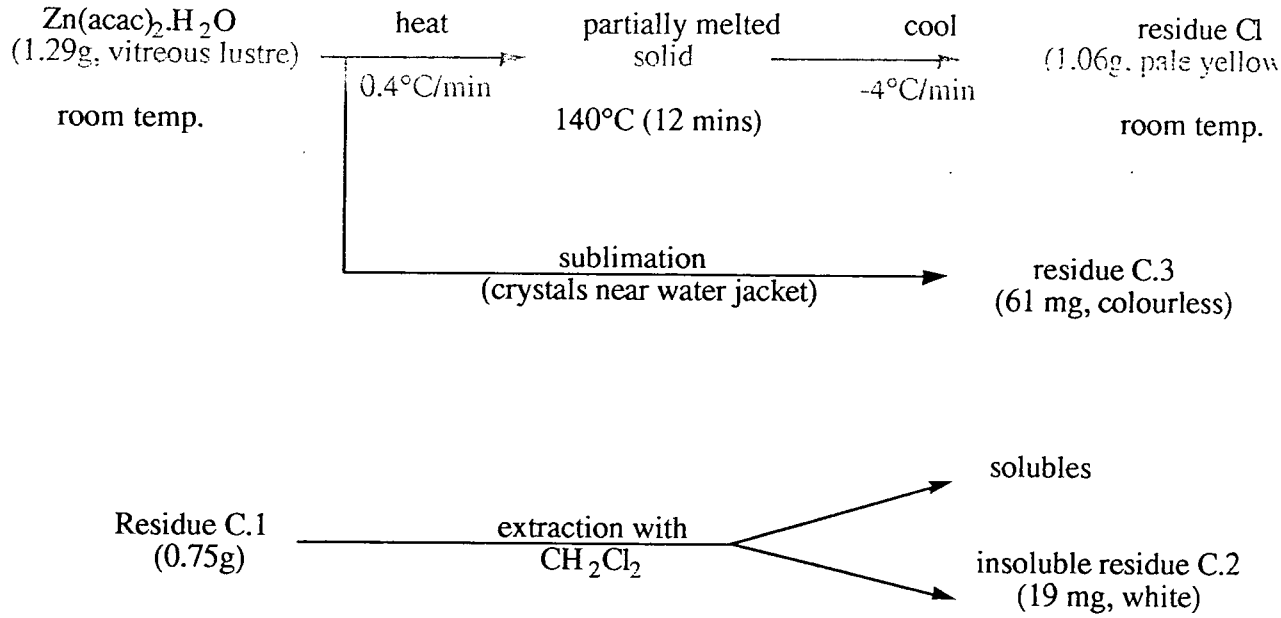

Analysis methods:

Residue C.1: C,H analysis, i.r., ^{1}H n.m.r.

Residue C.2: X-ray diffraction

Residue C.3: C,H analysis, i.r.

5.2.4: Thermolysis Experiment D (0.4°C/min, 120°C, 12 min dwell).

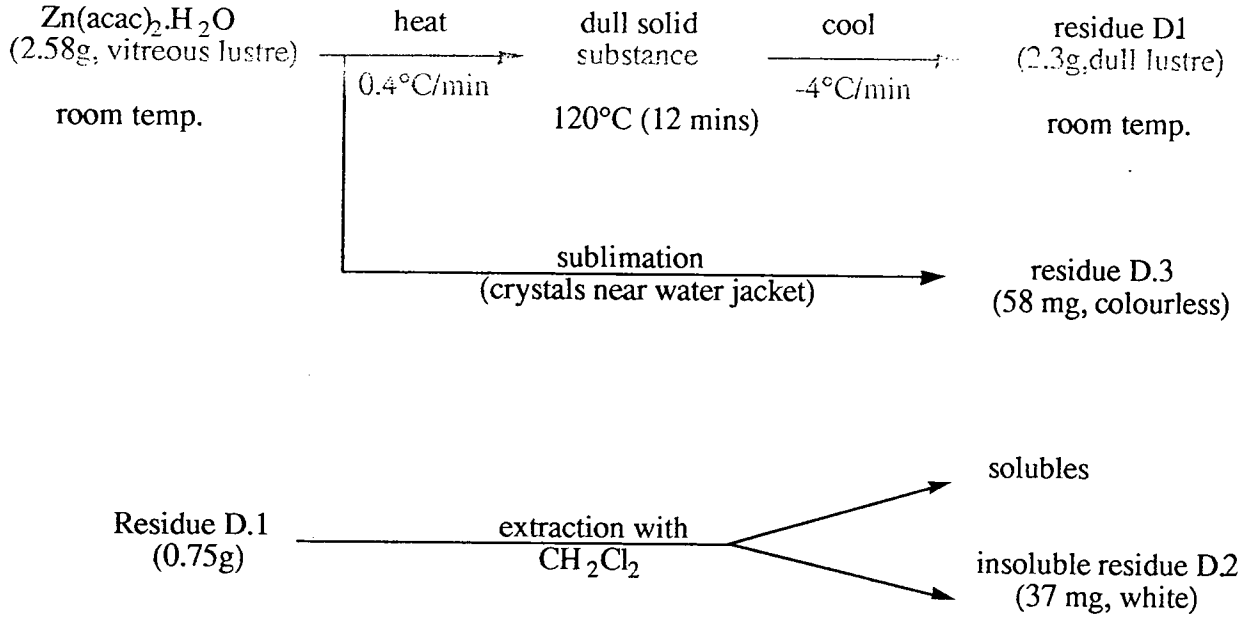

Analysis methods:

Residue D.2: C,H and Zn elemental analysis and i.r.

5.2.5: Thermolysis Experiment E (0.4°C/min, 120°C, 2 hour dwell).

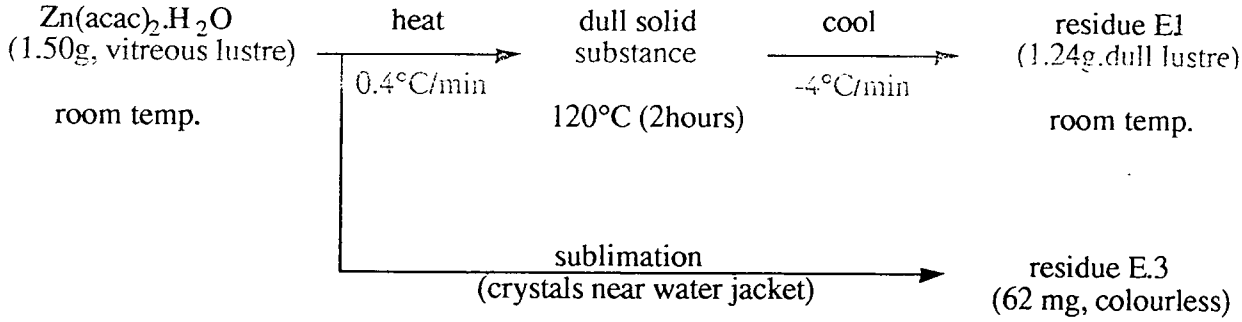

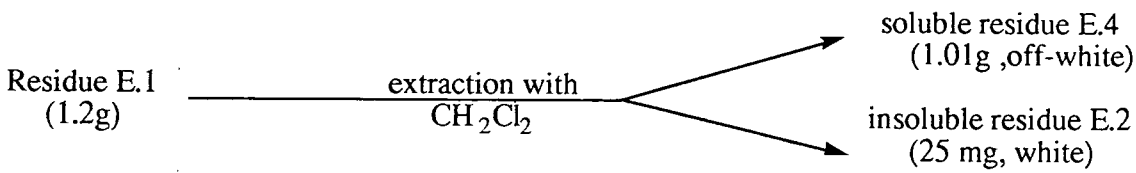

Analysis methods:

Residue E.2: C,H and Zn elemental analysis, i.r.

Residue E.4: C,H and Zn elemental analysis, i.r.

5.2.6: Thermolysis Experiment F (2°C/min, 120°C, 12 min dwell).

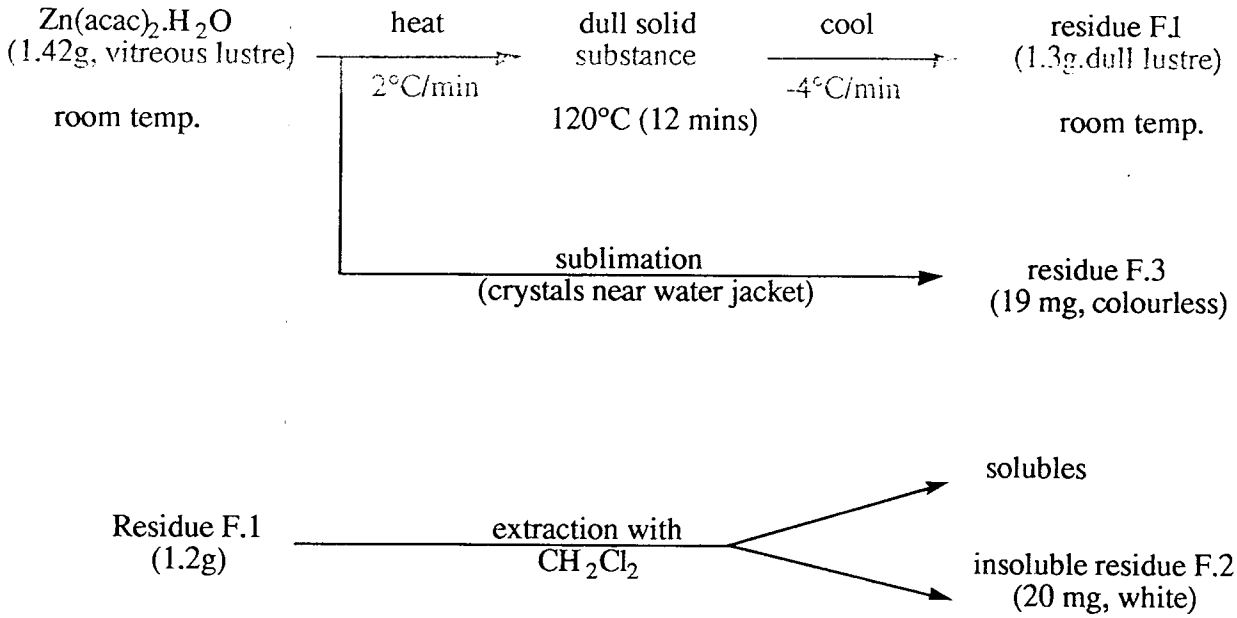

Analysis methods:

Residue F.1: C &H elemental analysis, i.r. , ^1H n.m.r.

Residue F.2.: C, H and Zn elemental analysis, i.r. , X-ray diffraction.

5.3. Analysis

R is a generic term used to represent experiments A to F (e.g. R.1 means A.1, B.1 etc.).

5.3.1 Elemental Analysis

	Element %		
Compound	C	H	Zn
A.1	44.5	5.2	
B.1	44.3	5.3	
C.1	44.9	5.2	
F.1	44.3	5.0	
D.2	13.0	1.7	36.3
E.2	11.6	1.4	40.3
F.2	26.8	3.3	22.9
B.3	45.2	5.0	
C.3	45.1	5.0	
E.4	45.3	5.3	25.6
$Zn(acac)_2.H_2O$	42.7	5.7	23.2
$Zn(acac)_2$	45.6	5.4	24.8
ZnO	----	----	80.3

Table 5.1

At first glance there appeared to be a marked contrast between the percentage carbon found in the R.1 (R=A,B,C or F) residues and that found in the d.s.c. residue (40.5%, *cf.* Section 5.1). However, the bulk of the R.I residues were anhydrous $Zn(acac)_2$ (see Section 5.3.3), whereas the majority of the d.s.c. residue was $Zn(acac)_2.H_2O$. Both sets of percentage carbon figures were slightly lower than would have been expected if the residues had been pure $Zn(acac)_2$ or $Zn(acac)_2.H_2O$;the shortfall indicated the presence of an imurity or impurities (with low carbon content) formed during the heating of $Zn(acac)_2.H_2O$.

Elemental analyses of a sample of each of the residues R.2 (R=D,E or F) were very

inconsistent, indicating that this insoluble material was an inhomogeneous mixture. However, there was some indication that the ratio of carbon to hydrogen in the mixture was roughly constant at 2:3.

5.3.2 Infra-red Spectroscopy

As the elemental analyses for each group of residues R.1, R.3 and R.4 indicated that they were all very similar, with the major component some form of $Zn(acac)_2$, it came as little surprise that their infra-red spectra were also similar. However, it was hoped that an insight into the slight differences between the residues would be gained.

A comparison was made between the recorded spectra and published infra-red work on $Zn(acac)_2$ and $[Zn(acac)_2]_3$[2-4], and adducts of $Zn(acac)_2$[5-10] contained in the literature. The major differences were noted in the region below 1300cm^{-1}; the absorption bands are listed in Table 5.2.

Before considering the examples from the literature it is worth noting that the absorption bands show that R.3 (sublimed product) and R.4 (solubles from extraction) were identical, and that R.1 (original solid residue) was a different, but closely related, compound or mixture.

The literature appeared to contain no definitive infra-red spectra for either monomeric or trimeric Zn(acac)2! Both Lawson[2] and Nakamoto *et al.*[3] purified their material by sublimation, which was also how the residues R.3 were produced. However, all three spectra were slightly different, e.g. in the region 700-900cm^{-1} Nakamoto *et al.*[3] noted one peak (769cm^{-1}), Lawson[2] noted two (769 and 780cm^{-1}), and this author noticed three (775, 785 and 804cm^{-1}). Single crystal studies of residue E.3, conducted by Prof. W. Clegg (University of Newcastle upon Tyne), showed it to have exactly the same space group and cell dimensions as

$[Zn(acac)_2]_3$[11]. From this, it seems reasonable to suggest that the materials studied by Lawson[2] and Nakamoto *et al.*[3] were predominantly $[Zn(acac)_2]_3$ with some contamination. The most likely source of this impurity would be $Zn(acac)_2.H_2O$ which is formed when $[Zn(acac)_2]_3$ is exposed to atmospheric moisture[11]. This theory is strengthened by the similarities evident between the spectrum of Nakamoto *et al.*[3] and that recorded by Niven and Thornton[5] for $Zn(acac)_2.H_2O$. (Niven and Thornton[5] used the same preparation as Lippert and Truter[12] used for their crystal structure determination.)

Having established residues R.3, and consequently R.4 , as the trimer, it did not appear unreasonable to suggest that R.1 was (at least mainly) the monomer, $Zn(acac)_2$. This would not be unexpected given the experimental conditions: R.3 and R.4 were formed in mobile environments (sublimation and solution respectively), whereas R.1 was produced under static conditions (solid state). However, it should be remembered that according to the literature[13] $Zn(acac)_2$ monomer is meta-stable, and on this basis it would not be surprising to see a gradual change in the i.r. spectrum due to slow formation of the trimer.

Fackler *et al.*[4] attempted to record the spectra of the two different forms (monomer and trimer) by trapping $Zn(acac)_2$ vapour in a carbon dioxide matrix at 77K, but again there were differences between their results and those of this author. In particular, the spectrum Fackler *et al.*[4] recorded for the "monomer" at room temperature, closely resembled the one this author recorded for the trimer, illustrating the tendency for the monomer to trimerise.

Most of the differences between the spectra of R.1 and R.3 (and R.4) appeared to be either slight shifts or splittings of the same bands. Only one band appeared unique to any spectrum - the one at $860cm^{-1}$ in R.1. Significantly, this band also occurred in the spectra of residues R.2, indicating that it belonged to the insoluble component of R.1. The otherwise inconsistent spectra of residues R.2 (insoluble material from CH_2Cl_2 extraction of R.1) also exhibited some bands consistent with

Table 5.2 Absorption bands occurring below 1300cm^{-1}

Author	Lawson[2]	Nakamoto *et al.*[3]		Fackler *et al.*[4]				Niven *et al.*[5]			
Compound	$[Zn(acac)_2]_x$	$[Zn(acac)_2]_x$ obs.	calc.	$Zn(acac)_2$ at 77K	at 298K	$[Zn(acac)_2]_3$ at 77K	at 298K	$Zn(acac)_2.H_2O$	R.1	R.3	R.4
Absorption bands (cm^{-1})	1269	1264	1266	1263/7m	1263s	1268m	1264s	1264	1267m	1263m	1260/7m
			1232								
	1208vw				1207w				1205vw	1209vw	1207vw
		1197		1198w	1197w	1198w	1197w	1191		1198vw	1197vw
	1022m	1019		1021m	1019m	1017m	1019m	1020	1014m	1017m	1017m
			937								
	927m	927		931m	928m	925m	927m	933	928m	935m	933m
			900								
									860vw		
					807w					804w	805m
					788w				785s	785w	785m
	780m			777m				779		775sh	
	769m	769		766m		773w	769w	772			
				728w							
				717w							
									678w		
	662w	666						656		667w	667w
		651							651w	650sh	650sh
			634							644w	645w
			590						580m		
								570		572w	572m
	565s	559						557		553w	553m
										545w	545w
									465m		
								439		450sh	450w
	426s	422	424					422		425m	422m
								413	412m		
	393m							388			
			373								
									275w		
			258								
			248					241	240m	248w	245m
								208			
			176					173			

$Zn(acac)_2$ and a broad band (400-600cm^{-1}) characteristic of zinc oxide.

5.3.3 ^1H n.m.r. Spectroscopy

^1H n.m.r. spectra in $CDCl_3$ were recorded for the residues A.1, B.1, C.1 and F.1. In all cases these showed data entirely consistent with $Zn(acac)_2$ in solution i.e. two singlets in a 1:6 ratio, the larger at 2.0 ppm (methyl protons) and the smaller at 5.4 ppm (CH proton). No other peaks were observed indicating that $Zn(acac)_2$ was the only soluble species (in $CDCl_3$) in residue R.1.

5.3.4 X-Ray Photography

X-Ray powder photographs were recorded for residues R.2 using a Guinea camera (see Chapter 2 for details). In contrast to the previous methods of analysis, all the photographs of R.2 were virtually identical. Close examination of the photographs indicated at least three components to the residue. One of these was $Zn(acac)_2$ which was probably present due to incomplete extraction. The lines belonging to this compound were very faint and inconsistent, indicating very small amounts. The second component was zinc oxide. Again the lines were faint but this was not necessarily an indication of small amounts as the material could well have been amorphous. The third component gave by far the strongest lines and the nine most significant are listed in Table 5.3 (below).

Table 5.3 X-Ray analysis of residues R.2

θ (°)	d (Å)	estimated intensity (100 = strongest)
11.72	3.79	80
15.11	2.96	100
18.16	2.47	50
21.85	2.07	40
23.98	1.90	20
24.70	1.85	30
24.88	1.83	40
29.04	1.59	30
30.84	1.50	20

Surprisingly, the literature did not reveal any compound that matched these d values. Either they were due to a mixture, which seemed unlikely given the simplicity of the photograph, or they were due to a compound (novel, new or otherwise) for which the powder photograph has not been previously recorded.

5.4 Conclusions

1. The differing heating rates, maximum temperatures and dwell times did not appear to significantly alter the chemistry that occurred when $Zn(acac)_2.H_2O$ was heated under a flow of nitrogen.

2. Three processes occurred during heating:

(a) Dehydration of $Zn(acac)_2.H_2O$ leaving the monomer, $Zn(acac)_2$.

(b) Sublimation of $Zn(acac)_2.H_2O/Zn(acac)_2$ which formed $[Zn(acac)_2]_3$ on condensation.

(c) A chemical reaction/decomposition producing zinc oxide and at least one other unidentified compound.

3. Extraction (CH_2Cl_2) of the residue (R.1) from the heating process produced $[Zn(acac)_2]_3$ from the solution and a solid residue containing zinc oxide and an unidentified compound.

4. Only one infra-red band (860cm^{-1}) was uniquely attributable to the unidentified compound and the X-ray powder photograph of this compound was unknown in the literature.

5.5 Conclusions to Chapters 4 and 5

Bearing in mind the close relationship between chapters 4 and 5, it is worth noting the overall conclusions these two chapters have produced.

1. When heated at a sufficiently low rate small quantities of $Zn(acac)_2.H_2O$ undergo a simple process: dehydration followed by melting of the resulting monomer, $Zn(acac)_2$.

2. When any of three variables - heating rate, sample size or particle size - are increased sufficiently, the process becomes significantly more complicated.

3. If complete dehydration has not occurred by a certain temperature the remaining water is involved in a reaction with $Zn(acac)_2.H_2O$ and/or $Zn(acac)_2$.

4. One product of this reaction is zinc oxide. However, other, as yet unidentified, compounds are produced. The literature[14,15] contains one example of the thermal decomposition of $Zn(acac)_2.H_2O$ where water is necessary. However, the products formed in this example [$Zn_2(acac)_3(OAc)$ and zinc acetate] were not produced in any of the experiments in chapters 4 and 5. Despite this, it seems likely that any reaction would involve water attacking the metal/acac ring unit.

5. When the above reactions take place, the d.s.c. trace contains four peaks: two are due to the simple processes of dehydration and $Zn(acac)_2$ melting.

6. The other two peaks are endothermic and must be related (either directly or indirectly) to the reaction described in conclusion 3, e.g. involving further reaction, evaporation, sublimation etc.

7. Throughout these processes sublimation of $Zn(acac)_2.H_2O$ and/or $Zn(acac)_2$ produces $[Zn(acac)_2]_3$ as condensate.

References

1. A.J.C. Fiddes, personal communication.
2. K.E. Lawson, *Spectrochim. Acta*, 1961, 17, 248.
3. K. Nakamoto, P.J. McCarthy and A.E. Martell, *J. Am. Chem. Soc.*, 1961, 83, 1272.
4. J.P. Fackler, M.L. Mittleman, H. Weigold and G.M. Barrow, *J. Phys. Chem.*, 1968, 72, 4631.
5. M.L. Niven and D.A. Thornton, *Spectrosc. Lett.*, 1980, 13, 419.
6. M.L. Niven and D.A. Thornton, *S. Afr. J. Chem.*, 1979, 32, 135.
7. Y. Nakamura and K. Nakamoto, *Inorg. Chem.*, 1975, 14, 63.
8. M.L. Niven and G.C. Percy, *Transition Met. Chem.*, 1978, 3, 267.
9. M. Yaqub, R.D. Koob and M.L. Morris, *J. Inorg. Nucl. Chem.*, 1971, 33, 1944.
10. D.G. Batyr, V.N. Scheinker, A.D. Garnovskii, V.D. Brega, V.A. Chetverikova, V.E. Nirka, Y.Y. Kharitonov and G.N. Marchenko, *Koord. Khim.*, 1978, 4, 1835.
11. M.J. Bannett, F.A. Cotton and R. Eiss, *Acta. Crystallogr.* , 1968, B24, 904.
12. E.L. Lippert and M.R. Truter, *J. Chem. Soc.*, 1960, 4996.
13. K. Takegoshi, K.J. Schenk and C.A. McDowell, *Inorg. chem.*,1978, 26, 2552.
14. G. Rudolph and M.C. Henry, *Inorg. Chem.*, 1964, 3, 1317.
15. G. Rudolph and M.C. Henry, *Inorg. Chem.*, 1965, 4, 1076.

Chapter 6

Spray Pyrolysis of Aqueous Solutions of Zinc Formate Dihydrate

6.1 Introduction

The object of the experiments described in this Chapter was to investigate the feasibility of producing a transparent crystalline zinc oxide film, suitable for use as a semiconductor, using the spray pyrolysis technique. Because of safety precautions and environmental considerations (especially for future large-scale production), it was decided to only use aqueous-based precursor solutions. It was hoped that film production might take place at a low enough substrate temperature to permit the deposition of good quality films onto plastic surfaces.

Zinc oxide is a well known and widely used compound and many authors have described a variety of methods of producing films of this material. Sputtering is a common technique both in oxygen[1-3] and oxygen/inert gas mixtures[4]. By using plasmas, the technique can be conducted at low temperatures (<400°C)[4]. The film quality is influenced by the nature of the substrate[5].

Chemical vapour deposition (CVD), another widespread technique, has also been used to produce films at low temperatures[6,7].

Other methods employed include Calcination of zinc napthenate[8], decomposition of a wet film of $Zn(OH)_2$[9], and reactive ionised cluster beam deposition[10,11].

Spray pyrolysis is also a widely employed technique[12,13], A considerable range of precursors have been used. Aranovich *et al.*[14] used aqueous solutions of zinc chloride, and Nükura *et al.*[15] and Bahadur *et al.*[16] used aqueous zinc nitrate. Jean[17] produce ZnO films at 400°C and Kamata and Matsumoto[18] created c-axis orientated films by reacting vaporised $Zn(acac)_2$ with steam at substrate temperatures as low as 90°C (optimum: 350-450°C). A large volume of work in this area concerns zinc acetate[19-24]. Nobbs and Gillespie[19] used aqueous solutions of this compound to produce c-axis orientated films on a 500°C substrate. Janda and Kubovy[20] used the

same precursor, remarking on the simplicity of the spray pyrolysis technique. The same authors[21] also calculated that the average grain size of ZnO films produced by this method was a function of the substrate temperature and the deposition rate. Major *et al.*[22] produced indium-doped films of ZnO using zinc acetate and $InCl_3$ in water/IPA mixtures (substrate temperature 300-450°C). Jaffe[23] found that the optimum substrate temperature for producing good quality ZnO films from the spray pyrolysis of water/alcohol solutions of zinc acetate was 620°C. Other precursors used by the same author included zinc chloride, zinc monochloroacetate, zinc trichloroacetate, zinc nitrate and zinc formate. Jaffe commented that zinc formate's lack of solubility in water made film production laborious.

Lack of solubility did not impede this author's choice of zinc formate dihydrate as a precursor. At the intended substrate temperatures (200-400°C) it was not envisaged that concentrations greater than 0.1M would be required, these being easily obtainable given the compound's 52g/l (0.27M) solubility at 20°C[25]. In addition to being easy to prepare and air stable, zinc formate dihydrate was chosen because it was relatively unstudied and contained a lower percentage carbon than the acetate - the author was concerned that carbon contamination might be significant for films deposited at low temperatures. Literature evidence [26-29] indicated little difference in the decomposition temperatures of $Zn(CH_3CO_2)_2.2H_2O$ and $Zn(HCO_2)_2.2H_2O$.

6.2 The experiments

6.2.1 Preparation and analysis of zinc formate dihydrate

The zinc formate dihydrate used in the spray experiments described in this chapter was prepared using a literature method[30].

129.6g (0.4 moles) of zinc basic carbonate [$ZnCO_3.2Zn(OH)_2$] were vigorously stirred in 2 litres of distilled water. To this was added 90.6 ml (2.4 mol) of formic

acid, causing effervescence and giving rise to a clear solution. This was filtered (to remove any untreated zinc basic carbonate) and the solvent (water) was removed using a rotary evaporator (water pump, 70°C bath) to yield a colourless crystalline solid. This was dried *in vacuo* (0.01 torr, 25°C, 7 hours) to give zinc formate dihydrate (215g, 93%). elemental analyses (Carbon : found 12.48%, theory 12.55%; Hydrogen : found 3.17%, theory 3.16%) showed that the purity was sufficiently high as to render recrystallisation unnecessary.

6.2.2 Spraying of aqueous solutions of zinc formate dihydrate

Details of the spraying kit are outlined in chapter 2.

The objective of the thirteen experiments described in this chapter was to explore the possibilities for producing zinc oxide semi-conducting films, from totally aqueous solutions of zinc formate dihydrate, at low (below 300°C) substrate temperatures. By varying the solution concentration and the substrate temperature it was hoped that the limits of the method would be identified, giving a basis on which decisions on future work could be made.

Three different solution concentrations (0.1M, 0.05M and 0.02M) were sprayed at four different substrate temperatures (250°C, 300°C, 350°C and 400°C). In addition, one run was conducted at 200°C with a 0.1M solution. All the experiments used solutions of zinc formate dihydrate (preparation described in 6.2.1) in demineralised water. In all cases the spray was shrouded with white spot nitrogen at 1 bar pressure and the spray solution was pumped at a pressure of 2 bar. The solutions were sprayed onto soda glass slides (3" x 1") situated on the substrate support (see Chapter 2). The central slide i.e. the one directly below the spray nozzle was used for analysis. Ceramic wool was placed around the edge of the substrate support to soak up any solution that fell outside the heated area. Details of the solution quantities and concentrations, substrate temperatures and spraying times are listed below.

Spray run SR1

Substrate temperature = 400°C.

350ml of 0.1M solution (6.70g of precursor) in 15 minutes.

Cooled for 15 minutes (400°C to 69°C) under N_2.

Spray run SR2

Substrate temperature 300°C.

350ml of 0.1M solution (6.70g of precursor) in 15 minutes.

Cooled for 15 minutes (300°C to 65°C) under N_2.

Spray run SR3

Substrate temperature 250°C

350ml of 0.1M solution (6.70g of precursor) in 17 minutes.

Cooled for 12 minutes (250°C to 65°C) under N_2.

Spray run SR4

Substrate temperature 300°C

700ml of 0.05M solution (6.70g of precursor) in 33 minutes.

Cooled for 15 minutes (300°C to 69°C) under N_2.

Spray run SR5

Substrate temperature 300°C

875ml of 0.02M solution (3.35g of precursor) in 43 minutes.

Cooled for 17 minutes (300°C to 45°C) under N_2.

Spray run SR6

Substrate temperature 200°C

350ml of 0.1M solution (6.70g of precursor) in 16 minutes.

Cooled for 10 minutes (200°C to 53°C) under N_2.

Spray run SR7

Substrate temperature 350°C

350ml of 0.1M solution (6.70g of precursor) in 17 minutes.

Cooled for 12 minutes (350°C to 60°C) under N_2.

Spray run SR8

Substrate temperature 350°C

700ml of 0.05M solution (6.70g of precursor) in 33 minutes.

Cooled for 13 minutes (350°C to 93°C) under N_2.

Spray run SR9

Substrate temperature 350°C

875ml of 0.02M solution (3.35g of precursor) in 65 minutes.

Cooled for 12 minutes (350°C to 66°C) under N_2.

Spray run SR10

Substrate temperature 400°C

875ml of 0.02M solution (6.70g of precursor) in 29 minutes.

Cooled for 15 minutes (400°C to 71°C) under N_2.

Spray run SR11

Substrate temperature 400°C

700ml of 0.05M solution (6.70g of precursor) in 29 minutes.

Cooled for 15 minutes (400°C to 71°C) under N_2.

Spray run SR12

Substrate temperature 250°C

875ml of 0.02M solution (3.35g of precursor) in 39 minutes.

Cooled for 15 minutes (250°C to 45°C) under N_2.

Spray run SR13

Substrate temperature 250˚C

700ml of 0.05M solution (6.70g of precursor) in 26 minutes.

Cooled for 13 minutes (250˚C to 62˚C) under N_2.

6.3 Analysis and Results

6.3.1 General

Generally speaking, spraying produced transparent films with a slightly white, frosted appearance. To study the films three types of analysis were employed. Thickness measurements were obtained using a α-step machine; spectrophotometer measurements in the region 300-1000nm were used to gauge optical transmittance; and grain size and preferred orientation were analysed using wide angle X-ray scattering (see Chapter 2 for details).

6.3.2 Thickness measurements

The following average thicknesses were obtained for the thirteen films.

	0.1M	0.05M	0.02M
200˚C	4,200nm (SR6)	--	--
250˚C	1,700nm (SR3)	1,700nm (SR13)	700nm (SR12)
300˚C	800 nm (SR2)	2,200nm (SR4)	1,200nm (SR5)
350˚C	4,100nm (SR7)	3,200nm (SR8)	800nm (SR9)
400˚C	800nm (SR1)	1,000nm (SR11)	500nm (SR10)

It should be remembered that for the 0.02M spray solutions only half the amount of zinc formate dihydrate was used as compared with the 0.01M and 0.05M solutions. Therefore, it was not surprising to note that the average thickness films produced using 0.02M solution was significantly lower than those for the films produced at the other two concentrations. Having stated this, it was not possible to ascertain any discernible trends, either with respect to substrate temperature or solution concentration, from the figures. This indicated that the films produced were rough, with variable thickness. The roughness was perhaps due to too quick a rate of deposition - the most consistent figures were obtained at the lowest concentrations (0.02M). With this in mind, future work should probably focus on using more diluted solutions (0.02M and below). Although this would make spraying less energy efficient (longer heating times required) it would open the possibility for using other, less soluble, zinc salts.

6.3.3 Optical Tranmittance Measurements

One of the criteria for semi-conductors used as the top layer in photovoltaic devices is that they must transmit optical light through to the base layer. For this reason, the percentage tranmittance at 890nm (wavelength used in previous work on this project) was recorded for all thirteen films. The results were as follows.

	0.1M	0.05M	0.02M
200˚C	63% (SR6)		
250˚C	62% (SR3)	73% (SR13)	64% (SR12)
300˚C	84% (SR2)	83% (SR4)	72% (SR5)
350˚C	75% (SR7)	73% (SR8)	74% (SR9)
400˚C	85% (SR1)	80% (SR11)	86% (SR10)

It is probably wise to show some caution with regard to these results given the variability in the film thicknesses. However, a clear trend can be noted with respect to the substrate temperature. All the films produced at 400°C had a transmittance of over 80% at 890nm, whereas, only one film (SR13) produced below 300°C had a transmittance over 65%. However, two of the three films produced at 300°C also recorded transmittances over 80%, and despite the slightly lower figures for films produced at 350°C (probably due to film thickness variation), the figures suggested that there was little difference in optical transmission for all films produced over 300°C.

The figures indicated no variation in optical transmittance with respect to spray solution concentration.

6.3.4 Wide angle X-ray scattering - preferred orientation

Wide angle X-ray scattering was used for two forms of analysis : grain size, using full width half maximum measurements, and preferred orientation, using relative intensities.

The first objective of the X-ray analysis was to identify the chemical nature of the films. Figures 6.1, 6.2 and 6.3 show X-ray patterns for zinc oxide, zinc formate dihydrate and the film from SR1 respectively. The figures clearly show that the film (SR1) was zinc oxide and was free from zinc formate dihydrate contamination.

Figure 6.1 also shows the relative intensities of the three main peaks in the X-ray pattern of powdered ZnO. These occur at 2θ values of 31.93, 34.57 and 36.40 and are due to the planes (100), (002) and (101) respectively[31]. The relative intensities (greatest = 100) are 57, 46 and 100 respectively. It is known[31] that dominance of the (101) peak indicates preferred orientation in the c-axis, which is desired for good semi-conductancy, and that dominance of the (002) peak indicates randomly orientated polycrystalline zinc oxide.

All the X-ray patterns for the films produced from SR1 to SR13 were similar. In all cases the dominant peak was (002) but the relative intensities of the three major peaks did vary. Given an intensity of 100 for the peak (002), the intensities for (100) and (101) are given below [(100) figure given first].

	0.01M	0.05M	0.02M
200˚C	18,39 (SR6)	--	--
250˚C	18,33 (SR3)	38,70 (SR13)	53,85 (SR12)
300˚C	46,48 (SR2)	28,53 (SR4)	32,52 (SR5)
350˚C	22,33 (SR7)	35,52 (SR8)	20,36 (SR9)
400˚C	64,90 (SR1)	46,59 (SR11)	17,27 (SR10)

These figures indicated that substrate temperature and solution concentration had no effect on the crystal formation in zinc oxide films produced by the spray pyrolysis of aqueous solutions of zinc formate dihydrate. In all cases the films were polycrystalline with no preferred orientation.

6.4.5 Wide angle X-ray scattering - grain size

Grain size is obviously important in semiconductors. Larger grains mean fewer grain boundaries per unit length and, consequently, less places where charge can be lost, leading to greater conductivity.

Grain size, ϵ, can be related to the full width half maximum of ZnO X-ray pattern peaks, B, by the following formulae[31].

$\epsilon = \kappa \lambda (\beta \cos \theta)^{-1}$ where $\beta = (B^2 - b^2)^{\frac{1}{2}}$

κ = 0.9

λ = X-ray wavelength

θ = diffraction angle

b = full width half maximum for a single crystal of GaAs.

Figure 6.1 Wide angle X-ray scattering pattern for powdered ZnO

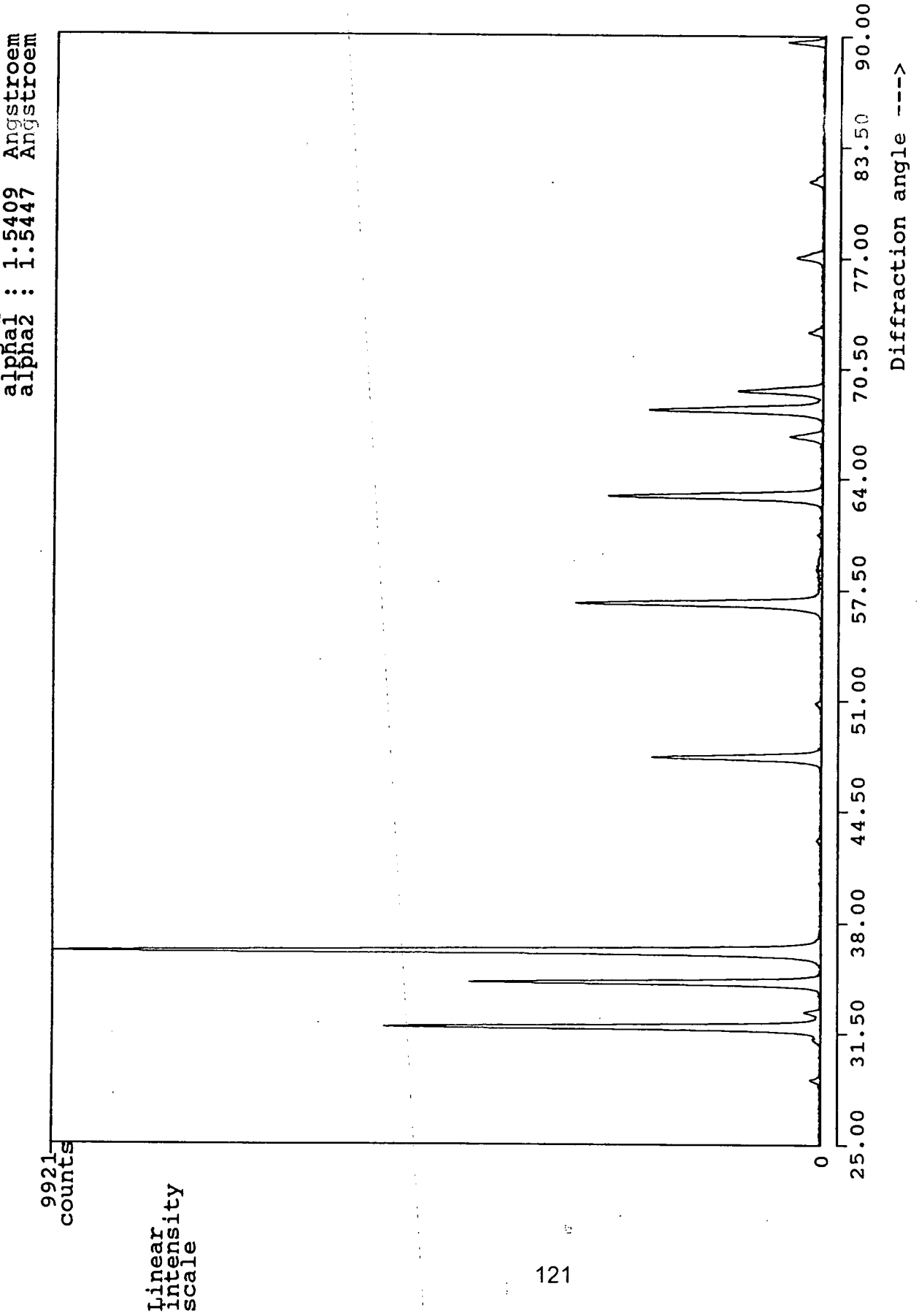

Figure 6.2 Wide angle X-ray scattering pattern for zinc formate dihydrate

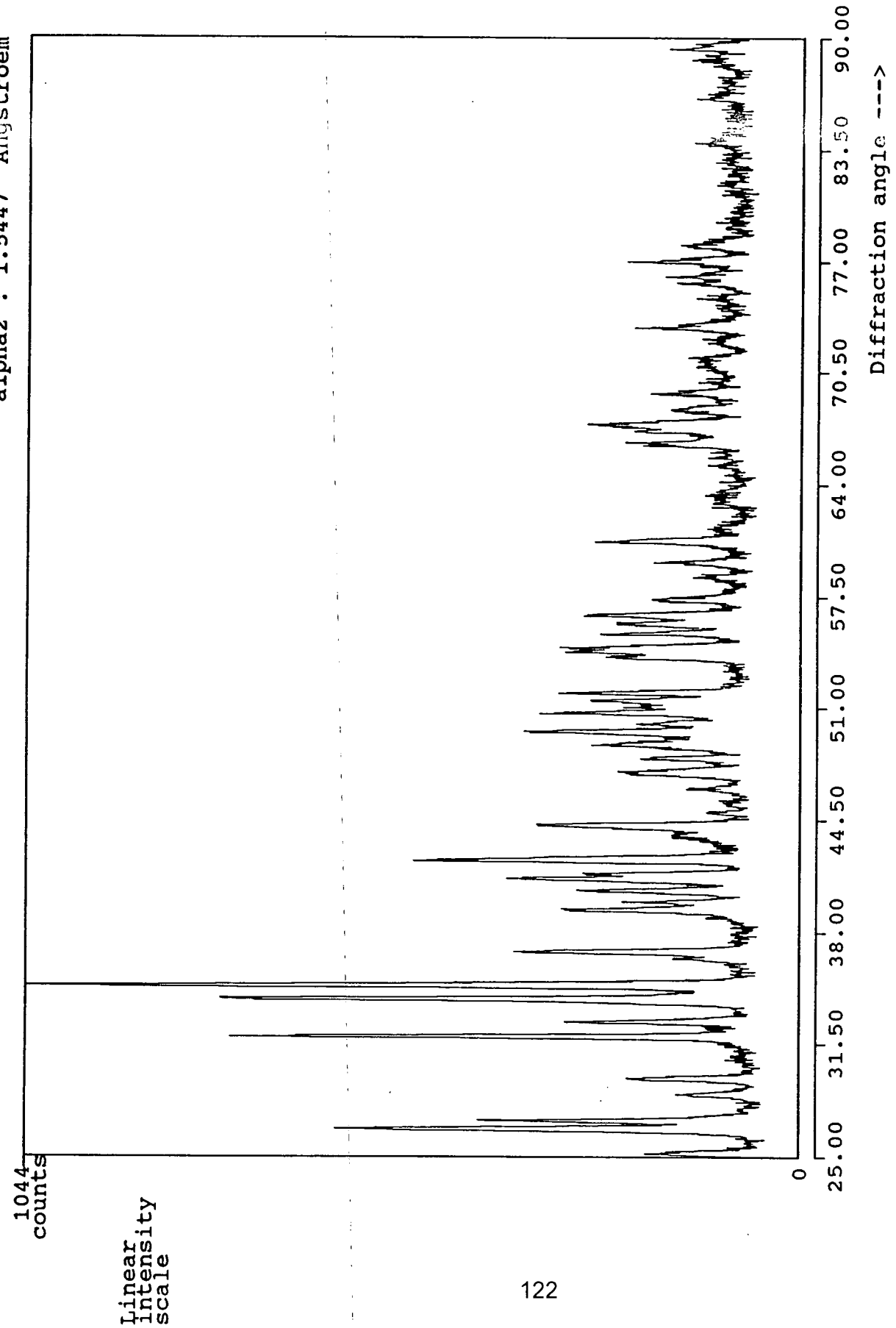

Figure 6.3 Wide angle X-ray scattering pattern for film from SR1

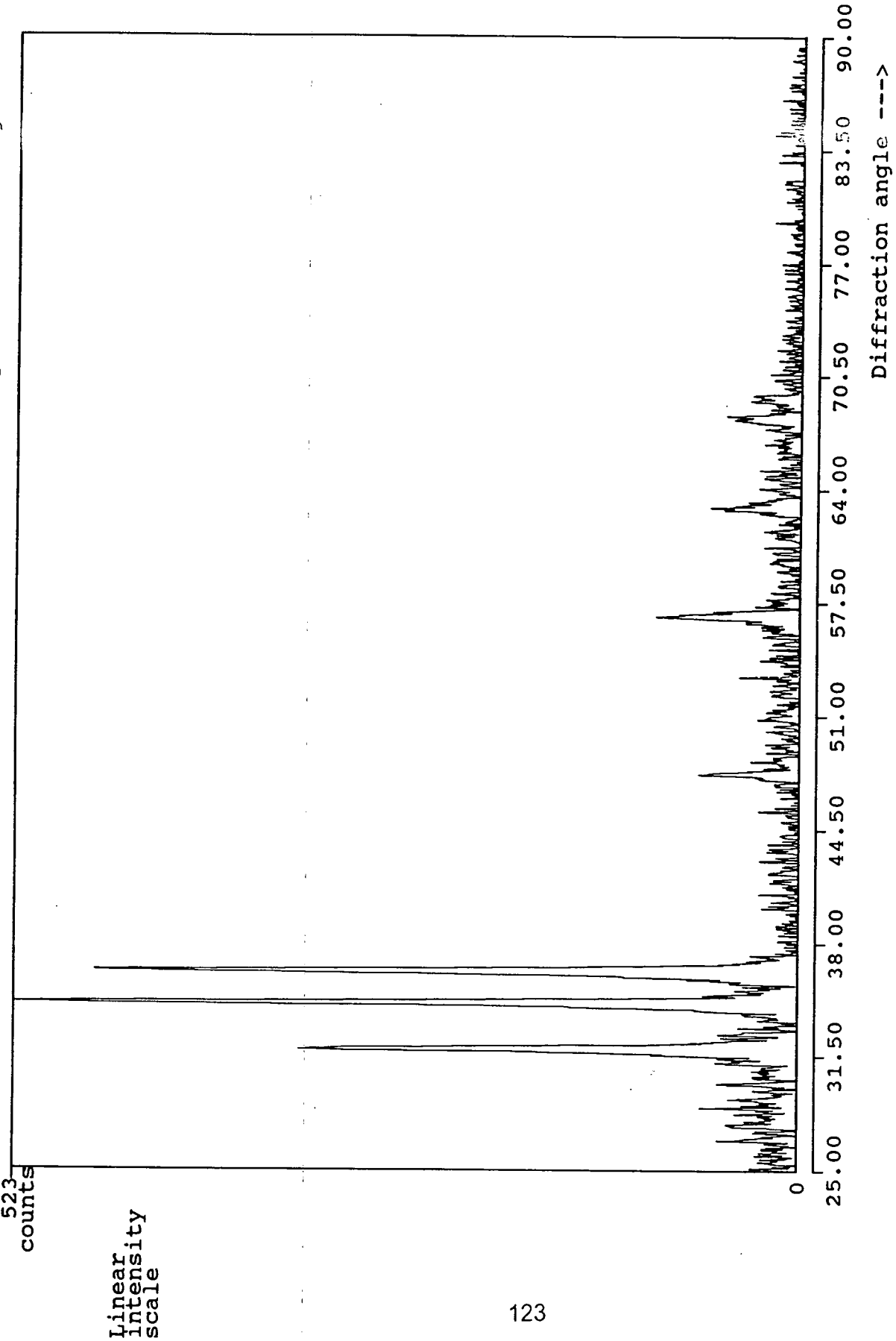

By deduction, the smaller the value of B the large the grain size. B values for the films produced in the thirteen experiments SR1 to SR13 are listed below. Values are given for the (002) peak.

	0.1M	0.05M	0.02M
200°C	0.46 (SR6)	--	--
250°C	0.50 (SR3)	0.48 (SR13)	0.45 (SR12)
300°C	0.51 (SR2)	0.51 (SR4)	0.43 (SR5)
350°C	0.49 (SR7)	0.42 (SR8)	0.36 (SR9)
400°C	0.30 (SR1)	0.45 (SR12)	0.30 (SR10)

In contrast to the preferred orientation figures, these results show two trends. Firstly, at a given solution concentration, higher substrate temperatures gave smaller B values, hence, larger grain sizes. Secondly, for a given substrate temperature, lower solution concentrations also gave smaller B values (larger grain sizes). Only the result for SR12 (400°C, 0.05M) was a major disagreement with these trends and should probably be disregarded as a "rogue" result. These results were in agreement with the work on zinc acetate by Janda and Kubovy.[20,21]

The figures indicated that maximum grain size could be achieved with a high substrate temperature and low solution concentration. The high temperature would provide the necessary energy for larger grain formation and the low solution concentration would provide a slower rate of growth allowing bigger grains to be formed.

6.4 Conclusions

Despite being inferior in terms of crystalline quality to the films produced from alcoholic solutions of $Zn(acac)_2 H_20$ by Mr A.J.C. Fiddes (SEAS, University of Durham)[32], there were some encouraging results from this initial study. Although no

preferred orientation was observed the films formed were polycrystalline. The clarity of the films formed was satisfactory and whilst sample thickness showed some variability, trends in the grain size pointed out the direction of future work. This would appear to lie with lower solution concentrations, which also provided films with a more even thickness. The use of a solvent (water) with a relatively high heat of evaporation will always be an obstacle, as this leaves less energy for the formation of preferentially orientated crystals. However, other precursors are available and further study will reveal the potential of spray pyrolysis of aqueous solutions at low temperatures.

References

1. G. Heiland, E. Mollwo and F. Stockman, *Solid State Phys.*, 1959, **8**, 191.
2. R.A. Mickelson and W.D. Kingery, *J. Appl. Phys.*, 1966, **37**, 3541.
3. B. Laville Saint Martin and B. Meyer, *Thin Films*, 1972, **2**, 139.
4. H.W. Lehmann and R. Widner, *J. Vac. Sci. & Techn.*, 1974, **11**, 41.
5. H.W. Lehmann and R. Widner, *Jap. J. Appl. Phys.*, 1974, **2**, 741.
6. H.H. Quon and D.P. Malanka, *Mater. Res. Bull.*, 1975, **10**, 349.
7. S.K. Ghandi and B.J. Field, *Appl. Phys. Lett.*, 1980, **37**, 449.
8. J. Fukushima, K. Kodaira, A. Tsunashima and T. Matsushita, *Yogyo Kyokai-Shi*, 1975, **83**, 535.
9. S.D. Sathaye and A.P.B. Sinha, *Thin Solid Films*, 1977, **44**, 57.
10. K. Matsubara, I. Yamada, N. Nagao, K. Tominaga and T. Takagi, *Surf. Sci.*, 1978, **86**, 290.
11. T. Ohkoda, N. Mutsukura and Y. Machi, *Res. Rep. Tokyo Denki Univ.*, 1979, **27**, 39.
12. J. Aranovich, A. Fahrenbruch and R. Bube, *XIV IEEE Photovoltaic Specialists Conf.*, San Diego, CA, U.S.A., 1980, 633.
13. R.L. Call, N.K. Jaber, K. Seshan and J.R. Whyte, *Sol. Energy Mater.*, 1980, **2**, 373.
14. J. Aranovich, A. Ortiz and R.H. Bube, *J. Vac. Sci. & Techn.*, 1979, **16**, 994.
15. I. Niikura, H. Watanabe and M. Wada,*Rec. Electr. & Commun. Eng. Conversazione Tohoku Univ.*, 1976, **45**, 27.
16. L. Bahadur, M. Hamdani, J. Koenig and P. Chartier, *Sol. Energy Mater.*, 1986, **14**, 107.
17. J.-H. Jean, *J. Mater. Sci. Lett.*, 1990, **9**, 127.
18. K. Kamata and S. Matsumoto, *Yogyo Kyokai-Shi*, 1981, **89**, 337.
19. J. McK. Nobbs and F.C. Gillespie, *J. Phys. Chem. Solids*, 1970, **31**, 2353.
20. M. Janda and A. Kubory, *Jemna Mech. & Opt.*, 1975, **20**, 66.
21. M. Janda and A Kubory, *Krist. & Techn.*, 1976, **11**, K53.
22. S. Major, A. Banerjee and K.L. Chopra, *Thin Solid Films*, 1983, **108**, 333.

23. M.S. Jaffa, *U.S. Patent No. 2,791,521,* 1957.
24. M. Islam, M. Hakim and H. Rahman, *J. Mater. Sci.*, 1987, **22**, 1379.
25. CRC Handbook of Chemistry and Physics, 60th edition, edited by R.C. Weast.
26. E.S. Osinorik, L.P. Kostynk-Kul'gavchuk and Z.M. Graboskaya, *Vest. Akad, Nauk Belarus. SSR, Ser. Khim. Nauk*, 1996, **4**, 112.
27. G. Djega-Mariadasson, A. Marques and G. Pannetier, *Bull. Soc. Chim. Fr.*, 1971, **9**, 3166.
28. Y. Masuda and S. Shishido, *Thermochim. Acta*, 1979, **28**, 377.
29. J. Mu and D.D. Perlmutter, *Thermochim. Acta*, 1981, **49**, 207.
30. K.N. Semenenko, *Zhur. Neorg. Khim.*, 1957, **2**, 2115.
31. Current topics in Materials Science, Volume 7, subchapter 3.0, 149, edited by E. Kaldis.
32. A.J.C. Fiddes, personal communication.

Appendices

APPENDIX 1

First Year Induction Courses: October 1988

The course consisted of a series of one hour lectures on the services available within the Department.

1. Departmental Organisation
2. Safety Matters
3. Electrical Appliances and Infra-Red Spectroscopy
4. Chromatography and Microanalysis
5. Atomic Absorption and Inorganic Analysis
6. Library Facilities
7. Mass Spectroscopy
8. Nuclear Magnetic Resonance Spectroscopy
9. Glassblowing Techniques

APPENDIX 2

UNIVERSITY OF DURHAM

Board of Studies in Chemistry

COLLOQUIA, LECTURES AND SEMINARS GIVEN BY INVITED SPEAKERS

1st August 1988 to 31st July 1989

SCHMUTZLER, Prof. R. (Technische Universität Braunschweig)

06.10.88

Fluorophosphines Revisited - New Contributions to an Old Theme

DINGWALL, Dr. J. (Ciba - Geigy) 18.10.88

Phosphorus - containing Amino Acids : Biologically Active Natural and Unnatural Products

*LUDMAN, Dr. C. J. (University of Durham) 18.10.88

The Energetics of Explosives

Von RAGUE SCHLEYER, Prof. P. (Universität Erlangen Nürnberg) 21.10.88

The Fruitful Interplay Between Calculational and Experimental Chemistry

REES, Prof. C. W. (Imperial College, London) 27.10.88

Some Very Heterocyclic Compounds

SINGH, Dr. G. (Teesside Polytechnic) 09.11.88

Towards Third Generation Anti - Leukaemics

*CADOGAN, Prof. J. I. G. (British Petroleum) 10.11.88

From Pure Science to Profit

McLAUCHLAN, Dr. K. A. (University of Oxford) 16.11.88

The Effect of Magnetic Fields on Chemical Reactions

*BALDWIN and WALKER, Drs. R. R. & R. W. (University of Hull) 24.11.88

Combustion : Some Burning Problems

*SNAITH, Dr. R. (University of Cambridge) 01.12.88

Egyptian Mummies : What, Where, Why and How?

HARDGROVE, Dr. G. (St. Olaf College, U.S.A.) 02.12.88

Polymers in the Physical Chemistry Laboratory

JÄGER, Dr. C. (Friedrich-Schiller University, Germany) 09.12.88

NMR Investigations of Fast Ion Conductors of the NASICON Type

HARWOOD, Dr. L. (University of Oxford) 25.01.89

Synthetic Approaches to Phorbols via Intramolecular Furan Diels-Alder Reactions : Chemistry under Pressure

*JENNINGS, Prof. R. R. (University of Warwick) 26.01.89

Chemistry of the Masses

*HALL, Prof. L. D. (Addenbrooke's Hospital, Cambridge) 02.02.89

NMR : A Window to the Human Body

*BALDWIN, Prof. J. E. (University of Oxford) 09.02.89

Recent Advances in the Bioorganic Chemistry of Penicillin Biosynthesis

*SCHROCK, Prof. R. R. (M. I. T.) 13.02.89

Recent Advances in Living Metathesis

BUTLER, Dr. A. R. (University of St. Andrews) 15.02.89

Cancer in Linxiam : The Chemical Dimension

*AYLETT, Prof. B. J. (Queen Mary College, London) 16.02.89

Silicon-Based Chips : The Chemists Contribution

MACDOUGALL, Dr. G. (University of Edinburgh) 22.02.89

Vibrational Spectroscopy of Model Catalytic Systems

*JOHNSON, Prof. B. F. G. (University of Cambridge) 23.02.89

The Binary Carbonyls

ERRINGTON, Dr. R. J. (University of Newcastle upon Tyne) 01.03.89

Polymetalate Assembly in Organic Solvents

MARKO, Dr. I. (University of Sheffield) 09.03.89

Catalytic Asymmetric Osmylation of Olefins

AVEYARD, Dr. R. (University of Hull) 15.03.89

Surfactants at your Surface

*GRADUATE CHEMISTS, (Polytechs and Universities in North East England) 12.04.89

R.S.C. Symposium for presentation of papers by postgraduate students

CASEY, Dr. M. (University of Salford) 20.04.89

Sulphoxides in Stereoselective Synthesis

CRICH, Dr. D. (University College, London) 27.04.89

Some Novel Uses of Free Radicals in Organic Synthesis

PAGE, Dr. P. C. B. (University of Liverpool) 03.05.89

Stereocontrol of Organic Reactions Using 1,3-Dithiane-1-oxides

WELLS, Prof. P. B. (University of Hull) 10.05.89

Catalyst Characterisation and Activity

FREY, Dr. J. (University of Southampton) 11.05.89

Spectroscopy of the Reaction Path : Photodissociation Raman Spectra of NOCl

STIBR, Dr. R. (Czechoslovak Academy of Sciences) 16.05.89

Recent Developments in the Chemistry of Intermediate - Sited Carboranes

MOODY, Dr. C. J. (Imperial College, London) 17.05.89

Reactive Intermediates in Heterocyclic Synthesis

PAETZOLD, Prof. P. (Aachen) 23.05.89

Iminoboranes : Inorganic Acetylenes?

POLA, Prof. J. (Czechoslovak Academy of Sciences) 15.06.89

Carbon Dioxide Laser-Induced Chemical Reactions - New Pathways in Gas - Phase Chemistry

UNIVERSITY OF DURHAM

Board of Studies in Chemistry

COLLOQUIA, LECTURES AND SEMINARS GIVEN BY INVITED SPEAKERS

1st August 1989 to 31st July 1990

*PALMER, Dr. F. (University of Nottingham) 17.10.89

Thunder and Lightning

FLORIANI, Prof. C. (University of Lausanne) 25.10.89

Molecular Aggregates - A Bridge Between Homogeneous and Heterogeneous Systems

BADYAL, Dr. J. P. S. (University of Durham) 01.11.89

Breakthroughs in Heterogeneous Catalysis

*GREENWOOD, Prof. N. N. (University of Leeds) 09.11.89

Novel Cluster Geometries in Metalloborane Chemistry

BERCAW, Prof. J. E. (California Institute of Technology) 10.11.89

Synthetic and Mechanistic Approaches to Ziegler - Natta Polymerization of Olefins

BECHER, Dr. J. (University of Odense) 13.11.89

Synthesis of New Macrocyclic Systems Using Heterocyclic Building Blocks

*PARKER, Dr. D. (University of Durham) 16.11.89

Macrocycles, Drugs and Rock 'n' Roll

COLE-HAMILTON, Prof. D. J. (University of St. Andrews) 29.11.89

New Polymers from Homogeneous Catalysis

*HUGHES, Dr. M. N. (King's College, London) 30.11.89

A Bug's Eye View of the Periodic Table

GRAHAM, Dr. D. (B. P. Research Centre) 04.12.89

How Proteins Adsorb to Interfaces

POWELL, Dr. R. L. (ICI) 06.12.89

The Development of C.F.C. Replacements

BUTLER, Dr. A. (University of St. Andrews) 07.12.89

The Discovery of Penicillin : Facts and Fancies

KLINOWSKI, Dr. J. (University of Cambridge) 13.12.89

Solid-State NMR Studies of Zeolite Catalysts

HUISGEN, Prof. R. (Universität München) 15.12.89

Recent Mechanistic Studies of [2 + 2] Additions

PERUTZ, Dr. R. N. (University of York) 24.01.90

Plotting the Course of C-H Activations with Organometallics

DYER, Dr. U. (Glaxo) 31.01.90

Synthesis and Conformation of C-Glycosides

*HOLLOWAY, Prof. J. H. (University of Leicester) 01.02.90

Noble Gas Chemistry

THOMPSON, Dr. D. P. (University of Newcastle upon Tyne) 07.02.90

The Role of Nitrogen in Extending Silicate Crystal Chemistry

*LANCASTER, Rev. R. (Kimbolton Fireworks) 08.02.90

Fireworks - Principles and Practice

LUNAZZI, Prof. L. (University of Bologna) 12.02.90

Application of Dynamic NMR to the Study of Conformational Enantiomerism

SUTTON, Prof. D. (Simon Fraser University, Vancouver) 14.02.90

Synthesis and Applications of Dinitrogen and Diazo Compounds of Rhenium and Iridium

CROMBIE, Prof. L. (University of Nottingham) 15.02.90

The Chemistry of Cannabis and Khat

BLEASDALE, Dr. C. (University of Newcastle upon Tyne) 21.02.90

The Mode of Action of some Anti - Tumour Agents

*CLARK, Prof. D.T. (ICI Wilton) 22.02.90

Spatially Resolved Chemistry (using Nature's Paradigm in the Advanced Materials Arena)

THOMAS, Dr. R. K. (University of Oxford) 28.02.90

Neutron Reflectometry from Surfaces

*STODDART, Dr. J. F. (University of Sheffield) 01.03.90

Molecular Lego

*CHEETHAM, Dr. A. K. (University of Oxford) 08.03.90

Chemistry of Zeolite Cages

POWIS, Dr. I. (University of Nottingham) 21.03.90

Spinning Off in a Huff : Photodissociation of Methyl Iodide

BOWMAN, Prof. J. M. (Emory University) 23.03.90

Fitting Experiment with Theory in Ar-OH

GERMAN, Prof. L. S. (Soviet Academy of Sciences) 09.07.90

New Syntheses in Fluoroaliphatic Chemistry : Recent Advances in the Chemistry of Fluorinated Oxiranes

PLATONOV, Prof. V.E. (Soviet Academy of Sciences, Novosibirsk) 09.07.90

Polyfluoroindanes : Synthesis and Transformation

ROZHKOV, Prof. I. N. (Soviet Academy of Sciences, Moscow) 09.07.90

Reactivity of Perfluoroalkyl Bromides

UNIVERSITY OF DURHAM

Board of Studies in Chemistry

COLLOQUIA, LECTURES AND SEMINARS GIVEN BY INVITED SPEAKERS

1st August 1990 to 31st July 1991

*MACDONALD, Dr. W.A. (ICI Wilton) 11.10.90

Materials for the Space Age

BOCHMANN, Dr. M. (University of East Anglia) 24.10.90

Synthesis, Reactions and Catalytic Activity of Cationic Titanium Alkyls

SOULEN, Prof. R. (South Western University, Texas) 26.10.90

Preparation and Reactions of Bicycloalkenes

JACKSON, Dr. R.F.W. (University of Newcastle upon Tyne) 31.10.90

New Synthetic Methods : α-Amino Acids and Small Rings

*LOGAN, Dr. N. (University of Nottingham) 01.11.90

Rocket Propellants

*KOCOVSKY, Dr. P. (University of Uppsala) 06.11.90

Stereo-Controlled Reactions Mediated by Transition and Non-Transition Metals

*GERRARD, Dr. D. (British Petroleum) 07.11.90

Raman Spectroscopy for Industrial Analysis

*SCOTT, Dr. S.K. (University of Leeds) 08.11.90

Clocks, Oscillations and Chaos

BELL, Prof. T. (SUNY, Stoney Brook, USA) 14.11.90

Functional Molecular Architecture and Molecular Recognition

PRITCHARD, Prof. J. (Queen Mary & Westfield College) 21.11.90

Copper Surfaces and Catalysts

WHITAKER, Dr. B.J. (University of Leeds) 28.11.90

Two-Dimensional Velocity Imaging of State-Selected Reaction Products

*CROUT, Prof. D. (University of Warwick) 29.11.90

Enzymes in Organic Synthesis

*PRINGLE, Dr. P.G. (University of Bristol) 05.12.90

Metal Complexes with Functionalised Phosphines

*COWLEY, Prof. A.H. (University of Texas) 13.12.90

New Organometallic Routes to Electronic Materials

*ALDER, Dr. B.J. (Lawrence Livermore Labs., California) 15.01.91

Hydrogen in all its Glory

SARRE, Dr. P. (University of Nottingham) 17.01.91

Comet Chemistry

*SADLER, Dr. P.J. (Birkbeck College London) 24.01.91

Design of Inorganic Drugs : Precious Metals, Hypertension & HIV

*SINN, Prof. E. (University of Hull) 30.01.91

Coupling of Little Electrons in Big Molecules : Implications for the Active Sites of Metalloproteins and other Macromolecules

*LACEY, Dr. D. (University of Hull) 31.01.91

Liquid Crystals

BUSHBY, Dr. R. (University of Leeds) 06.02.91

Biradicals and Organic Magnets

*PETTY, Dr. M.C. (Durham University) 14.02.91

Molecular Electronics

SHAW, Prof. B.L. (University of Leeds) 20.02.91

Syntheses with Coordinated, Unsaturated Phosphine Ligands

BROWN, Dr. J. (University of Oxford) 28.02.91

Can Chemistry Provide Catalysts Superior to Enzymes?

DOBSON, Dr. C.M. (University of Oxford) 06.03.91

NMR Studies of Dynamics in Molecular Crystals

*MARKAM, Dr. J. (ICI Pharmaceuticals) 07.03.91

DNA Fingerprinting

*SCHROCK, Prof. R.R. (M.I.T.) 24.04.91

Metal-Ligand Multiple Bonds and Metathesis Initiators

HUDLICKY, Prof. T. (Virginia Polytechnic Institute) 25.04.91

Biocatalysis and Symmetry Based Approaches to the Efficient Synthesis of Complex Natural Products

BROOKHART, Prof. M.S. (University of North Carolina) 20.06.91

Olefin Polymerizations, Oligomerizations and Dimerizations Using Electrophilic Late Transition Metal Catalysts

BRIMBLE, Dr. M.A. (Massey University, New Zealand) 29.07.91

Synthetic Studies Towards the Antibiotic Griseusin-A